LA-9328-MS

281

Los Alamos National Laboratory is operated by the University of California for the United States Department of Energy under contract W-7405-ENG-36.

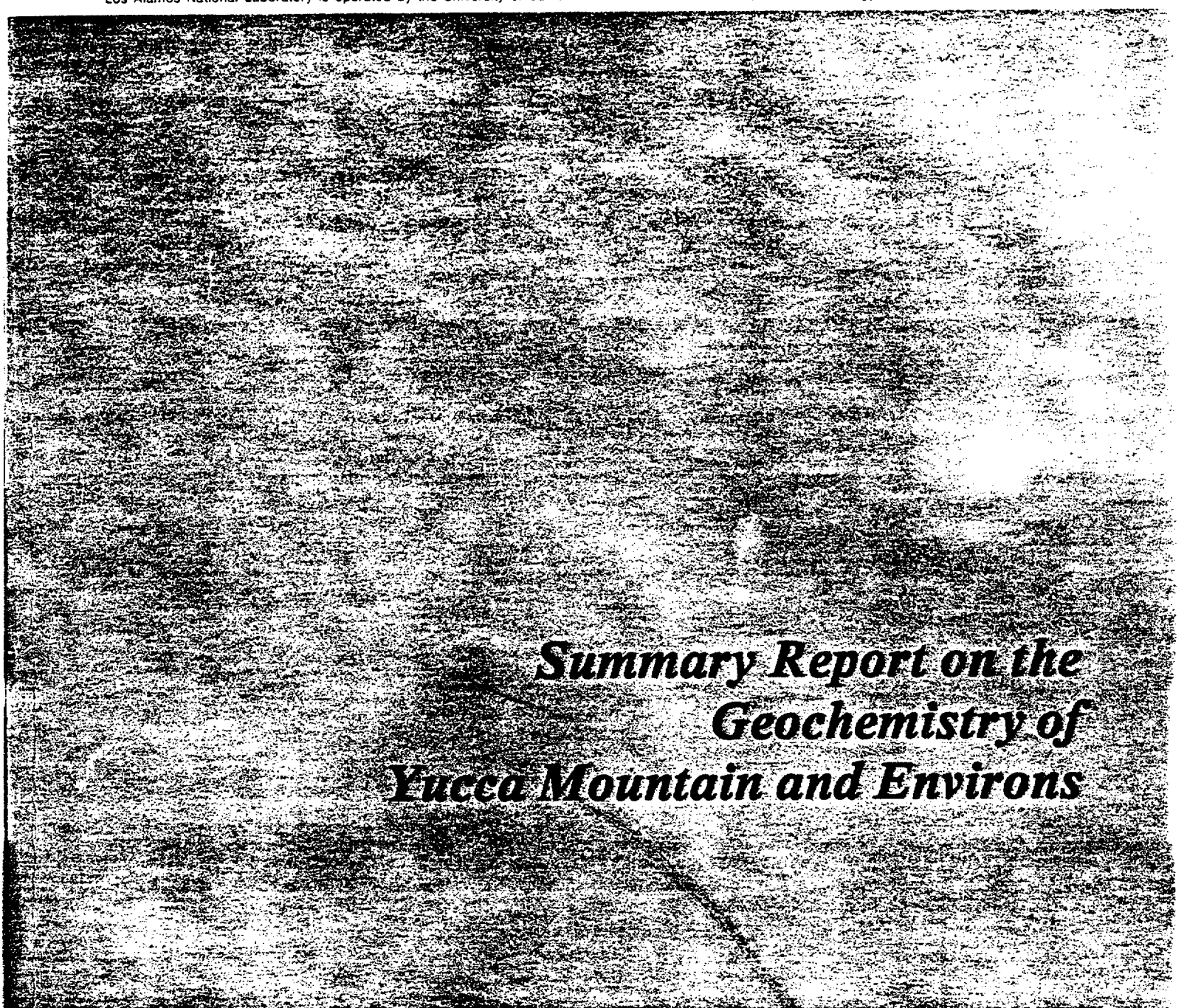

Summary Report on the Geochemistry of Yucca Mountain and Environs

Los Alamos
Los Alamos National Laboratory
Los Alamos, New Mexico 87545

This report was prepared by the Los Alamos National Laboratory as part of the Nevada Nuclear Waste Storage Investigations managed by the Nevada Operations Office of the US Department of Energy. Based upon their applicability to the investigations, some results from the Radionuclide Migration Project, managed by the Nevada Operations Office of the US Department of Energy, are included in this report.

Edited by Jody Heiken

LA-9328-MS

UC-70
Issued: December 1982

Summary Report on the Geochemistry of Yucca Mountain and Environs

W. R. Daniels
K. Wolfsberg
R. S. Rundberg
A. E. Ogard
J. F. Kerrisk
C. J. Duffy
T. W. Newton
J. L. Thompson*
B. P. Bayhurst
D. L. Bish
J. D. Blacic
B. M. Crowe
B. R. Erdal
J. F. Griffith
S. D. Knight
F. O. Lawrence
V. L. Rundberg
M. L. Skyes
G. M. Thompson**
B. J. Travis
E. N. Treher
R. J. Vidale
G. R. Walter**
R. D. Aguilar
M. R. Cisneros
S. Maestas
A. J. Mitchell
P. Q. Oliver
N. A. Raybold
P. L. Wanek

*Department of Chemistry, Idaho State University, Pocatello ID 83209.
**Department of Hydrology and Water Resources, University of Arizona, Tucson AZ 85721.

Los Alamos National Laboratory
Los Alamos, New Mexico 87545

CONTENTS

CONTENTS (Cont)

SUMMARY REPORT ON THE GEOCHEMISTRY OF YUCCA MOUNTAIN AND ENVIRONS

by

W. R. Daniels
K. Wolfsberg
R. S. Rundberg
A. E. Ogard
J. F. Kerrisk
C. J. Duffy
T. W. Newton
J. L. Thompson
B. P. Bayhurst
D. L. Bish
J. D. Blacic
B. M. Crowe
B. R. Erdal
J. F. Griffith
S. D. Knight
F. O. Lawrence
V. L. Rundberg
M. L. Sykes
G. M. Thompson
B. J. Travis
E. N. Treher
R. J. Vidale
G. R. Walter
R. D. Aguilar
M. R. Cisneros
S. Maestas
A. J. Mitchell
P. Q. Oliver
N. A. Raybold
P. L. Wanek

ABSTRACT

This report gives a detailed description of work at Los Alamos that will help resolve geochemical issues pertinent to siting a high-level nuclear waste repository in tuff at Yucca Mountain, Nevada. It is necessary to understand the properties and setting of the host tuff because this rock provides the first natural barrier to migration of waste elements from a repository. The geochemistry of tuff is being investigated with particular emphasis on retardation processes. This report addresses the various aspects of sorption by tuff, physical and chemical makeup of tuff, diffusion processes, tuff/groundwater chemistry, waste element chemistry under expected repository conditions, transport processes involved in porous and fracture flow, and geochemical and transport modeling.

Executive Summary

This report gives a detailed description of technical contributions of the Los Alamos National Laboratory to the Nevada Nuclear Waste Storage Investigations (NNWSI) managed by the Nevada Operations Office of the US Department of Energy from the time of the Laboratory's first involvement with the project in FY 1977 until March of 1982. Efforts have been primarily devoted to resolving geochemistry issues pertinent to siting a nuclear waste repository in tuff at the Nevada Test Site (NTS), with emphasis on the Yucca Mountain area.

Water from the producing well (J-13) nearest the potential repository site at Yucca Mountain has been selected as the reference groundwater for laboratory experiments. For use in experiments on sorption of waste elements on tuff, the well J-13 reference groundwater was pretreated with tuff from individual strata of Yucca Mountain. Before being used in sorption experiments, the water was also filtered through 0.05-μm Nuclepore membranes to remove solid material. The well J-13 water composition is altered by contact with tuff of different strata; the sodium content decreases as much as 50%, and there is a variable, but slight, decrease in the potassium, calcium, and magnesium contents of the water. An additional significant point is the importance of filtration on the analyzed composition of the water. The results of experiments show that filtration through a 0.45-μm crossed-fiber membrane yields erroneously high results for the iron content; the filtration should be done through a 0.05-μm membrane having uniform pore sizes. This is especially important because the iron concentration in solution is a part of the measure of the oxidation-reduction potential (Eh) of the solution.

To determine or estimate the effect of the groundwater composition on the waste package, on the waste itself or its compounds, and on retardation mechanisms, it is necessary to determine the composition of the formation water for each particular stratum under consideration for a repository or a transport path. The groundwater composition is also important in its effect on forming or dissolving the newly formed minerals brought about by the temperature gradient exerted on the repository by the waste package. Wells in the vicinity of Yucca Mountain and Pahute Mesa have been sampled in various ways in an attempt to determine the composition of the groundwaters as a function of location. Results from analysis of groundwaters from hydrology wells at Yucca Mountain indicate that deep waters may be oxygen deficient compared to water

at the standing waste level. The presence of Fe 2+ and Fe 3+ influences the Eh of groundwater in geologic systems. Analysis of the concentration of these ions in groundwater may be used as part of the measure of the Eh. An alternative approach is to measure the concentration of Fe 2+ and Fe 3+ in different tuff strata and then to estimate the total oxidation-reduction capacity of the tuff mass. Attempts are being made to develop both alternatives as complementary information.

Short-term experiments have been done in which three tuffs from Yucca Mountain were contacted with groundwater at 152 ± 1°C to study possible reactions between the solid and solution phases. Three tuff samples of different lithologies were used, Topopah Spring, tuffaceous beds of Calico Hills, and Bullfrog II. Before contact with groundwater, the samples were examined with a scanning electron microscope (SEM) to observe general surface features and mineral phases. After contact with well J-13 water for 3 weeks at 152°C, the tuff samples were examined again by SEM and the waters analyzed. The Bullfrog tuff showed little reaction other than some rounding of surfaces and precipitation of clays. The Topopah Spring tuff showed greatly increased amounts of clays or other fine-grained sheet silicates, which had formed on glass edges. The tuffaceous beds of Calico Hills showed marked dissolution of clinoptilolite crystals. The main changes in the composition of the contacting water were large increases in sodium, potassium, and silicon concentrations and large decreases in the magnesium and calcium concentrations.

Prediction of the hazards caused by actinides escaping from a repository depends upon knowledge of the chemical processes that can take place in the repository and along the routes to the accessible environment. Information is needed concerning solubility and speciation of actinides under repository conditions and under conditions encountered by mobile species along flow paths toward the accessible environment. Factors that affect the solubility of actinides and the chemical form of the dissolved species and thus mobility include (1) the chemical and physical state of the waste form; (2) the Eh, pH, and concentration of dissolved material in the groundwater; (3) the temperature and flow rate of the groundwater; and (4) the physical and chemical state of the tuff encountered along the flow path. Each of these factors may vary with time and distance from the repository.

A number of studies that are relevant to understanding actinide solubility and speciation have been carried out: a method has been developed for preparing

groundwater solutions traced with actinides for sorption studies with tuff, including methods of separating solid and aqueous phases after contact; plutonium chemistry in near-neutral solutions, including development of systems for controlling the Eh through use of osmium complexes or other Eh buffers, is being investigated; and particulate transport, which includes preparation of plutonium polymers, is being studied. One difficulty encountered in laboratory experiments with plutonium is control of Eh, and thus, control of the oxidation state in the pH range of interest. Osmium complexes are potentially useful as Eh buffers because (1) the redox potentials of the Os(II)-Os(III) couples are independent of pH in near-neutral solutions, (2) the standard potential of the couple can be changed by varying the coordinated ligands, (3) the complexes are unlikely to complex actinide species, and (4) Os(II) complexes are highly colored and thus optically measurable at low concentrations. Nine osmium complexes, most of them synthesized at this laboratory, were examined for their suitability as Eh buffers. Equivalent weights were determined, absorption spectra recorded, extinction coefficients obtained, and formal oxidation potentials determined. Many of these complexes were found to be stable in solution for periods of days or weeks, even when held at elevated temperatures and exposed to light.

A number of reactions between osmium complexes and the various oxidation states of plutonium were investigated, and apparent second-order rate constants measured. By use of an osmium bipyridine complex, the standard potential for the Pu(V)-Pu(VI) couple was determined.

A number of Eh indicator systems that might be used as Eh buffers have been studied. Both Indigo Carmine and thionine show promise, although there is some evidence of slow attainment of chemical equilibrium. Equipment that enables us to conduct these studies in air or under a rigorously controlled inert atmosphere has been assembled.

Plutonium (IV) forms a polymer under certain conditions, so experiments have been initiated to characterize this polymer under conditions likely to exist in a repository. A technique is being investigated to measure the solubility of the polymer, that is, the extent to which the polymer converts to Pu(IV) ions. Measurements of this solubility, using ^{239}Pu, were somewhat tentative because of radiolysis caused by the intense alpha activity of this nuclide. These measurements are being repeated using ^{242}Pu, which has a lower specific activity. Experiments have been conducted in which the polymer appears to form over a broad range of concentration levels and pH values.

One mechanism by which radionuclides may move through geologic media is particulate transport. Particulates may include radioactive elements aggregated as colloids or colloids formed by sorption of radioactive species on microscopic particles. Such material may form from radionuclides initially in solution or as a consequence of leaching of solid waste forms. Microautoradiographic procedures have been used to identify particulates containing americium and plutonium in the effluents of crushed-rock columns. Colloids of Pu(IV) in a controlled size range are being prepared so that this material may be used in future transport studies. Plastic spheres incorporating fluorescent dye or radioactive material to aid in their detection are also being used to study particulate transport.

Possible changes in the solid phases at Yucca Mountain caused by the presence of a repository are of concern because they could affect rock properties, especially sorption, strength, permeability, and porosity. This is especially true in the near field where temperature will rise as a result of the repository emplacement. The phases most likely to change are the clays, zeolites, and glasses, all of which may be expected to alter to less hydrous phases of smaller volume. There may also be hydration of anhydrous phase assemblages, such as feldspar and silica, to zeolites or clays. Experiments to examine the phase changes in tuffs of varying mineral composition at known values of pressure and temperature have been started. The samples are ground and enclosed in gold capsules with water present. The capsules are then placed in standard cold-seal pressure vessels, which are pressurized and heated to the desired conditions. Preliminary hydrothermal experiments have provided evidence for the upper thermal stabilities of clinoptilolite and mordenite at 400 bars water pressure. The upper stability of mordenite is probably between 300 and 400°C; that for clinoptilolite appears to be below 300°C.

A study has been initiated to evaluate the geochemical stability of potential shaft and borehole sealing materials in the felsic volcanic-tuff environment of Yucca Mountain. The investigation deals with the chemical compatibility of potential sealing materials and felsic tuff.

The term "sorption" has generally been used to describe processes by which elements are removed from solution by rock, such as ion-exchange phenomena, chemisorption, and diffusion into the rock matrix. Precipitation or coprecipitation can also occur and remove elements. Los Alamos has used batch and

several types of column techniques in the laboratory to provide information on sorption processes, speciation, kinetics, diffusion, and surface effects. Sorption data have been obtained for samples from drill holes J-13, UE25a-1, and USW-G1 under different conditions (contact time, temperature, atmosphere, and particle size). Detailed data are given in the body and appendixes of this report.

The variation in the abundance of clinoptilolite, as well as that of other minerals in tuff, is related to the mode of emplacement and to alteration processes during cooling and by interaction with groundwater. Strontium, cesium, and barium are thought to sorb mainly by ion-exchange reactions. Their lowest sorption ratios or R_d values (defined in the introduction) are associated with devitrified tuffs, which are generally welded to some degree and contain principally quartz, cristobalite, and alkali feldspar (plus some clays). The maximum sorption ratios correspond to nonwelded tuffs that contain the zeolite clinoptilolite. The variations of sorption of cerium, europium, plutonium, and americium with stratigraphy are not as regular as those for strontium, cesium, and barium. The chemistry of these elements is more complex in the near-neutral groundwater. The sorption ratios for plutonium cover a fairly narrow range, independent of sample location or mineralogy. In comparing americium's sorption ratios with its mineralogy, there is a rough correlation of high sorption with samples containing clinoptilolite or smectite and a correlation of low sorption with samples containing devitrification minerals. Although sorption of technetium, uranium, and neptunium has not been measured for many samples, the sorption ratios are relatively low; correlations with stratigraphic position cannot be made from the available data.

Sorption ratios for each element have been plotted as a function of clinoptilolite abundance for all the samples studied. The samples containing no clinoptilolite have significantly lower sorption ratios than those containing more than a few per cent of the zeolite. If the abundance of this zeolite is the only factor influencing sorption ratios, with no differences in sorptive properties caused by the exact composition of the clinoptilolite (or heulandite), then there should be a linear relationship between the distribution coefficient K_d and clinoptilolite abundance. Least squares fits to our data points, for which the abundance of clinoptilolite is $\geq$10%, give sorption ratios of 6.9×10^4 and 4.3×10^4 mℓ/g for 100% of the pure minerals. These values are compared with those calculated using simplifying assumptions from available thermodynamic

data for different mineral samples of 1.8×10^5 and 3.8×10^4 mℓ/g for strontium and cesium, respectively.

Sorption ratios for technetium, cerium, europium, and americium show no obvious correlations or trends with abundance of the zeolite clinoptilolite. Sorption ratios of samples with no clinoptilolite scatter among those for samples with the zeolite. Sorption ratios for neptunium, uranium, and plutonium are higher for the zeolitized tuffs than for the nonzeolitized ones, although there are no trends with degree of zeolitization. There is an absence of any obvious trend for cesium sorption when considering smectite alone in nonzeolitized samples. Possible explanations are that trace quantities of clinoptilolite, not detected by x-ray diffraction, may mask any influence of smectites; that other minerals such as illite also contribute to sorption; and that sorption on clays involves other factors such as their texture or their availability to the groundwater. Sorption ratios for samples containing the zeolite analcime are not as large as those ratios expected for samples containing clinoptilolite, an effect related to the structures of the zeolites.

A model based on a sorptive mineral content (SMC) concept has been shown to agree well with experimental values for sorption of cesium on a variety of tuffs. Because tuff may be composed of more than one sorbing mineral, the SMC concept is used to predict sorption by combining the effects of several minerals. The combined effect is defined as a weighted sum $SMC = \Sigma W_i X_i$, where W_i is the weighting factor for each mineral phase relative to that of clinoptilolite and X_i is the abundance (%) of each phase. The weighting factors are relative to clinoptilolite, and they are calculated from published thermodynamic data, using some simplifying assumptions. Clinoptilolite, mortmorillonite, mordenite, analcime, and glass were considered. For cesium, sorption ratios plotted as a function of SMC normally follow the same trend as if clinoptilolite were the only sorbing mineral in a sample. The SMC concept will be extended to other elements.

In general, R_d values from desorption experiments are slightly higher than those from sorption experiments. The results for strontium and cesium from the two methods agree within ~20% for most measurements. For barium there is reasonable agreement when sorption ratios are low (devitrified tuffs). For some of the zeolitized tuffs, values for barium from desorption experiments are greater than those from sorption experiments by factors of ~2 for most samples but are as great as ~10 for a few. It appears that barium sorbs on

clinoptilolite somewhat more irreversibly than do strontium and cesium. For cerium, europium, and americium, the differences in sorption ratios (which are reasonably high) obtained by the sorption and desorption methods are greater. A large fraction of these elements are sorbed irreversibly, although in most cases the trends from the sorption measurements with stratigraphic position are qualitatively retained in the desorption results. The differences for plutonium, which do not show discernible trends, are also approximately a factor of 10. It should be noted that sorption ratios for technetium, uranium, and neptunium, which are low, are nevertheless significantly greater for desorption than for sorption. Sorption ratios for plutonium cover a fairly narrow range (less than a factor of 10), independent of sample location or mineralogy. Based on the limited data available, neptunium exhibits similar behavior with a range of less than a factor of 5, although the R_d values are about an order of magnitude less than those for plutonium. Americium sorption ratios show a much wider variation, from just over 100 mℓ/g to nearly 30 000 mℓ/g, but again with essentially no correlation to mineralogy. Sorption ratios for technetium and uranium are low; correlations with stratigraphic position or mineralogy cannot be made from the limited data available.

Results from three batch sorption experiments performed at 70°C have been compared with those performed at room temperature. Values are similar, with those for 70° being generally higher by factors up to 5 than those for room temperature.

The presence of very fine particles (<38 μm) in rock fractions of larger particle size apparently can change the observed sorption ratio of an element by a factor of 2 to 5, especially for devitrified tuffs. It is, therefore, advisable that larger size fractions be wet-sieved to avoid the presence of fine particles, which may increase the observed sorption in an irreproducible manner. The removal of small particles may result in measurements being made on material that is not completely representative of the tuff; however, the observed results are useful for comparison purposes and are probably not far from the "true" values. Any errors should be in the conservative direction, that is, too low R_d values for samples that do not contain very fine particles.

Because reducing conditions are expected for some groundwater/rock systems, it may be anticipated that the sorptive behavior of some elements in such systems will be different from that under normal atmospheric conditions. These effects were investigated by comparing the results of batch studies

performed in a nitrogen atmosphere (<0.2 ppm oxygen and <20 ppm carbon dioxide) with similar measurements made under normal atmospheric conditions on the same geologic materials. Depending upon the element, sorption was observed to be lower, higher, or unchanged for different elements in the nonoxidizing atmosphere. Technetium, in particular, showed the effects of the atmosphere, giving R_d values in the nitrogen atmosphere greater than 10 times those in air.

The circulating system used at Los Alamos for sorption measurements incorporates features of both batch and column methodologies. The batch and circulating-system procedures are similar in some ways, but the solid phase remains stationary in the circulating system and is not subject to the possible self-grinding of the batch measurements. The presence of smaller particles could result in greater sorption as a result of greater surface area or differences in mineralogy. In most cases, the results from the two methods fall within the spread of individual experimental values. Devitritied tuffs tend to give slightly higher sorption ratios by the batch method than by the circulating-system method. The observed difference could well be the result of the presence of smaller particles in the batch measurements.

The study of sorption isotherms is important for several reasons; it will be used to (a) determine the influence of groundwater/tuff interactions on the sorptive properties of tuff, (b) accurately model the retardation of waste elements under various source-term and groundwater conditions, (c) detect irreversible sorption processes, which would be a potentially highly positive property if present in tuff, (d) correctly interpret and model diffusion into the tuff matrix as would occur in fracture flow, and (e) explain the observed dependence of the sorption ratio (distribution coefficient) on the solution-to-solid ratio. The Langmuir and Freundlich isotherms have been used for these applications as well as to determine a relationship from mass-action equilibrium. Experimental fits to the Freundlich isotherms for strontium, cesium, barium, cerium, and europium generally indicate nonlinear behavior for nonzeolitized, welded tuffs and linear behavior for zeolitized tuffs. For plutonium, there appears to be little correlation between sorption ratio and the element concentration; the sorption isotherm for the zeolitized tuff is linear, whereas that of the devitrified tuff deviates. The effects of nonlinear isotherms on sorption phenomena have also been studied, and equations and computer programs to solve the diffusion equations with nonlinear isotherms have been developed.

Some simple relations have been derived that can explain the dependence of K_d on the solution-to-solid ratio. Experimental results in which the solution-to-solid ratio was varied can be directly compared with the results of measurements in which the element concentration was varied (isotherm determinations). These relationships are important because of the difference in solution-to-solid ratios between laboratory batch determinations and real situations.

Laboratory measurement of permeability and storage capacity has been accomplished by a transient pressure pulse method. Porosity has been obtained by measuring the wet and dry weights of the samples, by grain density measurements, and by mercury porosimetry. These measurements are basic to understanding the transport of waste elements in groundwater through tuff. Data for both permeability and storage capacity are necessary for comparison with field tests and to predict flow through unfractured tuff in response to a pressure gradient; this gradient might be the regional hydrologic gradient or the result of heating by the repository. Porosity is a necessary parameter in calculating the effects of diffusion. The combined results for permeability, storage capacity, and porosity can be used to gain insight into the pore structure of the tuff. This understanding of pore structure is important to the understanding of diffusion because it will help estimate constrictivity and tortuosity parameters. The permeability of tuff is quite low and contrasts with the relatively high porosity (7 to 40%) of the samples tested. Porosity clearly does not determine permeability because there is no correlation between the two. Mercury porosimetry indicates the permeability is more closely related to pore size. In tuffs, low permeabilities are probably caused by small connections between larger pores, which suggests that the constrictivity of tuff may be relatively large. Permeability shows only a slight variation with effective confining pressure. The storage capacity and porosity values taken together indicate that the pore compressibility of tuff is quite small, and as a consequence the porosity of tuff also varies little with effective confining pressure. Because the permeability does not show a marked decrease with increasing effective confining pressure, it seems likely that the stiffness of the pores indicated by the pore compressibility applies to the small connections as well as to the larger pores that make up most of the porosity. Therefore, studies of the pore structure of tuff made on unpressurized samples should apply well to the rock at depth. Permeability measurements on tuff samples before and after heating wet at 120°C for 5.5 months show no significant change in permeability in samples composed predominantly of zeolites. However,

some increase in permeability was observed in samples with quartz, cristobalite, and potassium feldspar as predominant phases.

Diffusion into the rock matrix is an important mechanism for retarding the transport of radionuclides through fractures in tuff. It is of particular importance for nonsorbing soluble species. The diffusion coefficient for a given radionuclide in tuff matrix depends on properties that are intrinsic to the chemical species, such as ionic mobility, and properties of the tuff, such as porosity, tortuosity, and R_d. It is, therefore, necessary to measure the diffusion coefficients of waste element species in various tuff units. An experimental program to accomplish this has been initiated using several techniques.

In general, the equations that have been used to describe fracture flow with matrix diffusion and simple diffusion into tuffaceous rock treated sorption as linear with concentration. This approach clearly has a serious deficiency because sorption on nonzeolitized tuff has already been shown to be nonlinear. Isotherm measurements on tuff YM-22 show that sorption of simple cations of strontium, cesium, and barium gives a Freundlich isotherm exponent <1.0. A nonlinear isotherm complicates the equations for matrix diffusion by giving the diffusion coefficient a concentration dependence, rendering the differential equations nonlinear. A computer program, using the finite difference method, is being developed to apply some of the mechanisms to matrix diffusion. Eventually, the program will be incorporated into a transport model so that a more realistic model can be developed.

Experiments specifically designed to examine transport in a single fracture provide information about the effectiveness of diffusion in retarding radionuclides and the effectiveness of sorption processes in rapidly flowing systems such as occur in a single fracture. The results of these experiments have been compared with transport model predictions to validate or demonstrate deficiencies in the models. The shape of the elution curve calculated for fracture flow in tuffs is not in agreement with the observed elution. The activity desorbs more slowly than would be expected for reversible, diffusion-controlled sorption. This observation is also consistent with previous measurements of sorption on tuff. In general, the R_d values determined by desorbing activity from tuff are considerably larger than those determined from the sorption process. The lack of agreement between the experimental and theoretical elution curves suggests a more complex sorption mechanism than simple linear sorption; sorption and matrix diffusion in tuff (especially welded tuff) appear to be more complex than expected.

Important conclusions resulting from laboratory fracture-flow studies are that (1) matrix diffusion is an important mechanism contributing to the retardation of radionuclides in fracture flow; however, simple analytic models do not appear to be adequate to predict accurately the transport of waste elements in tuff fractures; (2) the high porosity of tuff makes matrix diffusion much more effective in retarding the movement of soluble species than does the low porosity of crystalline rock such as granite; and (3) undisplaced, induced Bullfrog- and Tram-Member tuff fractures subjected to a simulated lithostatic stress of 3000 psi sealed to cause a fracture permeability comparable to that of the undisturbed matrix.

Experiments examining the transport of radionuclides through porous media have been conducted in an effort to determine the radionuclide retardation that will be provided by geochemical processes along flow paths. These experiments, using both crushed-tuff and solid-tuff columns, provide intermediate steps in the laboratory-to-field link. Chromatographic columns packed with crushed rock have been used for most of the studies. The following radionucides have been used: ^{131}I, ^{85}Sr, ^{137}Cs, ^{133}Ba, ^{141}Ce, ^{152}Eu, $^{95}Tc^{m}$, and ^{3}H. Some of the columns have been run at two flow rates. The crushed-rock columns have begun to provide information on dynamic effects in radionuclide transport through porous media. In addition to the crushed-rock columns, some solid-core columns have been run and more solid-core column experiments are being run. These columns are providing data to establish whether minerals are made available by crushing that are not naturally available and also to examine dynamic effects. General conclusions from these studies are as follows. (1) The sorption ratios determined by using column methods agree with those determined by the batch techniques within a factor of 10. Recent studies indicate that much of the previously reported disparity between batch and column results may be caused by particle fractionation. When the same particle-size distributions are used, the results are in reasonable agreement. (2) At water velocities comparable to regional flow velocities ($\sim 10^{-5}$ cm/second), the shapes of peak elutions for some simple ions are comparable to what would be expected from diffusional broadening alone. This may indicate that at these velocities, kinetics is not an important factor. (3) The anion exclusion effect may have been observed in a highly zeolitized tuff. (4) Plutonium particulate matter was filtered out by flow through a solid-core column.

Kinetic sorption experiments (sorption as a function of time) have been performed on thin tablets of tuff. The uptake of activity has been measured

as a function of time for a number of elements on several tuffs. These data should fit the solution for diffusion into a plane sheet if one ignores any edge effect. When the analytic solution to a one-dimensional plane sheet is applied to the data, a good fit cannot be achieved. This is typical of the nonsteady state diffusion experiments that have been performed with tuff samples.

Some new fluorobenzoate tracers, with very low detection limits, have been developed to use in field experiments. The diffusion coefficients of these tracers have been measured so that their usefulness as diffusing tracers in characterizing fracture-flow systems can be evaluated. The ionic diffusion coefficients are generally close to 8.0×10^{-6} cm^2/second. This is considerably lower than the diffusivity of tritiated water (2.4×10^{-5} cm^2/second) and has potential application to field experiments.

The study of natural analogues to waste repository environments can give important information on long-term chemical reaction and transport. Such analogues can be used to extrapolate experimental data from laboratory time, days and months, to "geologic time," the hundreds to hundreds of thousands of years that may be required for isolation of waste in a repository. A potentially important source of information on the long-term behavior of Yucca Mountain tuffs in a hydrothermal gradient is the study of hot-spring environments in felsic tuffs in Nevada. The mineral alteration in these localities can give information about (1) the response of the near-field repository environment to the thermal pulse that is expected after the initial emplacement of the waste and (2) the response to the normal geothermal gradient, the natural increase of temperature with depth. Another useful analog study may be the investigation of rock matrix diffusion of elements near ore bodies. Matrix diffusion has been proposed as a process that would retard the transport of elements in media in which the hydrology is dominated by fracture flow. Recent measurements of lead isotope abundance in a rock core from the Oklo uranium mines suggest that lead may have diffused into a crystalline rock matrix from a fracture that was an aqueous transport channel in past geologic times.

Field experiments are performed to collect radionuclide migration data under conditions that approximate those of a nuclear waste repository more closely than can be obtained in laboratory measurements. Data from field experiments will be used for two primary purposes: to verify the accuracy of

models used for repository performance assessment and to determine the extent to which laboratory measurements can be scaled to give results valid for field conditions.

The techniques used in field migration studies are of two types: one addresses aqueous flow and transport through a fracture, and the other addresses diffusion into the rock matrix from water but without aqueous flow. Three fracture-flow experiments performed by others have been reported in some detail; all are in granitic rock. A nuclide migration field experiment in tuff was begun, but geochemical and hydraulic conductivity measurements showed that a more suitable tuff and location than the one originally chosen must be selected for this work.

Geochemical and transport models have been developed and tested both in support of the nuclear waste management programs at Los Alamos and to contribute to development of an overall performance model. The efforts in geochemical modeling have concentrated on testing the available codes and improving the thermodynamic data base. Geochemical models can be used to predict the chemical species that should occur in a groundwater system and also the mineral solubility and solubility limits for the waste element species. These predictions influence the expected retardation of the waste elements. For instance, an anionic species would not be sorbed by zeolite minerals, whereas most cations are strongly sorbed. Currently the data base for these geochemical models is being updated to include thermodynamic data for the minerals composing Yucca Mountain tuff. The geochemical model EQ3 has been used to calculate uranium and plutonium solubilities in water from well J-13.

Several transport codes available at Los Alamos can be used to model a variety of problems, including multiphase flow, unsaturated flow, the inverse problem, fracture flow, and three-dimensional systems. Transport models are being updated to include appropriate sorption mechanisms and to account for the dependence of sorption on concentration, that is, nonlinear isotherms. These codes will provide a means of modeling field and laboratory experiments. In the near future it is hoped that some of these codes can be validated by designing and executing appropriate experiments in the laboratory and field. Code TRACR3D simulates transient air, water, and tracer flow in permeable media for a three-dimensional geometry. Tracer motion can occur in either the air phase or the liquid phase. Transport mechanisms include advection, molecular diffusion, mechanical dispersion, and capillary action. Several equili-

brium sorption models as well as nonequilibrium sorption model are included. Material properties such as permeability can vary spatially. The code also has the capability of simulating flow in a fracture system with transport into or out of a porous material surrounding the fractures. This code has been used to model a field experiment with a single fracture to predict the effect of partial saturation and to aid in the design of such experiments.

The second part of this report delineates the proposed experimental program that will be necessary to resolve those geochemistry issues of importance to the use of the Yucca Mountain area of the NTS as a nuclear waste repository site. For the most part, these studies will be natural extensions of those already in progress and described above, with the addition of some complementary experiments. In particular, Los Alamos has not been using isotopic techniques to obtain information about Yucca Mountain, and believes such techniques used by the US Geological Survey for Yucca Mountain investigations have been limited to ^{14}C and ^{18}O analyses. The information that can potentially be obtained from isotopic analyses includes (1) origins of the groundwaters and pore waters, (2) flow paths and mixing of aquifers, (3) age and age gradients of the water, (4) paleoclimate information, and (5) natural water/rock interactions and geothermometry.

Work is planned that will use cosmogenically produced ^{36}Cl (half-life 3×10^5 years) to measure the ages of old groundwaters and "bomb pulse" ^{36}Cl to measure the ages of old groundwaters and "bomb pulse" ^{36}Cl to measure recent rates of water movement in the unsaturated zone. Other nuclides being considered are ^{2}H, ^{3}H, ^{4}He, ^{13}C, ^{14}C, ^{18}O, ^{34}S, ^{39}Ar, ^{81}Kr, ^{129}I, and uranium and radium isotopes and their daughters.

Obviously, isotope techniques can yield useful information about how the natural system has behaved over recent and geologic time. Interpretation requires wise selection of the proper models.

Chapter 1:

INVESTIGATIONS OF THE GEOCHEMISTRY OF YUCCA MOUNTAIN AND ENVIRONS

I. INTRODUCTION

This report details the technical contributions of Los Alamos National Laboratory to the Nevada Nuclear Waste Storage Investigations (NNWSI) project since the time of its inception in FY 1977 (as the NTS Terminal Waste Storage project) until March of 1982. The NNWSI project is managed by the Nevada Operations Office of the Department of Energy. Efforts have been devoted primarily to resolving geochemistry issues pertinent to siting a nuclear waste repository in tuff at the Nevada Test Site (NTS).

The Los Alamos National Laboratory studies of the sorptive behavior of tuff and transport of radionuclides through tuff have been partly generic in nature (to understand the sorptive behavior of tuff as a function of many variables) and partly site specific (to obtain data for a possible repository site in tuff). It is necessary to have an understanding of the mechanisms of radionuclide transport and retardation in tuff, as well as to have a data base of sorptive behavior, to perform the required safety assessment dealing with possible releases from a repository in tuff. Previous reports in this series are Refs. 1, 2, and 3.

When the work was initiated, the only appropriate tuff samples for this study were from drill hole (later well) J-13 (Ref. 4) in western Jackass Flats at the NTS. When the NNWSI identified Yucca Mountain as a possible repository location and undertook an exploratory drilling program, samples from additional drill holes became available.

Tuffaceous groundwater used in these studies has been obtained from well J-13 in Jackass Flats except for studies of the Yucca Mountain groundwaters themselves. To better simulate water in contact with the rocks under investigation, the water from well J-13 is pretreated with the particular rock of interest. Analyses of the water before and after such treatment have indicated only minor changes in composition.

Perhaps a more critical problem is simulation of the redox conditions that exist in the actual rock/groundwater systems. If the underground conditions are reducing, as is postulated for many deep geologic systems, then the sorptive behavior of elements such as technetium, uranium, neptunium, and plutonium will be different from that under the normal, mildly oxidizing conditions in air. In their lower oxidation states, these elements are generally more insoluble or sorb better on geologic media and, consequently, should be retarded more than in the higher states. However, at the present time, there is no

definitive description of the actual redox conditions in the tuff formations under investigation or of conditions that might be in possible release scenarios. Preliminary observations of the alteration features of the mafic minerals in zones of the bedded tuff of Calico Hills and Prow Pass Member of the Crater Flat Tuff suggest possible oxidizing conditions, at least at the time when alteration was occurring. Observations of the dissolved oxygen content of water pumped from the J-13 well and drill holes at Yucca Mountain also suggest oxidizing conditions; however, results from the analysis of groundwaters from hydrology wells at Yucca Mountain indicate that deeper waters may be oxygen deficient when compared to water at the standing water level. Independent work by the US Geological Survey (USGS) has shown that there are significant concentrations of dissolved oxygen in water from tuffaceous wells (J-12 and J-13), as well as in some other deep water.[5] However, contact of crushed tuff with groundwater under a controlled atmosphere (≦0.2 ppm oxygen, ≦20 ppm carbon dioxide) gave apparently negative Eh values.[3] The crushing may have exposed previously unexposed minerals. Investigations have been conducted under both atmospheric and near-oxygen-free conditions and there are plans to do experiments under controlled Eh conditions.

Buffers are being developed to control the oxidation potential during laboratory experiments. Formation and transport of particles containing actinides (and presumably other radionuclides) have been found to be important in waste element mobility. Because Pu(4+) polymer may be mobile, its behavior and rate of formation are being studied. Waste element sorption has been found to correlate with stratigraphy and mineralogy. The capability has been developed to predict retardation properties, based on thermodynamics and the sorptive mineral content. A strategy for identifying and obtaining geochemical thermodynamic data was developed and implemented. Matrix diffusion and hydraulic properties were found to correlate with pore structure. Predictions of diffusion of nonsorbing tracers agree with experiments, but problems have been encountered in predicting the behavior of sorbing elements, presumably because of slow kinetics and nonequilibrium. A field test program has been defined and will be used to validate geochemical transport models.

The sorption ratio, designated by R_d, is used as a measure of sorption as a function of many parameters. It is defined as

$$R_d = \frac{\text{activity in solid phase per unit mass of solid}}{\text{activity in solution per unit volume of solution}}$$

Many authors refer to this ratio as the distribution coefficient K_d. Los Alamos prefers not to use this term, which implies equilibrium, knowing that reversible equilibrium is usually not attained. If equilibrium is attained, then K_d is related to a retardation factor, R_f, in a uniform flowing system by

$$R_f = K_d\ (\rho/\varepsilon) + 1 \quad ,$$

where ρ is the bulk density and ε is the porosity.

A detailed listing of the measured sorption ratios is given in App. A. The origin of the tuff samples studied and their mineralogic composition have been discussed in an earlier report[6] or are given in this report. Petrographic descriptions of tuff thin sections are given in App. B. The prefix JA- indicates the sample was obtained from hole J-13; the prefix YM- from hole UE25a-1. The prefix G# indicates the sample was obtained from drill hole USW-G#; the four numbers following the prefix give the depth in feet from which the sample was obtained.

These investigations were performed under the Los Alamos quality assurance program for the NNWSI, which is designed to ensure that the data and interpretive reports produced are consistent with formally specified procedures and reviews.

Responsibility for the planning and implementation of the Los Alamos quality assurance program rests with the Materials Science and Technology Division (MST) quality assurance organization. Reference 7 contains a complete account of the Los Alamos NNWSI quality assurance program, including the Quality Assurance Program Plan and the detailed procedures developed for the project.

The quality assurance program developed for the NNWSI at Los Alamos is outlined in the Quality Assurance Program Plan (QAPP), which is updated to meet changing requirements. It is structured to meet the requirements of 10-CFR-50, App. B,[8] as applied to the evaluation of major geologic formations with regard to their suitability as locations of permanent repositories for high-level radioactive wastes. The Los Alamos Quality Assurance Manual[9] (now being revised) is used as a primary compliance document. The procedures described therein are applicable unless otherwise stated in the QAPP or specific procedure documents issued for the NNWSI.

Work Plans are the primary planning documents covering the Los Alamos technical activities for the NNWSI. These Work Plans are written to provide

an adequate description of the scope and purpose of the task. They include, directly or by reference, the quality assurance requirements with regard to data validity and documentation. Review boards are used for the quality assurance program acceptance of the Work Plans, as well as for review and acceptance of design and acceptance of final documents. The review board consists of, at a minimum, a management member, a quality assurance member, and an independent technical reviewer who is experienced and competent in the field under review but has no direct program responsibility.

In addition to the QAPP, quality assurance procedures specific to the Los Alamos effort in the NNWSI have been established for document control and procurement. These procedures supplement the guidelines in the Quality Assurance Manual; they are given in full in Ref. 7. Detailed quality assurance procedures have also been prepared for most of the technical areas of the project, including all facets of obtaining, handling, and shipping geologic samples; mineralogical and petrological tests; geophysical and geochemical measurements; and radionuclide interactions with geologic materials in both laboratory and in situ experiments. Revisions of these technical procedures are prepared as necessary as more experience is gained or better techniques are developed. Reference 7 contains the current versions of these quality assurance procedures. A one-time research effort may be documented in a Los Alamos notebook with, as a minimum, technical approval at defined intervals.

Periodic surveillance in accordance with pre-established check lists is used to maintain quality assurance standards in technical efforts. Measuring and testing equipment that require calibration is controlled in accordance with the applicable sections of the Quality Assurance Manual. Corrective action for significant conditions adverse to quality is provided in accordance with Sec. QMR 12 of the manual. Compilance with the quality assurance program is verified by periodic audits that are planned, documented, and carried out in accordance with Sec. QMR 15 of the Quality Assurance Manual.

II. GROUNDWATER GEOCHEMISTRY

A. Groundwater Chemistry

1. Reference Groundwater for Laboratory Experiments. In a laboratory sorption experiment that duplicates field conditions for a specific location, one problem is the selection of the reference composition of the groundwater. Ideally, water from individual tuff layers in Yucca Mountain would be used, but at this time there is no producing well at Yucca Mountain and no way of obtaining formation water from particular tuff layers. Therefore, the water from well J-13, the nearest producing well, was chosen as reference water, and it has been used for several years in all sorption experiments. At the end of 1980, this reference-water composition was as shown in Table I, based on multiple analyses of well J-13 water by the USGS. Because the composition of the water directly from the well may change slightly over time depending on well usage, a standard composition for well J-13 water composition was established.

TABLE I

REFERENCE GROUNDWATER COMPOSITION FOR TUFF FILTERED THROUGH 0.45-μm MILLIPORE FILTER

Emission Spectroscopy	Concentration (mg/ℓ)
Magnesium	2.1
Silicon	31
Iron	0.04
Strontium	0.05
Barium	0.003
Calcium	14
Lithium	0.05
Potassium	4.9
Aluminum	0.03
Sodium	51
Anion Chromatography	
Fluoride	2.2
Chloride	7.5
Phosphate	0.12
Nitrate	5.6
Sulfate	22
Carbonate	0.0
Bicarbonate	120
Other Conditions	
pH - slightly basic (7.1)	

Examples of well J-13 water composition now and the extent of change during specific time periods are shown in Table II. The first six analyses are of water collected in plastic-lined barrels in June 1981 over several hours. The last analysis is of water collected in January 1982. Before analysis the waters were filtered through 0.05-μm Nuclepore membranes and then acidified with ultrapure HNO_3 for cation analysis. This table shows that with time there are minor variations in composition beyond the standard deviation and limits of detection of the elements; however, these variations are minor when compared to other variables in experiments in which the water is used.

The techniques to determine the cation and anion concentrations listed in the tables of this section are state-of-the-art techniques. Cations are analyzed on acid-stabilized solutions with a Spectrometrics, Inc., 20-channel, direct-current, plasma-source, emission spectrometer. Analyses for anion concentrations are performed on a Dionex Ion Chromatograph; alkalinity and pH are measured on a Brinkmann Metrohm Dosimat and Titroprocessor.

The analytical techniques for NO_2^- and NO_3^-, arsenic at <0.1 mg/ℓ, and Fe^{2+} at <0.02 mg/ℓ need further development. These analyses are especially important because the ions may be the major oxidizing-reducing species in Yucca Mountain waters.

As pumped from the well, J-13 water contains ~5.5 ppm oxygen and exhibits a pH of ~7.1. As the water stands, the pH slowly increases--presumably the result of a loss of CO_2 from the water.

2. Water for Sorption Experiments. In preparation for experiments to determine the sorption of waste elements on tuff, well J-13 reference groundwater was precontacted with tuff from individual strata of Yucca Mountain and then was filtered through 0.05-μm Nuclepore membranes. The three parts of Table III illustrate changes in the composition of well J-13 water that occur when it is contacted with tuff for ~3 weeks. The sample number in the table reflects the depth in feet in the drill hole from which the sample was taken (for example, sample G1-1854 was taken from well USW-G1 at 1854-ft depth) and the sample sequence number in the J-13 drill hole (JA-18).

The tuff sample JA-18 water results are derived from contacting well J-13 water with tuff from the lower Topapah Spring Member, which was sampled during the drilling of the J-13 well and is from the approximate region of main water production in the well. It was expected that this tuff would be already in equilibrium with the water, but, as shown in Table III, the magnesium concen-

TABLE II
COMPOSITION OF WELL J-13 GROUNDWATER

Date-ID	Concentration (mg/ℓ) Mg	Mn	Si	Fe	Sr	Ba	V	Ti	Ca	Li	K	Al	Na
6/81-51	1.76	0.012	31.8	0.011	0.039	0.001	0.021	0.028	11.5	0.060	5.26	0.025	45.1
52	0.74	0.009	29.9	0.063	0.040	0.002	0.018	0.014	11.6	0.076	5.36	0.028	46.1
53	1.71	0.022	29.4	0.060	0.039	0.002	0.036	0.030	11.4	0.064	5.25	0.028	44.5
54	1.71	0.007	29.5	0.017	0.040	0.003	0.038	0.028	11.4	0.074	5.33	0.026	45.2
55	1.73	0.012	29.6	0.042	0.041	0.002	0.039	0.038	11.5	0.076	5.65	0.023	45.5
56	1.72	0.001	29.8	0.069	0.041	0.004	0.042	0.044	11.6	0.069	5.99	0.026	44.7
1/82-1	2.15	0.014	37.6	0.039	0.045	0.004	0.013	<0.001	14.2	0.059	4.96	0.040	50.2
Limits of Detection	0.001	0.001	0.05	0.007	0.0001	0.0001	0.0001	0.0001	0.0001	0.0001	0.05	0.0001	0.1
Typical Standard Deviation of Instrumental Analysis	0.016	0.001	0.42	0.007	0.005	0.005	0.001	0.005	0.13	0.005	0.09	0.005	0.9

Date-ID	F^-	Cl^-	PO_4^{3-}	NO_3^-	SO_4^{2-}	Alk	pH
6/81-51	2.1[a]	6.4[a]	0.1[a]	10.1[a]	18.1[a]	2.339[b]	6.9
1/82-1	1.8	6.3	<0.1	9.1	18.3	2.089	8.3
Typical Standard Deviation	0.1	0.4	0.01	0.4	0.1	0.04	

[a] mg/ℓ.

[b] Alkalinity in meq/ℓ.

TABLE III

COMPOSITION OF WELL J-13 GROUNDWATER

AFTER CONTACT WITH USW-G1 AND J-13 TUFFS

	Concentration (mg/ℓ)												
	Mg	Mn	Si	Fe	Sr	Ba	V	Ti	Ca	Li	K	Al	Na
Original groundwater[a]													
	2.17 (0.22)	0.16 (0.02)	30.7 (2.3)	0.001 (0.020)	0.09 (0.06)	0.021 (0.014)	0.023 (0.016)	0.000 (0.013)	12.2 (1.2)	0.16 (0.16)	6.8 (2.0)	0.003 (0.011)	51.7 (3.5)
Tuff filtered through 0.45-μm membrane													
G1-1854	0.016	0.008	31.8	0.027	0.000	0.001	0.017	0.009	0.082	0.080	1.89	0.125	80.7
G1-2333	1.51	0.009	28.6	0.101	0.042	0.013	0.050	0.019	10.3	0.123	4.88	0.056	57.9
G1-2410	0.981	0.012	29.4	0.045	0.038	0.005	0.017	0.010	9.34	0.085	4.68	0.025	64.3
G1-2476	1.35	0.013	29.7	0.033	0.034	0.000	0.010	0.004	9.50	0.093	6.00	0.016	68.9
G1-2840	1.75	0.009	32.0	0.027	0.043	0.005	0.011	0.003	12.1	0.086	5.73	0.033	61.2
G1-2854	1.80	0.011	32.2	0.053	0.043	0.014	0.018	0.009	11.4	0.099	6.47	0.156	64.9
Tuff filtered through 0.05-μm membrane													
G1-2289	0.121	0.004	32.3	<0.007	0.001	0.006	0.007	<0.0001	0.414	0.048	1.29	0.008	75.5
G1-2363	1.04	0.008	31.0	<0.007	0.036	0.034	0.007	<0.0001	10.3	0.058	4.81	0.011	53.5
G1-2476	1.03	0.050	26.6	<0.007	0.040	0.149	0.002	<0.0001	10.4	0.066	8.71	0.009	67.3
G1-2539	0.848	0.012	25.5	0.0316	0.012	<0.0001	0.011	<0.0001	4.66	0.067	10.1	0.062	69.7
G1-2840	1.66	0.009	33.2	<0.007	0.037	0.002	0.010	0.001	11.9	0.057	5.07	0.010	48.3
JA-18	0.949	0.007	33.4	0.004	0.002	0.001	0.011	<0.005	11.0	0.054	6.4	0.015	54.1

[a]Well J-13 water; no contact with solid. Mean of seven measurements made over preceding 6-month period. Value in parentheses is the standard deviation of the mean for the well J-13 water.

tration of the water does change on further equilibration. No conclusive explanation can be given at this time; the carbon dioxide content of the water in the laboratory is probably less than at depth, the temperature is lower in the laboratory by 4°C, and the groundwater may actually not be in equilibrium with the tuff.

Table III also illustrates changes observed in well J-13 water that is contacted with tuffs from various depths of the USW-G1 drill hole. The main differences are a decrease in sodium content and an increase in the magnesium content of the water with depth in the drill hole. There is also a difference in waters filtered through 0.05-μm Nuclepore membranes rather than 0.45-μm Millipore filters. For example, the iron content is drastically reduced when filtered through the finer membrane. Because accurate iron contents may be very important for estimating the oxidation-reduction capabilities of solutions, the Los Alamos procedure recommends filtering all solutions through 0.05-μm Nuclepore membranes. With state-of-the-art equipment, filtration through membranes with smaller pores is too difficult and time consuming.

An additional example of the importance of filtration is given in Table IV. This well J-13 water was contacted with tuffs from the NTS G tunnel (outside the proposed repository site) and then was filtered in various ways. The tuff from the G-tunnel beds exhibited a much greater tendency to produce small particles and colloids than any of the tuffs studied in the NNWSI program.

3. Temperature Effects on Groundwater Composition. A major question to be answered by this study is whether or not a temperature increase such as that caused by the heat from the waste package will change the water composition enough to affect the transport of waste elements in the groundwater. In short-term experiments three tuffs from Yucca Mountain were contacted with groundwater at 152 ± 1°C to study possible reactions between the solid and solution phases.

Three tuff samples of different lithologies were used (Tables V and VI). Before contact with groundwater, the samples (~2 mm thick by 19 mm in diameter) were examined with a scanning electron microscope (SEM) to observe general surface features and mineral phases. The tuff wafers were then contacted with water from well J-13 in Teflon-lined Parr bombs. A Teflon screen separated the wafer and solution, and contact between the two was made by inverting the Parr bomb during the experiment. In future experiments the waters will be filtered at temperature before analysis because the increases in silicon and

TABLE IV

EFFECT OF FILTRATION ON APPARENT COMPOSITION OF WELL J-13 WATER[a]

Element	Concentration (mg/ℓ) 0.45 μm[b]	0.40 μm[c]	0.05 μm[c]
Mg	4.0	0.11	0.08
Mn	7.4	0.058	0.021
Si	219	28.3	27.1
Fe	82.0	1.5	0.6
Sr	0.045	0.000	0.001
Ba	9.0	0.05	0.12
V	0.17	0.005	0.008
Ti	14	0.09	0.00
Ca	5.4	0.70	0.56
Li	80	0.059	0.050
K	30	4.5	4.9
Al	39	0.7	0.009
Na	102.5	94.1	89.0

[a]Well J-13 water was contacted with matrix tuff for 3 weeks and centrifuged before successive filtrations.

[b]Millipore, HA membrane.

[c]Nuclepore, polycarbonate membrane.

TABLE V

TUFF SAMPLES FOR INITIAL ALTERATION STUDY

Sample	Unit	Rock Type
G1-1292	Topopah Spring	vitrophyre
G1-1436	Tuffaceous beds of Calico Hills	zeolitized nonwelded tuff
G1-2476	Bullfrog II	devitrified welded tuff

TABLE VI

MINERALOGY OF TEST SAMPLES USED IN ALTERATION STUDY

Sample	Glass (%)	Clay[a] (%)	Zeolite[b] (%)	Alkali Feldspar (%)	SiO_2[c] (%)
G1-1292	80-90	tr mnt	0	5-10	5-10 cr
G1-1436	0	tr i/m	65-85	5-10	10-20 qz
					2-5 cr
G1-2476	0	tr mnt	0	30-50	25-40 qz
		2-5 i/m			5-10 cr

[a] tr = trace; mnt = montmorillonite; i/m = illite/mica.

[b] clinoptilolite.

[c] cr = cristobalite; qz = quartz.

iron may be in the form of suspended colloids or polymers that will be filtered out of solution.

After a contact time of 3 weeks at elevated temperature, the bombs were reinverted to separate the phases and were allowed to cool. The tuff samples were again examined by SEM to determine if reaction had occurred. Sample G1-2476 containing cristobalite, alkali feldspar, and silica showed little reaction other than some rounding of surfaces and precipitation of clays. The vitrophyre, sample G1-1292, showed greatly increased amounts of clays or other fine-grained sheet silicates, which had formed on glass edges. Globules, analyzed as pure SiO_2, also were observed. An unusual surface fracture network developed (Fig. 1), and in some cases these fractures were filled with a phase of the same composition as that of the glass. Sample G1-1436 showed marked dissolution of clinoptilolite crystals, and the latest formed phases, mordenite and cristobalite, which were observed by SEM before reaction, apparently dissolved. The SEM photographs (Figs. 2 and 3) show sample G1-1436 before and after contact with well J-13 water. Figure 2 shows clumps of fresh cristobalite crystals over clinoptilolite before the experiment. After soaking at elevated temperature, the cristobalite is no longer present and the clinoptilolite is distinctly etched (Fig. 3).

In Table VII cation concentrations in the solutions after contact at 152°C are compared with cation concentrations in well J-13 water treated with

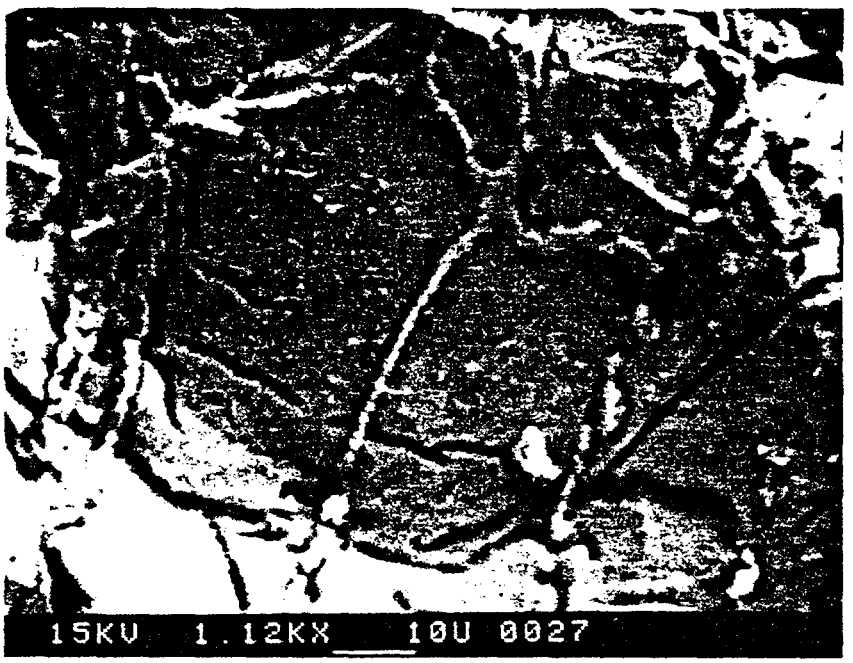

Fig. 1. SEM photograph of sample G1-1292 after contact with water from well J-13 at 152°C for 3 weeks.

Fig. 2. SEM photograph of sample G1-1436 before contact with well J-13 water.

Fig. 3. SEM photograph of sample G1-1436 after contact with well J-13 water.

the same tuffs at 22°C. Significant increases in the concentrations of silicon, iron, potassium, and sodium and decreases in the concentration of magnesium were observed after reaction of samples G1-2476 and G1-1292 at the higher temperature; these changes represent dissolution and precipitation, respectively.

4. Oxidation-Reduction Potential of Groundwater. The oxidation-reduction potentials (Eh) of groundwaters at Yucca Mountain cannot currently be measured without ambiguity because they do not contain sufficiently high concentrations ($>10^{-5}$ M) of oxidizable or reducible species. Therefore, oxygen and sulfide poisoning of the Eh electrode are very real problems.[10] If the water as sampled contains measurable oxygen of >0.1 ppm, redox potential measurements will be meaningless because the electrode is poisoned. A reading of ~350 mV at pH 7 will be obtained. In the presence of large amounts of sulfide, the electrode may also be poisoned so that measurements below -200 mV are probably in error.

Although most waters at the NTS do not contain measurable quantities of sulfide ions, the sulfide electrode can help estimate when the Eh electrode would be poisoned by oxygen. Theoretically, the Eh electrode and sulfide

TABLE VII

COMPOSITION OF WELL J-13 GROUNDWATER AFTER CONTACT WITH USW-G1 TUFFS AT 22° AND 152°C

	Concentration (mg/ℓ)					
	G1-2476		G1-1436		G1-1292	
Cation	22°C	152°C	22°C	152°C	22°C	152°C
Mg	1.35	0.042	0.009	0.015	1.79	0.006
Mn	0.013	0.044	0.020	0.022	0.010	0.018
Si	29.7	>60	30.8	>60	32.3	>60
Fe	0.033	0.120	0.064	0.285	0.020	0.063
Sr	0.034	0.013	0.000	0.019	0.090	0.011
Ba	0.000	0.000	0.002	0.000	0.000	0.000
V	0.010	0.000	0.019	0.000	0.000	0.021
Ti	0.004	1.02	0.000	0.549	1.72	0.000
Ca	9.50	0.657	0.176	0.031	13.1	0.534
Li	0.093	0.223	0.074	0.099	0.084	0.086
K	6.00	7.68	3.51	>10	5.02	>10
Al	0.016	0.418	0.042	0.000	0.000	3.26
Na	68.9	122 ± 4	78 ± 5	134 ± 6	57 ± 4	128 ± 2

electrode readings should be ~180 mV apart for the same solution, with the Eh electrode showing the more positive measurement.[11] For this reason the conditions where sulfide electrodes are usable have been investigated.

The sulfide-ion electrode contains a silver sulfide membrane. The voltage across this membrane is a function of the Ag^+ concentration and can be expressed in terms of the S^{2-} concentration by using the solubility product of Ag_2S. The potential of the electrode can then be expressed by the Nernst equation

$$E_{S^{2-}} = (E^{\circ}_{S^{2-}}) - \frac{RT}{2F} \ln(S^{2-}) \quad . \qquad (1)$$

A plot of measured $E_{S^{2-}}$ vs log (S^{2-}) should be a straight line of slope -29.58 mV for each decade change of concentration. Figure 4 shows the results for a

change in the sulfide-electrode potential as the S^{2-} concentration is varied in the range of 4×10^{-3} to 4×10^{-9} M. The four sets of experiments were either done at pH 8, or the measurements were corrected to pH 8. The lower limit of accurate detection of S^{2-} from this graph is $\sim 4 \times 10^{-5}$ M (±20%). However, the sulfide electrode is qualitatively useful to concentrations as low as 10^{-9} M.

Figure 5 shows the effect of ionic strength on the electrode potential of S^{2-} solutions. Sulfide solutions were prepared over the concentration range of 4×10^{-3} to 4×10^{-9} M and adjusted to pH 8 ± 1; then the S^{2-} potentials were measured. Sufficient KCl was added to each solution to make it 0.1 M in KCl, and the S^{2-} potentials of the solutions were again measured with the sulfide-ion electrode. From Fig. 5 it can be seen that at S^{2-} concentrations below 4×10^{-6} M, the ionic strength of the solution has a large effect.

Complexes of H^+ and S^{2-} form as the pH of a solution is increased. At pH 11 the major species in solution is S^{2-}, whereas at pH 7 and pH 4 the major species are HS^- and H_2S, respectively. Because the sulfide-ion electrode responds only to S^{2-}, all electrode manufacturers have recommended that the pH of a solution be adjusted to pH 11 before measurement. Boulègue[11] has shown that this is not necessary. The S^{2-} concentration and electrode potential can be calculated for any pH and total H_2S concentration and can be used to form calibration curves as $E_{S^{2-}}$ vs pH. Figure 6 also shows that the electrode-measured S^{2-} potentials agree quite well with the calculated values. Eight sets of experiments in which the S^{2-} concentration was 10^{-3} M are shown on the graph. Also included are calculated $E_{S^{2-}}$ vs pH lines.

The electrode manufacturers also recommend using an antioxidant such as ascorbic acid in the solution so that the S^{2-} will not oxidize. The reaction of S^{2-} with air is reasonably slow, and the antioxidant is not necessary if the measurements are carried out within a reasonable time (a few hours) after sampling (Fig. 6). At most, the measured potential increases by 20 mV when air is present in the solution.

A platinum Eh electrode can be used in a sulfide system to measure the potential of the half-cell $S^{2-} = S + 2e^-$. Using Eq. (1), $Eh = E^\circ - 0.0295 \log (S^{2-})$. When this equation is combined with that for the potential of a sulfide-ion electrode, $Eh = E_{S^{2-}} + (E^\circ - E^\circ_{S^{2-}})$. Boulègue and Michard[12] estimated from thermodynamic data that $(E^\circ - E^\circ_{S^{2-}})$ is 180 mV. Therefore, $Eh = (E_{S^{2-}}) + 180$ mV. This equation is plotted in Fig. 7 with measurements (shown as x and +) of Eh

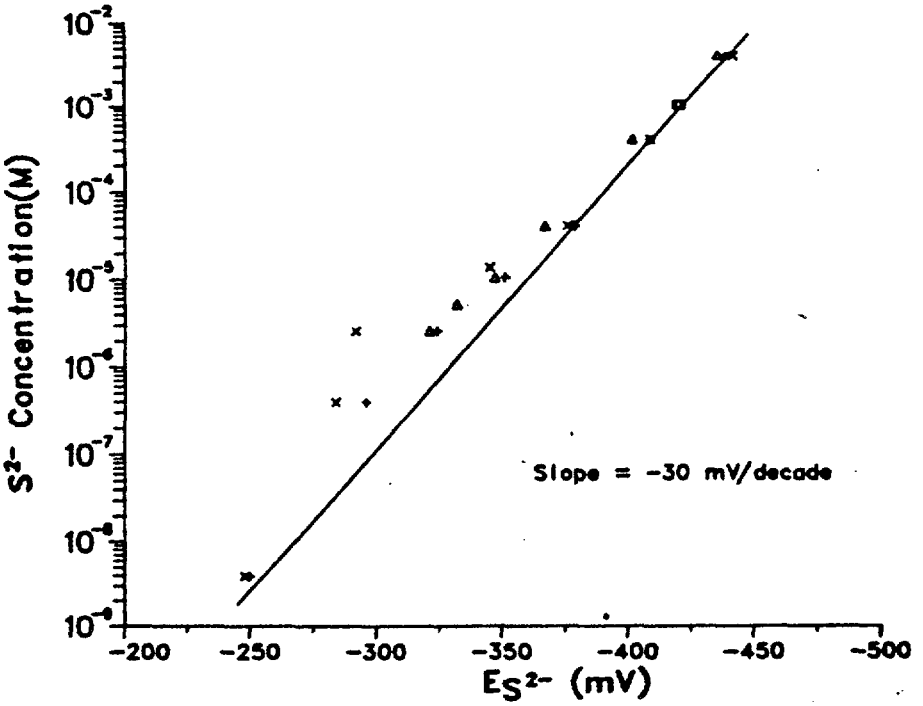

Fig. 4. Variation of sulfide-electrode potential with sulfide concentration.

and E_{S2-} carried out in the oxygen-free nitrogen atmosphere of a Vacuum-Atmosphere glove box. In an oxygen-free atmosphere the Eh-E_{S2-} relationship is very good.

In addition, Eh and E_{S2-} measurements were plotted for solutions of constant S^{2-} concentration but with different oxygen contents. The vertical lines (Fig. 7) connect experiments of equal pH and, supposedly, the same Eh and E_{S2-}. The uppermost measurements on each line represent solutions either in air or in a poor glove box that had air leaks. The middle points represent these same solutions after ascorbic acid was added to remove the oxygen in the solution. Three conclusions can be drawn from this figure: (1) the Eh electrode measurements are influenced by oxygen contamination, even in a sulfide environment; (2) the sulfide electrode is not affected to a large extent by the oxygen contamination; and (3) ascorbic acid either does not eliminate all the oxygen in a solution or does not clean the Eh electrode enough to give a reading that represents the absence of oxygen.

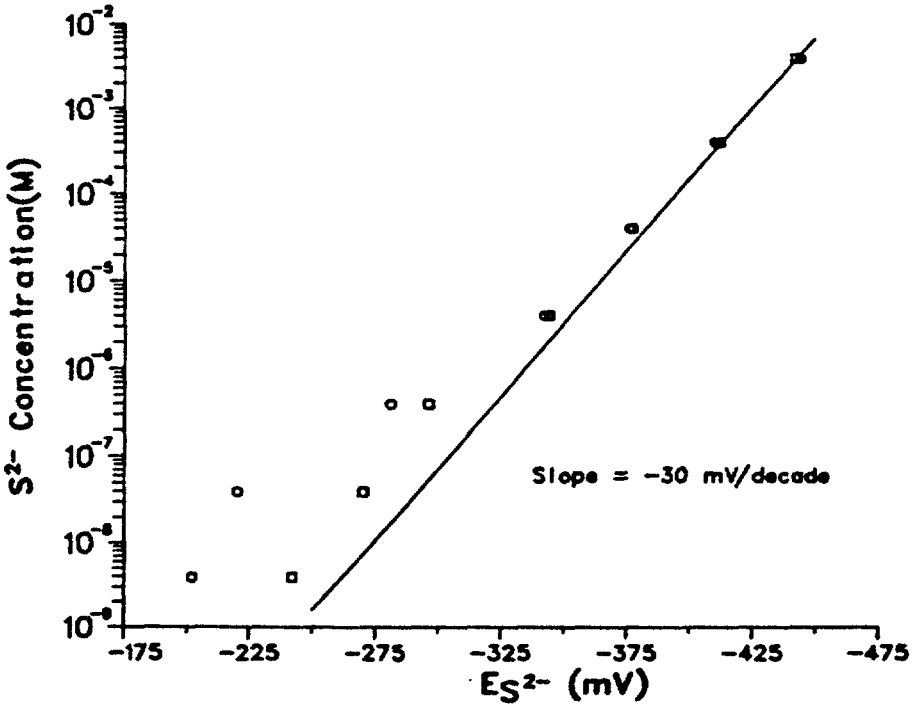

Fig. 5. Effect of ionic strength on sulfide-electrode potentials.

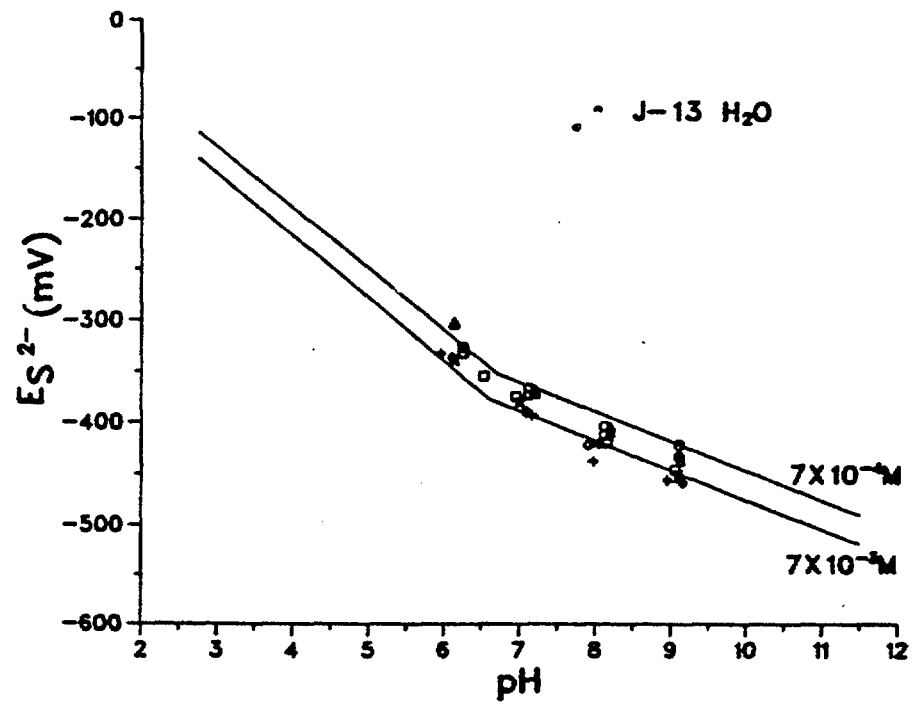

Fig. 6. Variation of sulfide-electrode potential with pH.

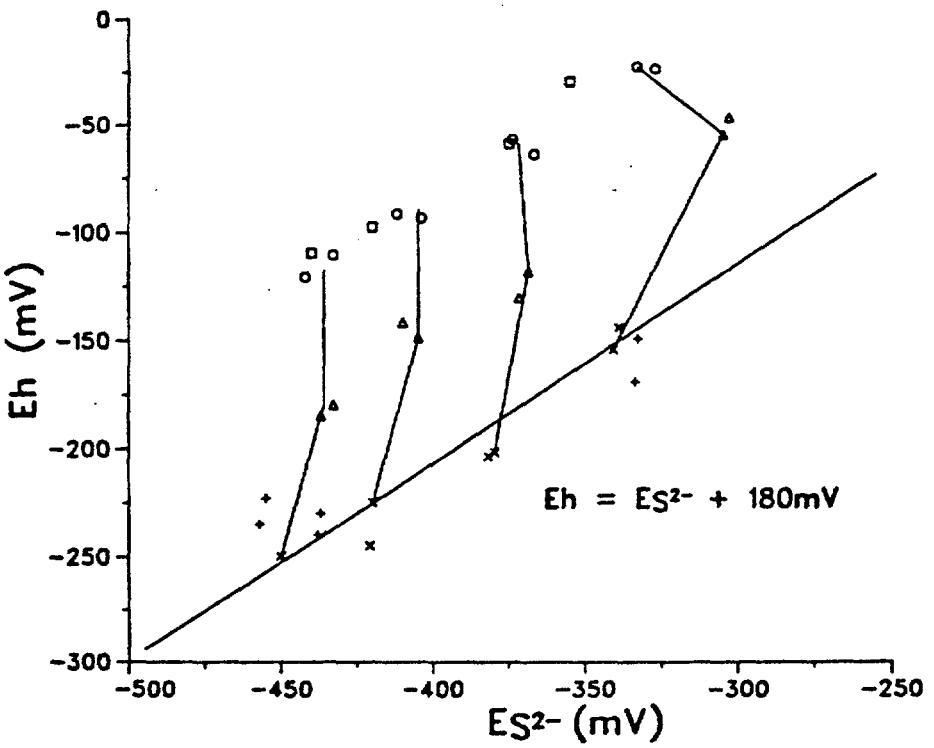

Fig. 7. Relationship of Eh and $E_{S^{2-}}$ for sulfide solutions with varying oxygen contents.

It would be interesting to pursue this study further to test whether the divergence of the Eh measurement from the Eh = ($E_{S^{2-}}$) + 180-mV relationship can be used as a measure of the oxygen content of the solution.

The Eh and $E_{S^{2-}}$ values were measured for well J-13 water inside the inert-atmosphere glove box. This water had been kept sealed in a container inside the glove box for most of the time since it was collected at the well-head. An Eh of +100 mV vs the H_2 electrode and an $E_{S^{2-}}$ of -100 mV were measured. The results agree quite well with the expression Eh = ($E_{S^{2-}}$) + 180 mV; however, the real significance of these measurements is still unclear because the S^{2-} concentration is below the limits of accurate detection (Figs. 4 and 6). Unfortunately, there are no known redox couples of sufficient concentration in well J-13 water to give a meaningful Eh measurement.

The Eh and sulfide electrodes have been tested on a producing well in which the dissolved iron concentration was known to be high enough, and therefore, the Eh reading is probably valid. An oxygen electrode was also included to measure any dissolved oxygen in the groundwater. Table VIII lists the chemical analysis and the electrode readings taken anaerobically on water from the Barmon-1 well at Chimayo, New Mexico.

It is possible to calculate from the chemical composition what could be expected for a measured Eh. Using a value of $K_{sp} = 10^{38}$ for the solubility product of $Fe(OH)_3$, pH = 7.2, standard $Fe^{2+} \rightarrow Fe^{3+} + e^-$ potential = 771 mV, and the measured Fe^{2+} concentration of 2.40 ± 0.02 mg/ℓ, an Eh between +25 and +100 mV can be calculated. Measurements of +75 mV were found in this case.

5. Composition of Yucca Mountain Groundwater. To determine or estimate the effect of the groundwater composition on the waste package, on the waste itself or its compounds, and on retardation mechanisms, it is necessary to determine the composition of the formation water in each particular stratum being considered for a repository or a transport path. The groundwater composition is also important in its effect on forming or dissolving the newly formed minerals brought about by the temperature gradient exerted on the repository by the waste package.

Wells in the vicinity of Yucca Mountain and Pahute Mesa have been sampled in various ways to determine the groundwater composition as a function of location. Wells 8, UE25b-1, and UE29a-2 were sampled while they were being pumped at a high rate. These samples were integral ones; the main contribution was made by the water from the permeable region (aquifer) nearest the pump intake. The water's Eh, pH, temperature, and oxygen were measured under anaerobic conditions for wells UE25b-1 and UE29a-2. Well USW-H1 was sampled under different conditions. Evacuated sample bottles were lowered by wire line to selected depths of the well. An electric valve on the bottle was opened to admit water, after which the valve was closed and the bottle was retrieved. These water samples were opened inside an inert-atmosphere glove box at Los Alamos, where Eh, sulfide and oxygen contents, and pH were measured before the samples were passed through 0.05-μm Nuclepore membranes and chemically analysized. Tables IX and X list the cation and anion compositions and electrode measurements for these samples. The nomenclature, or the sample number, for samples taken from well USW-H1 again indicates the depth from which the sample was taken.

TABLE VIII

COMPOSITION OF BARMON-1 WELL (NEW MEXICO) GROUNDWATER[a]

Concentration (mg/ℓ)												
Mg	Mn	Si	Fe	Sr	Ba	V	Ti	Ca	Li	K	Al	Na
10.5	0.29	5.9	3.1[b]	1.00	0.15	N.D.[c]	N.D.	69.7	0.12	5.5	0.08	7.7

Concentration (mg/ℓ)										
F^-	Cl^-	NO^-	PO_4^{3-}	NO_3^-	SO_4^{2-}	S^{2-}	O_2	Alk[d]	pH	Eh[e]
0.8	6.8	N.D.	N.D.	N.D.	12.0	0.032	<1.2	5.904	7.16	75

[a] Each sample was passed through 0.05-μm Nuclepore membrane.

[b] Fe^{2+} content is 2.4 mg/ℓ.

[c] N.D. = not detected.

[d] Alkalinity in meq/ℓ.

[e] mV vs a hydrogen electrode.

TABLE IX
CATION COMPOSITION OF GROUNDWATERS[a]

Well	Concentration (mg/ℓ)												
	Mg	Mn	Si	Fe	Sr	Ba	V	Ti	Ca	Li	K	Al	Na
8	1.377	0.005	25.6	0.009	0.007	<0.0001	0.003	<0.0001	8.2	0.045	4.13	0.035	36.5
UE25b-1													
8/7/81	(0.740)	(0.192)	(30.1)	(0.154)	(0.051)	(0.005)	(0.010)	(0.023)	(20.4)	(0.834)	(3.62)	(0.044)	(59.8)
8/7/81	0.833	0.193	31.6	0.047	0.055	0.005	0.011	0.015	22.5	0.873	3.69	0.032	63.0
9/11/81	(0.616)	(0.004)	(28.1)	(0.34)	(0.041)	(0.006)	(0.006)	(0.014)	(17.3)	(0.262)	(3.19)	(0.015)	(53.6)
9/11/81	0.677	0.004	31.5	0.035	0.046	0.007	0.015	0.026	19.7	0.283	3.28	0.028	55.8
UE29a-2	(0.303)	(<0.002)	(25.9)	(0.008)	(0.037)	(0.001)	(0.002)	(<0.0001)	(10.3)	(0.094)	(1.13)	(0.016)	(50.1)
	0.343	0.034	25.8	0.048	0.041	0.03	0.003	<0.0001	11.1	0.105	1.17	0.041	50.8
H1-2000	0.196	0.112	3.55	0.019	0.027	0.38	0.001	0.004	3.45	0.074	6.38	0.017	106.0
3000	0.087	0.08	11.5	0.143	0.035	0.007	0.005	0.004	5.23	0.092	1.37	0.028	153.0
4000	0.074	0.036	12.9	0.026	0.043	0.008	0.007	0.003	1.68	0.112	1.45	0.018	166.0
5900	0.149	0.146	16.1	0.214	0.106	0.013	0.006	<0.001	6.18	0.143	2.19	0.022	120.0

[a]Values in parentheses for waters that were not filtered through 0.05-μm Nuclepore membranes.

TABLE X
COMPOSITION OF GROUNDWATER

Well	Concentration (mg/ℓ) F^-	Cl^-	PO_4^{3-}	NO_3^-	SO_4^{2-}	O_2 [c]	S^{2-}	Alk [b]	pH	Eh [d]
8	0.5	6.9	N.D.[a]	5.4	14.6			1.407	6.6	
UE25b-1										
8/7/81	1.07	11.4	N.D.	N.D.	21.1	1.8	N.D.	3.421	8.7	220
9/11/81	1.2	7.1	N.D.	0.6	20.6			2.213	7.7	
UE29a-2	0.56	8.3	<0.2	18.7	22.7	5.7	N.D.	1.769	7.0	305
H1-2000	2.7	24.6	N.D.	N.D.	13.9	3.4	N.D.	3.494	7.2	270
3000	17.7	8.3	N.D.	N.D.	34.4	1.3	0.064	5.861	7.0	-40
4000	13.1	8.4	N.D.	N.D.	60.9	1.3	0.000064	5.898	8.0	-25
5900	16.8	9.5	N.D.	N.D.	50.0	<1.2[e]	0.032	4.253	7.6	-105

[a] N.D. = not detected.

[b] Alkalinity in meq/ℓ.

[c] Measured after return to Los Alamos.

[d] mV vs a hydrogen electrode.

[e] The 1.2 was the minimum detectable.

When making comparisons among the results for the wells, the pumping history of each well must be kept in mind. Wells 8 and J-13 are producing wells that are still in use. Well UE25b-1 was pumped for more than 1.3×10^7 gal., but the water still contained detergent from the drilling of the well. Well UE29a-2 was pumped for a relatively short time and also contained detergent, and well USW-H1 was a stagnant hole that had not been pumped for over 6 months.

Despite the differences in pumping histories, several generalizations can be made.

(1) Well 8 water composition is very similar to that of well J-13. The concentrations of cations and anions in well 8 are all lower but are at approximately the same ratios to each other as those for well J-13 water.

(2) Well UE25b-1 water, however, contains higher sodium and calcium and lower magnesium and potassium concentrations. There is a large drop in manganese concentration in well UE25b-1 with time. The difference in results for unfiltered and filtered water from well UE25b-1 again shows the importance of filtration through 0.05-μm Nuclepore membranes when measuring iron concentration. An Eh of 220 mV was measured for this water, representing a solution without measurable quantities of oxygen present (<0.1 ppm). Oxygen analysis on the water after it was shipped to Los Alamos gave the high value of 1.8 ppm, which must be considered as a maximum because of the handling involved. Using the same constants and procedure that were used to calculate the measured iron concentration for well UE25b-1 (Table IX), the calculated Eh would be +110 ± 30 mV. The measured Eh of +220 mV (Table X) is too positive and may indicate poisoning by some oxygen in the system or during sample handling. The difference between the Eh and sulfide-electrode measurements (290 mV) is also greater than 180 mV,[9] indicating that the Eh electrode was poisoned by oxygen and was giving too positive a reading. The higher measurement may also be a result of mixing the water from two aquifers, one of which contains oxygen, during pumping.

(3) Well UE29a-2 water is very similar to well J-13 water except for a lower magnesium concentration and lower alkalinity. This water, like well J-13 water, contained ~5.7 ppm dissolved oxygen. Both well UE29a-2 and well J-13 produce water in a permeable zone at or near the standing water level; therefore, it is not surprising to see high oxygen contents. Well UE25b-1, however, produces water from several zones.

(4) The results on the at-depth samples from well USW-H1 are very different from those of pumped wells. The sodium is very high, whereas magnesium,

calcium, and potassium are low. At several depths the sulfide and iron concentrations are very high; these depths approximate the strata in which pyrite is found. The fluoride, chloride, and sulfate concentrations and the alkalinity are very high in these same samples, and a negative Eh is measured. At the time these measurements were taken, 1.2 mg/ℓ was the minimum detectable oxygen using the Yellow Springs Instrument electrode. These results probably represent reactions that can take place with time after drilling rather than conditions that existed before drilling. The difference in NO_3^- results between wells may be an indication that wells USW-H1 and UE25b-1 are not fed by the same aquifer as wells 8, J-13, and UE29a-1 and that well UE29a-1 may be unique.

These results are important because there is now some evidence that all groundwaters at NTS are not highly oxidizing with measurable amounts of dissolved oxygen. Therefore, samples of formation water from particular strata must be obtained.

6. Determination of Fe^{2+} in Water. The presence of Fe^{2+} and Fe^{3+} in groundwaters has important effects on the oxidation potential in geologic systems. Total iron can easily be determined, but measuring the Fe^{2+} content is usually difficult in the presence of Fe^{3+}. However, using a procedure adopted originally from Lee and Stumm,[13] there seems to be very little interference from Fe^{3+}. The reagent, 4,7 diphenyl-1,10 phenanthroline, commonly called bathophenanthroline, is more sensitive and the color developed is more stable than other phenanthrolines. Ferric iron does form a slightly colored complex with the bathophenanthroline, but unless large quantities of ferric iron are present its contribution to the absorbance can be considered negligible. If needed, correction for large amounts of ferric iron can be made by establishing a calibration curve for ferric iron; however, the solubility of Fe^{3+} at pH 7 should be very low.

Reagents are prepared iron free by extractions to reduce the blank. The present lower limit for the procedure is ~1 μg Fe^{2+}, which is 0.0125 mg/ℓ for an 80-mℓ sample.

None of the common anions chloride, nitrate, acetate, or sulfate interfere in the determination of iron with bathophenanthroline, nor do the alkali and alkaline earth cations. Results for several groundwater samples are presented in Table XI.

TABLE XI

Fe^{2+} IN GROUNDWATER

Water	Filter (μm)	Fe^{2+} Concentration (ppm ≤)[a]
G Tunnel[b]	none[c]	0.057
G Tunnel[b]	0.05	0.0125
YM-46[b]	0.45	0.037
YM-54[b]	0.45	0.023[d]
Barmon No. 1[e]	0.40	3.0
Barmon No. 1[e]	none	3.0

[a]Reported as ≤ because the small contribution of Fe(III) has not been subtracted.

[b]Well J-13 water contacted with indicated tuff cores.

[c]Not originally filtered. A precipitate formed after boiling with acid. The solids were filtered out on No. 541 Whatman filter paper before extraction. Iron results may be low if the precipitate trapped iron.

[d]Limit is high because only a small sample was available.

[e]New Mexico well used to test equipment.

7. Determination of Fe^{2+} in Silicate Rocks. The presence of Fe^{2+} and Fe^{3+} influences the oxidation potential in geologic systems. An estimate of the total quantity of Fe^{2+} and Fe^{3+} in tuffs could be an indication of the total oxidation-reduction capacity of the tuff in Yucca Mountain. Total iron can easily be determined; however, a good method for determinating Fe^{2+} in silicate rocks must involve special techniques to prevent Fe^{2+} from oxidizing during separation or at other times when it is not being measured. Using a modification of Banerjee's technique,[14] in which the silicate rock is dissolved, the Los Alamos method includes a simultaneous oxidation of Fe^{2+} by ICl to form I_2. Iodine monochloride has a lower oxidation potential than either permanganate or dichromate, other oxidizing agents that might have been used; however, the use of ICl as oxidant precludes interference by Mn(II) or Cr(III). Pertinent half-cell reactions are

$$MnO_4^- + 8H^+ + 5e^- = Mn^{2+} + 4H_2O \qquad E° = 1.52\ V$$

$$Cr_2O_7^{2-} + 14H^+ + 6e^- = 2\ Cr^{3+} + 7H_2O \qquad E° = 1.33\ V$$

$$MnO_2 + 4H^+ + 2e^- = Mn^{2+} + 2H_2O \qquad E° = 1.23\ V$$

$$2(I^+Cl^-) + 2e^- = I_2 + 2Cl^- \qquad E° = 1.19\ V$$

$$Fe^{3+} + e^- = Fe^{2+} \qquad E° = 0.77\ V$$

The Los Alamos procedure uses ^{131}I-tagged ICl. The $^{131}I_2$ is reduced with $NaHSO_3$, extracted from an organic into an aqueous phase, and counted on a Ge(Li) detector. Standards are run at the same time for calibration. The method uses hydrofluoric acid in the dissolution, which limits the vessels that can be used. The FEP Oak Ridge-type centrifuge cones (50 mℓ) and fluoropolymer screw caps (Nalgene 3114) are suitable; most other plastics cannot be used because I_2 sorbs or diffuses into them. Several USGS "standard" rocks were analyzed, with a 2.0% average deviation from the published results.

In previous analyses, the Fe^{2+} was detectable in YM-22, YM-38, and YM-46 tuffs. These analyses will be repeated, however, because a less sensitive analysis of I_2 than the ^{131}I tracer method was used. Two analyses using the radioactive method were completed on G-Tunnel core U12G-RNM9. The Fe^{2+} content was <0.1%.

The procedures must be improved before they can be used for routine rock analyses.

B. Actinide Behavior

To assess the radiochemical hazards that would be associated with dissolved actinides in the repository, the geochemical processes along possible flow paths from the repository to the accessible environment must be known. The principal issues concerning actinide chemistry are:

(1) Speciation
  (a) oxidation state
  (b) hydrolyzed forms
  (c) complex ions
  (d) polymeric forms

(2) Solubility of oxides and hydrous oxides
  (a) effect of Eh and pH
  (b) effect of temperature
  (c) effect of complexing anions [closely related to (1c) above]
  (d) rates of precipitation and dissolution.

These issues must to be resolved before reasonable predictions of the behavior of plutonium and other actinides in the environment can be made. These issues are not strictly site specific; many are dependent upon the composition of the groundwater and rock.

The behavior of an element in solution under various conditions will depend on the species present. Thus, speciation is an important underlying issue in any discussion of the effect of groundwater chemistry on the behavior of waste elements. For elements that can exist in more than one oxidation state, the species present will depend on the Eh, the pH, and the concentration of complexing anions.

For plutonium and the other lighter actinides (An), the species present in acid solutions are well understood: An^{3+}, An^{4+}, AnO_2^+, and AnO_2^{2+} for the III, IV, V, and VI oxidation states, respectively, in the absence of significant concentrations of complexing ions. Plutonium (VII) is a very strong oxidizing agent and is not stable in acid solutions. At lower acidities, hydrolysis becomes important, and for plutonium significant concentrations of $PuOH^{2+}$, $PuOH^{3+}$, PuO_2OH, and PuO_2OH^+ appear at pH values of ~8.0, 0.5, 9.7, and 5.6, respectively.[15] More highly hydrolyzed species are known for PuO_2^{2+} and are almost certainly important for Pu^{4+} as well. However, Pu(IV) forms polymers in the pH region where more highly hydrolyzed species are expected, and no data exist.

The species present in acid solutions of many complexing agents are known, and a number of complexing constants have been determined.[16] Complex ions are expected to hydrolyze, but very little has been reported on these mixed complexes.[17]

The very low solubilities of the An(IV) oxides and hydrous oxides often limit the available concentrations in the environment and in the laboratory. Direct spectrophotometric methods for studying speciation usually require concentrations of $\sim 10^{-4}$ M, and determination of the oxidation state usually requires $\sim 10^{-6}$ M, much higher concentrations than those expected under environmental conditions. To determine an average charge (a step toward understanding speciation) by electrophoretic methods requires concentrations that are high enough that sorption on the medium is not important. Species present at low concentrations can sometimes be inferred by the effects that pH, Eh, and complexing ion concentrations have on the solubility equilibria and various distribution equilibria (for example, ion exchange and solvent extraction).

Quantitative consideration of any plausible set of solubility products, hydrolysis constants, and oxidation potentials for plutonium, uranium, and neptunium shows that the net solubility in noncomplexing media is a complicated function of both Eh and pH. The most stable solid phase is Pu(IV) oxide or hydrous oxide for most of the accessible Eh-pH region, but there are large regions where Pu(III) and Pu(V) are the principal solution species.[18]

A number of studies that are relevant to actinide solubility and speciation have been carried out. Los Alamos' experience in determining sorption ratios for actinides in tuff is outlined below, including the methods of preparation of the feed solutions and techniques for separating the solid and aqueous phases after contact. Studies of plutonium chemistry in near-neutral solutions are reviewed, including work with osmium complexes and observations concerning Pu(IV) polymeric material. Finally, the preliminary work related to particulate transport is reported, including production of actinides in the form of polymers or colloids.

1. Preparing Actinide Feed Solutions and Separating Solid and Aqueous Phases After Contact in Batch Sorption Measurements. Introducing plutonium or americium into groundwater is difficult because both elements tend to behave unpredictably in near-neutral solutions. Precipitation, polymerization, and/or colloid formation frequently result if great care is not taken in the preparation of the traced feed solutions and separation of the final aqueous and solid phases. Most traced feed solutions were prepared by evaporation of the tracer, violent agitation with groundwater, and finally, filtration through two different size filters. Sample separation problems were caused primarily by actinide sorption on very fine particles and filters and also by the the difficulty in removing such particles from the contacted groundwater. To determine, as far as possible, what species might be present in both plutonium and americium "solutions," a number of sample and traced feed solutions were characterized by microautoradiographs of the filters used in their preparation.

The traced solutions were normally prepared using rock-pretreated groundwaters, isotopically pure ^{241}Am tracer from Oak Ridge National Laboratory, ^{239}Pu tracer (weapons grade) from Los Alamos, and ^{237}Pu tracer from Argonne National Laboratory. Tracer purities were checked by both alpha and gamma spectroscopy. Feed solutions were usually prepared to contain ~2 x 10^6 dpm/mℓ of ^{241}Am, and/or ~3 x 10^5 dpm/mℓ of ^{239}Pu, or ~2.4 x 10^3 dpm/mℓ ^{237}Pu at 100%

yield of tracer, which was generally not obtained. These correspond to mass concentrations of ~1 x 10^{-6} M americium, ~1 x 10^{-5} M plutonium when ^{239}Pu was used, and ~4 x 10^{-13} M plutonium when ^{237}Pu was used. The ^{237}Pu tracer was treated with $NaNO_2$ so that the plutonium was in the IV oxidation state at the beginning, which resulted in the addition of ~10^{-4} M sodium ion to the feed solutions containing ^{237}Pu. Batches of traced feed solution were prepared in sufficient quantity to contact a predetermined number of crushed-rock samples, to aliquot for concentration determination, and to measure the pH value.

The "pH-adjusted" feed solutions were prepared by adding tracer solution directly to the groundwater and then adjusting the pH to the original value by adding NaOH solution, which resulted in the addition of ~10^{-2} sodium ion. "Dried" feed solutions were prepared by first evaporating an aliquot of tracer solution in air at room temperature in a polypropylene tube. The dried activity was then contacted several times with 20-mℓ volumes of groundwater for periods of from a few minutes to overnight. After each contact the tube was centrifuged for 1 hour at 12 000 rpm (~28 000 g), and the aqueous phase was added to a large polyethylene bottle. These two contact processes were continued until no significant decrease in γ-ray activity was observed in the tube; generally, this required three contacts. Groundwater was added then to the bulk of the feed solution in the bottle to give a volume ~20 mℓ less than the desired final volume, and this bulk solution was shaken overnight. At the same time, the final contact was being made in the original tube. The next day the tube was centrifuged, and the solution was added to the bottle. Water was added to give the desired final volume, and the bottle was shaken for at least 1 hour. The solution was then centrifuged for 1 hour at $\geq$6000 rpm and transferred to a new bottle.

In early experiments, feed solutions were not filtered. The yields of the traced feed solutions generally varied from ~5 to 70%. The procedure currently in use to prepare traced feed solutions is described in Sec. IV.A.2. Within 1 hour after preparation of a feed solution, an aliquot was taken and acidified for later assay for the initial concentration of each tracer, and 20-mℓ portions were added to crushed-rock samples in polypropylene tubes and to empty tubes for use as "controls." The pH value of the remaining solution was then measured.

The results of experiments using the pH-adjusted feed solution differed
m measurements using feed solution prepared from dried tracer. Individual
le sorption ratio values are presented in Ref. 2; average values are

presented here in Table XII. Differences are presumably the result of differences in speciation that were caused by the alternate methods of feed solution preparation.

Feed solutions for early actinide sorption experiments were prepared in a manner to optimize the actinide concentration of the feed solution, and ensure, as far as possible, the exclusion of any polymeric or colloidal particles. However, the centrifugation described in Ref. 1 probably did not eliminate any particles because the feed solution was transferred from the centrifugation bottle by decanting. For all later experiments, the centrifugation was omitted, and the feed solutions were passed directly through a double filter (0.4 and 0.05 μm), thus eliminating two container changes. The method removing activity from the tube in which it is dried was changed to include a 2- or 3-minute contact with rock-treated water using a vibrator or

TABLE XII

SORPTION RATIOS[a] (mℓ/g) FOR AMERICIUM AND PLUTONIUM DETERMINED USING TWO METHODS FOR PREPARING FEED SOLUTIONS

			Feed Solutions[a]			
			Dried		pH Adjusted	
Element	Core	Temp (°C)	Sorption	Desorption	Sorption	Desorption
Am	JA-18	22	180(30)	1100(260)	435(6)	960(15)
		70	230(30)	3400(300)		
	JA-32	22	130(30)	2200(650)	1100(120)	2300(310)
		70	110(30)			
	JA-37	22	670(210)	17000(3500)	8800(1100)	12000(2000)
		70	970(240)		34000(6000)	5300(720)
Pu	JA-18	22	140(30)	350(140)		
	JA-32	22	~110		1200(210)	750(170)
	JA-37	22	280(100)		3300(1200)	3800(950)
		70	~240			

[a]Traced feed solutions were not filtered before use. They are averaged over 1-, 2-, 4-, and 8-week contact times; 106- to 150- and 355- to 500-μm particle sizes, and ~10^{-6} and ~10^{-13} M plutonium concentrations. Values in parentheses are the absolute-value standard deviation of the means.

ultrasonic bath and then a second 2- or 3-minute contact with a fresh portion of rock-treated water, again using an ultrasonic bath. Subsequent contacts removed successively smaller portions of the remaining dried tracer; in general, 90 to 99% of the activity that can be removed is removed in the first two contacts.

Investigations detected the presence of centrifugable or filterable actinide species generated during feed preparation and sorption procedure. Improvements were made in the method used to separate solid and liquid phases after contact, presumably reducing the amount of particulates present in the aqueous phase and, thereby, giving more accurate results. A few operations were added to examine (1) container sorption for samples and controls, (2) the fraction of centrifugable species in the controls, (3) the effect of filtering successive portions of the same "postcontact" solution through the same filter membrane, (4) the effects of filtering postcontact solutions through filter membranes with different pore sizes, and (5) the effects of centrifuging postcontact solutions a different number of times and for different durations. The procedure to separate phases after contact was usually three centrifugings, for 1, 1, and 2 hours, respectively, at 12 000 rpm (28 000 g). Extreme care was taken to avoid transferring any particulates from the bottom of the tube or in surface films. The centrifuged solutions were then filtered in various ways. The relative difference in sorption values obtained from pH-adjusted feed solutions but different postcontact phase-separation procedures is shown in Table XIII. The higher R_d values observed with the improved phase-separation procedure indicate a more efficient removal of solid particles (with their associated high count rates) from the aqueous phase before counting. In some cases, aliquots were taken for counting after each centrifuging and each filtering.

Sorption on container walls during tuff contacts was measured by transferring the contents after contact, without centrifuging, to new tubes and counting the original tubes. Sorption on the container walls when solids were present was measured for twenty-four ^{241}Am and seven ^{237}Pu samples. The amount of activity sorbed on the container, with the possibility of retention of a small amount of solid even after transfer, averaged 2.1% for americium and 2.5% for plutonium. For controls (no solids present), container sorption averaged 24% for nine americium solutions at room temperature, 74% for four americium solutions at 70°C, and 16% for two plutonium solutions at room temperature.

TABLE XIII

SORPTION RATIOS[a] (mℓ/g) FOR AMERICIUM AND PLUTONIUM DETERMINED USING DIFFERENT METHODS OF SEPARATING SOLID AND AQUEOUS PHASES[b]

Type of Phase Separation	Americium		Plutonium[c]	
	Sorption	Desorption	Sorption	Desorption
Original procedure				
JA-32	950(160)[d]	920	1200(200)	750(170)
JA-37	5000(800)	4000(1300)	8000(1400)	1100(300)
Improved procedure				
JA-32	1400(110)	2700(430)		
JA-37	12000(410)	14000(2100)	700(210)	4600(1000)

[a]Sorption ratios are averaged values for two particle sizes (106 to 150 and 355 to 500 μm).

[b]Experiments run in air at ambient temperature. Feed solutions prepared by addition of acid solution of tracer and readjustment of pH. Data given for post-contact solutions after centrifugation but before filtration.

[c]These two experiments also differed in the concentration of plutonium used; the first used ~10^{-13} M ^{237}Pu and the second used ~10^{-6} M ^{236}Pu. See Sec. IV.C.3 for a discussion of concentration effects.

[d]Values in parentheses are the absolute-value standard deviation of the means.

The amount of plutonium or americium activity remaining on the containers is obviously much lower for the samples than for the controls.

For comparison, container sorption during experiments with argillite samples from the Eleana formation at NTS was also investigated. The measurement methods were essentially the same as those used on the tuff except that the control samples were centrifuged and the aqueous phase was transferred to another tube. The activity observed in a control tube, therefore, represented the sum of wall sorption and centrifugable species. Sorption on the container walls when solids were present was measured for thirteen ^{241}Am and nine ^{237}Pu samples. The amount of activity sorbed on the container averaged 1.2% for americium and 0.6% for plutonium, with the possibility of retaining a small amount of solid even after transfer. For the controls, the americium activity remaining in the container averaged 13% for 13 solutions at ambient temperature and 90% for 4 solutions at 70°C.

For two plutonium controls at each temperature, the values were 43% at ambient and 88% at elevated temperature. Again, container sorption was much higher for the controls than for samples containing crushed rock.

To determine the distribution of activity sorbed on the tuff control tubes, the bottoms of 6 tubes were washed twice with 2.5-mℓ portions of 3 M HCl; the activity removed was assumed to represent that which sorbed on the bottom of the tube. The tubes were then completely washed with two 2.5-mℓ portions of 3 M HCl, and the activity removed from each tube was again assumed to represent that which sorbed on the walls. The final "clean" tubes were checked by gamma counting. The activity was calculated per unit area; the ratio of the activity on the bottom to the activity on the walls varied from 0.3 to 1.1 with an average of 0.7. The activity on control tubes appears to have been sorbed fairly evenly on the surface. The above results for container sorption suggest that sorption is dependent on available surface area, so when crushed tuff is present, container sorption is negligible.

For the tuff controls described above, the fraction of centrifugable species was measured by centrifuging the contents of the new tubes after the first transfer, again transferring the liquid, and counting the activity left in the tubes. The average fraction of the activity in the solution after contact that was removed by one 1-hour centrifuging was 17% for nine americium controls at room temperature, 37% for four americium controls at 70°C, and 13% for two plutonium controls at room temperature. Because there was a significant amount of centrifugable species in the control solutions, presumably a similar fraction of the activity was also present with the samples; there it would have been combined with the crushed rock and counted with the sorbed activity. Each of three centrifugings (1, 1, and 2 hours) removed additional activity from americium solutions after contact and, therefore, would appear to be necessary. (These measurements were not repeated with plutonium solutions.)

In an experiment to see if effects related to the filtering process would result in a change in the radionuclide concentration of solutions after contact, three ~3-mℓ portions of a solution were passed through the same 0.4-μm polycarbonate membrane. Each portion was aliquoted and counted after passing through the membrane. Filtering successive portions of the same postcontact solution through the same filter membrane did not appear to result in a significant difference in the concentration of plutonium or americium in the solution.

The effects of centrifuging the postcontact solutions and passing them through filters with various pore sizes were examined by counting aliquots of

the solution after each step. Data for a number of samples and controls are given in Table XIV. The filter sequences were 1.0/0.4/0.05 μm, 0.4/0.4 μm, and 0.05/0.05 μm. The most recent procedure for postcontact centrifuging and transferring produced plutonium solutions from which no additional plutonium was removed by filtering. This was not true for americium, where a factor of 2 or more of the activity was sometimes removed by filtering the centrifuged solutions, the results varied with the contact temperature. These results suggest that plutonium does not significantly sorb on polycarbonate filter membranes, at least in the time required for filtration. The activity present in a plutonium solution after it has been centrifuged three times is, therefore, probably the correct value for calculating sorption ratios. For americium, it appears that centrifuging the solution after contact establishes a lower limit to the sorption ratio because crushed-rock particles and particulates remaining with the solution tend to lower the calculated R_d.

In an attempt to better understand the mechanism by which americium is retained on filter membranes, 38 membranes from the sequential filterings listed in Table XIV were examined by a microautoradiographic technique. Approximately one-half to one-third of each filter membrane was mounted on a glass slide by coating it with a thin layer of parlodion (a 2% solution in isopentyl acetate). The slide was then alpha counted to determine the length of exposure time needed (calculated to give $\sim 10^7$ total disintegrations) and clamped together with a second slide on which a Kodak AR.10 strippable emulsion had been mounted. Mounting the emulsion directly onto the coated filter made it difficult to see single tracks. To ensure that the emulsion adhered well to blank glass slides, the slides were first etched with a dilute solution of HF, then dried and coated with a solution of 2% parlodion in isopentyl acetate, dried again, and finally coated with a thin gelatin layer by dipping the slide in a water solution containing 0.5% gelatin and 0.06% $KCr(SO_4)_2 \cdot 12H_2O$.

Microautoradiography of the "sorption" membranes (those from solutions after initial sorption experiments) showed not only single-alpha tracks but also clusters and stars, indicating the presence of large complex species, polymers, or colloids in the so-called solutions, even after multiple centrifugings. Some sorption solutions were filtered successively through several membranes with the same or decreasing pore sizes (Table XIV); essentially all these membranes were found to retain americium in clusters, stars, and single tracks. Americium species in these solutions probably exist in a broad range of particle sizes. In contrast, the "desorption" membranes (those from

TABLE XIV

AVERAGE ACTIVITY[a] REMOVED FROM SOLUTIONS BY CENTRIFUGING AND FILTERING

Treatment	Samples (%)			Controls (%)		
	^{237}Pu	^{241}Am	^{241}Am[b]	^{237}Pu	^{241}Am	^{241}Am[b]
2nd Centrifuge[c] 1 hour		28	51		14	8
3rd Centrifuge 2 hours		24	26		6	8
Filter	0	10		3	28	0
0.1 μm						
0.4 μm	0	13		2	26	0
0.05 μm	0	27		1	28	48
or						
0.4 μm	22		2	26	6	
0.4 μm	11			24	3	
or						
0.05 μm	0	39	70		40	
0.05 μm	0	21	6		32	

[a]Decreases in activity are in per cent of input activity for a given operation removed by that operation.

[b]For 70°C solutions.

[c]All centrifugings were at 12 000 rpm.

solutions after desorption experiments) generally showed only single-alpha tracks, suggesting that some americium sorbed on the membranes and that large particulates were neither removed from the solids during desorption nor formed in the aqueous phase during contact.

Some caution must be exercised in interpreting these autoradiograms because radiocolloids and particles coated with radioactive material often produce a similar pattern of tracks. It is sometimes possible to distinguish between them by viewing the original particle or colloid with reflected as well as transmitted light. In related work, Allard* has observed sorption

*From information received from B. M. Allard, Chalmers University, Göteborg, Sweden.

ratios for Millipore filter paper that are comparable to ratios for rock-forming minerals during batch sorption experiments with americium in simulated groundwater.

Considering the above results, a conservative approach was taken in calculating americium sorption ratios; the results from the solutions after they been centrifuged but not filtered were used. After the early postcontact experiments described here, all feed solutions were prepared by drying the tracer and redissolving it in groundwater (Sec. IV.2).[7]

It must be emphasized that the measured sorption ratios for plutonium and americium include effects other than sorption. There may well be differences in the behavior of plutonium or americium even between supposedly identical solutions at pH 8 to 8.5; for example, the degree of polymerization and radiocolloid formation and hydrolysis result in variations in species (including charge) and particle size. Grebenshchikova and Davydov[19] reported that the charge on colloidal Pu(IV) species may be either positive (at low pH values) or negative (at high values) and that the isoelectric pH, or point of zero charge, is in the pH region 8.0 to 8.5. Polzer and Miner[20] presented a plot of effective charge (caused by hydrolysis) of the americium species vs pH for a 0.1 M $LiClO_4$ solution. Between pH 8.0 and 8.5 the average effective positive charge per atom of americium varied from ~1.3 to ~0.0. Therefore, large variations in the behavior of both plutonium and americium can be expected in this pH range.

2. Plutonium Chemistry in Near-Neutral Solutions. In an effort to control the Eh in laboratory experiments involving plutonium and other multivalent elements, several systems are being investigated. A number of osmium complexes that could be used for this purpose have also been prepared and tested. Because of the importance of the Pu(IV) polymer as a possible migrating species from a repository (as described in Sec. II.B.2.e), its rate of formation at very low concentrations and its ionic dissociation are being studied. Because the Pu(V)-Pu(VI) potential in speciation and solubility at Eh greater than ~0.9 V and pH less than ~7 is important, measurements of the equilibrium in selected Pu(VI)-Os(II) reactions are being used for an independent determination of the Pu(V)-Pu(VI) potential at low acid concentrations and ionic strengths.

a. Eh Control. Measurements of Eh in the laboratory have been made with either a platinum or a gold electrode referenced to a standard calomel

electrode. Standards of +430 and -388 mV, relative to the normal hydrogen electrode, have been used for calibration.

Measurements of Eh on unpoised or complex systems are difficult to interpret.[21] A weak signal can be undetectable because of electrical noise in the system. Laboratory measurements of both aerated and oxygen-free groundwaters in the absence or presence of many rock samples studied (tuff, Climax Stock granite, and Eleana argillite) have generally shown positive potentials. However, mixtures of tuffs YM-54 (divitrified) or tuff YM-38 (zeolitized) and water from well J-13 that have been shaken in a controlled atmosphere for more than a year show slightly lower Eh values, -20 to -140 mV, compared to values of +300 to +350 mV for aerated solutions with pH values of ~8.

Next, $NH_2OH \cdot HCl$ was examined as a reducing agent. Solutions were sparged for several hours with argon gas to remove some of the oxygen, $NH_2OH \cdot HCl$ was added, and the pH was adjusted with dilute NaOH to neutral or slightly basic. The Eh was measured as a function of pH, and an approximately linear correlation was found. At pH 7, Eh $\cong$ 120 mV; at pH 10.8, Eh $\cong$ -130 mV.

Before a potentiostat was obtained and set up, a preliminary experiment was run with 10^{-6} M Nile Blue in sodium carbonate solution; ferrous iron was used as reductant to decrease the Eh to the Nile Blue theoretical value of -160 mV at pH 8.3. This reading was maintained for several hours with the addition of ferrous ammonium sulfate. It is unclear which couple was actually measured: Ottaway[22] states that concentrations of $\leq 10^{-7}$ M are needed for true solution behavior of Nile Blue.

A potentiostat cell similar to those of Harrar[23] and Rai et al.[24] was built with a 3.6-cm diam and 7.5-cm height. The bottom has a convex indentation to hold a 5/8-in. Spinfin for magnetic stirring, which allows the very vigorous mixing needed to deoxygenate any solution used under controlled Eh conditions.[23] The working electrode is a 3.3-cm-diam, platinum-gauze cylinder. The counter electrode is a folded 5- by 2-cm platinum gauze isolated in a glass cell with a porous Vycor frit making contact with the solution. A salt bridge contains a calomel reference electrode. Inlet and outlet tubes for inert-gas sparging and a sample port with a stopper are included.

Control of pH is necessary when working with Eh buffer-potentiostat systems. Although tris-(hydroxymethyl)-amino-methane makes usable buffers in the desired (underground systems) pH range, the borate-boric acid systems have been the most useful and probably are less likely to interfere in the rock-groundwater systems.

Work at Eh values below that of the H_2O_2-O_2 couple (0.68 - 0.059 x pH)V is difficult because of oxidation by oxygen in the air. It is necessary to work in an inert-atmosphere glove box when studying systems with Eh values $\lesssim$0.1 V. A Vacuum Atmospheres controlled-inert-atmosphere glove box with a Dri-Train purification system is used. The oxygen content is $\leq$0.2 ppm and the carbon dioxide content is $\leq$20 ppm in the atmosphere of the box. Argon gas that has been through a chromous-perchlorate, zinc-amalgam scrubber and an acid scrubber is piped into the box so that various solutions under study can be sparged in the box.

The first investigations of possible redox buffers have focused on redox indicators because a wide range of potentials is available.[22] However, in addition to having an appropriate potential, a satisfactory Eh buffer system must be relatively stable in both oxidized and reduced forms; it must also show a relatively rapid redox reaction rate with the species of interest, but must not react in other ways.

The first work in Los Alamos involved the organic redox indicator Indigo Carmine. The formal potential (that given by equimolar concentrations of oxidized and reduced forms) for Indigo Carmine is reported[22] to be (0.291 - 0.059·pH)V. Using this dye, Los Alamos scientists have maintained stable Eh values of (-0.19 ± 0.02)V at pH 7 for several days. Indigo Carmine, however, has some drawbacks; unstable Eh values are observed if attempts are made to reduce the last 0.01% using a potentiostat. Also, Los Alamos has been unable to reproduce the reported Eh-pH function--the values at pH = 1.1 and 7.6 are 0.1 V lower and 0.04 V higher, respectively, than published values.[22]

Preliminary experiments with thionine show that it may be useful at Eh values somewhat higher than those provided by Indigo Carmine. The range might be useful for experiments with technetium. The formal potentials are reported to be 0.563 and 0.064 V at pH = 0 and 7, respectively. Reasonably satisfactory behavior was observed at pH 5.6 after stirring the solution and sparging it with argon for several days and then reducing with a potentiostat. After this treatment the measured formal potential came to within 0.003 V of the theoretical value in 3 days. This time may indicate slow attainment of equilibrium at the electrodes.

b. Osmium Complexes. Couples involving selected osmium complexes will probably be useful as Eh buffers or moderators. H. Taube,* who has had con-

*From information provided by H. Taube, Stanford University, Stanford, CA 94305 (1980).

siderable experience with a wide variety of inorganic complexes, suggested that although many ruthenium complex couples have desirable potentials, they are probably not stable enough for these purposes. Certain osmium complexes are much more stable, and Taube suggested that the II-III couples such as $Os(bipyridyl)_3$ and $Os(bipyridyl)_2(CN)_2$ should be tried. This section describes the preparation and some of the properties of these complexes. Osmium complexes have the advantages that (a) the redox potentials of the Os(II)-Os(III) couples are essentially independent of pH in the range of interest, (b) the standard potential of the couple can be changed by varying the coordinated ligands, (c) the complexes are neutral or positively charged so they are not expected to complex plutonium or other actinide species, and (d) the Os(II) complexes are highly colored so that reactions can be studied at low concentrations. Long-term stability with respect to decomposition in solution and rapidity of redox reaction with plutonium or other actinide species are additional properties required for suitability of complexes as buffers or moderators. If the complexes were to be used as moderators in conjunction with a potentiostat, rapid electrochemical reversibility would also be required.

Preparation. The tris complexes $[Os(bipy)_3]Cl_2$ (identified as complex A), $[Os(dimebipy)_3]Cl_2$ (B), $[Os(diphenbipy)_3]Cl_2$ (C), and $[Os(nitrophen)_3]Cl_2$ (D)* were prepared by refluxing an excess of ligand with $(NH_4)_2OsCl_6$ in ethylene glycol according to the procedure described by Fabian et al.[25] Excess solvent was removed under vacuum, methanol was added, and the product was recovered using a column of Sephadex LH-20 with methanol as eluant. Complexes A, B, and D were recrystallized from methyl ethyl ketone-methanol mixtures under vacuum using a rotating flask. Complex C was precipitated from methanol by an excess of ethyl ether.

The other complexes, $[Os(en)(bipy)_2]I_2$ (E), $[OsCl(py)(bipy)_2]ClO_4$ (F), and $[OsCl(py)(dimebipy)_2]Cl$ (G), were prepared from the appropriate dichloro-complexes using modifications of the procedures described by Buckingham et al.[26] Complex F was precipitated from the reaction mixture using $NaClO_4$, separated from a large amount of by-product using the Sephadex column, and finally precipitated from the methanol solution using ethyl ether. The preparation of complex G was similar to that of complex F except that the reaction

---

* Abbreviations for the ligands are bipy = 2,2'bipyridine; dimebipy = 4,4'-dimethyl-2 2'-bipyridine; diphenbipy = 4,4'-diphenyl-2,2'-bipyridine; nitrophen = 5-nitro-orthophenanthroline; en = ethylenediamine; py = pyridine; and acac = acetonylacetonate.

mixture was taken to small volume under vacuum, methanol was added, and the solution was transferred directly to the Sephadex LH-20 column. The product was repurified by a second passage through the column and recovered by removing the methanol at ~45°C.

Solutions of the Os(II) complexes were assayed by spectrophotometric titrations based on the colors of the complexes. Standard solutions of Ce(IV) or Mn(VII) were used as oxidants. The equivalent weights and peak extinction coefficients determined for some of the complexes are listed in Table XV. The absorption spectra between 300 and 600 nm have been used to identify complexes to indicate chemical change.

Properties. Formal oxidation potentials were determined in dilute sulfuric acid by titration with Ce(IV) or Mn(VII) in cells equipped with bright platinum and silver-silver chloride or mercury-calomel electrodes. Because the oxidation potential for $Os(bipy)_3^{2+}$ is accurately known,[27] it was used as a standard for the other complexes. Tritrations of this complex were run consecutively with the other complexes to calibrate the electrodes and the procedure. The titration data, that is, cell potential vs volume of oxidant added, were fit to the Nernst equation, and the formal cell potential was determined by a least squares procedure. The standard potentials were determined by comparing the formal cell potentials with the measurements taken with $Os(bipy)_3^{2+}$ made at approximately the same time. Standard potentials determined in this way are included in Table XV.

The stabilities of the complexes in solution were determined by observing changes in the spectra as a function of time.

Solutions of $Os(bipy)_3^{2+}$ were stored in water for several months at room temperature without significant changes in the spectra. A sample of the material was refluxed in 6 M NaCl for 16 hours, again with no significant changes. A solution of $Os(bipy)_3^{3+}$ was prepared from the Os(II) complex by oxidizing it with chlorine, drying it on a vacuum line, and redissolving it in water. After 72 days at room temperature in the dark, this solution showed large amounts of the Os(II) complex. The potentials are such that the Os(III) complex can oxidize water in near-neutral solutions.

Long-term experiments have not been done on solutions of $Os(dimebipy)_3^{2+}$, but it is expected to be as stable as the corresponding bipy complex. The spectrum of $Os(dimebipy)_3^{3+}$ in water was found to be unchanged after 90 hours at room temperature or 15 minutes at 90°C. However, a 200-minute exposure to daylight caused a 20% decrease in the absorption peak at 488 nm.

TABLE XV

PROPERTIES OF SELECTED OSMIUM COMPLEXES

Complex	Equivalent Weight (g/equiv)	λ_{max} (nm)	Extinction Coefficient ($M^{-1}cm^{-1}$)	Oxidation Potential (V)
A. $[Os(bipy)_3]Cl_2$	782[a] (784,3)[c]	480	1.36×10^4	0.8846[b]
B. $[Os(dimebipy)_3]Cl_2$	837 ± 6[a] (832,1)[c]	488	1.42×10^4	0.694 ± 0.002
C. $[Os(diphenbipy)_3]Cl_2$	1155 ± 38 (1186,0)[c]	502	2.45×10^4	0.849 ± 0.004
D. $[Os(nitrophen)_3]Cl_2$		470		~1.05[e]
E. $[Os(en)(bipy)_2]I_2$		505		
F. $[OsCl(py)(bipy)_2]ClO_4$	741 (735,1)[c]	345	1.17×10^4	0.476 ± 0.005 0.4836[b]
G. $[OsCl(py)(dimebipy)_2]Cl$		473		0.421
H. $[Os(acac)(bipy)_2]Cl$[(d)]		515		0.153[b]
I. $[Os(2\text{-}(2'\text{-pyridyl})quinoline)_3]Cl_2$[(d)]		503		0.990 ± 0.003
J. $[Os(6\text{-methyl-}2,2'bipyridine)_3]Cl_2$[(d)]				~0.90[e]

[a]Heated to ~50°C under vacuum.

[b]Reference 25.

[c]Calculated equivalent weight for indicated hydrate.

[d]Material furnished by D. M. Klassen, Department of Chemistry, McMurry College, Abilene, TX 79605.

[e]Potential is only approximate because of serious drifts.

The stabilities of the bis-(bipy) and bis-(dimebipy) complexes were examined in experiments in which the complexes were dissolved in argon-swept water and sealed into 13-mm-o.d. Pyrex tubes. The +3 oxidation states were prepared using iodine as the oxidizing agent. The spectra were determined, and the absorbances at characteristic peaks and valleys were recorded for periods of a week or more; the results are summarized in Table XVI. Except for two of the oxidized forms, $[Os(acac)(bipy)_2]Cl_2$ and $[OsCl(py)(dimebipy)_2]Cl_2$, the spectral changes are quite small. Also, $[OsCl(py)(bipy)_2]ClO_4$ was found to be relatively unstable in solution at pH 3.

After the room temperature experiments were completed, the sealed samples were subjected to a temperature of ~90°C for 2.5 hours and then room temperature under daylight for ~50 hours. Neither of these treatments caused drastic changes; in all cases the spectra of the final solutions were similar to the original ones. $[Os(acac)(bipy)_2]Cl_2$ and $[OsCl(py)(bipy)_2](ClO_4)_2$ appeared to be the least stable, showing absorbance changes up to 12 and 43%, respectively.

c. Reaction Rates Between Plutonium Species and Osmium Complexes. The rates of a number of reactions between osmium complexes and the various oxidation states of plutonium were investigated because such data are required when evaluating the complexes for possible use as Eh buffers and moderators.

TABLE XVI

STABILITY OF VARIOUS OSMIUM COMPLEXES IN WATER AT ROOM TEMPERATURE

Complex	Observation Period (days)	Spectral Changes (% day^{-1})
E. $[Os(en)(bipy)_2]I_2$	73	+0.01 to +0.03
$[Os(en)(bipy)_2]I_3$	11	0 to -0.23
F. $[OsCl(py)(bipy)_2]ClO_4$[a]	3	-0.10 to +0.40[b]
$[OsCl(py)(bipy)_2](ClO_4)_2$	11	-0.30 to -0.50
G. $[OsCl(py)(dimebipy)_2]Cl$	13	-0.08 to -0.23
$[OsCl(py)(dimebipy)_2]Cl_2$	13	-0.11 to -1.44
H. $[Os(acac)(bipy)_2]Cl$	20	0 to -0.05
$[Os(acac)(bipy)_2]Cl_2$	12	-1.0 to -4.0

[a] Run in ordinary 1.00-cm cell.

[b] Values were -1.8 to -3.3% day^{-1} at pH 3.

Plutonium(III) solutions were prepared by dissolving weighed pieces of electrorefined ^{239}Pu metal in concentrated $HClO_4$ and diluting to the desired concentration or by reducing other oxidation states on zinc-amalgam. Plutonium(VI) was made from Pu(III) by oxidation in strongly fuming $HClO_4$. Plutonium(IV) solutions were made by mixing appropriate amounts of Pu(III) and Pu(VI) in 3 M acid.

The reactions were studied spectrophotometrically at room temperature, and the results are summarized in Table XVII. Rapidly stirred 10-cm absorption cells were used for the faster reactions. Except for the reduction of Pu(V), the rates are sufficiently rapid for satisfactory Eh buffer behavior.

The reaction

$$Pu(III) + 2Os(bipy)_3^{3+} = Pu(V) + 2Os(bipy)_3^{2+}$$

was studied at pH values of 3.0 and 3.8, using a great excess of the Os(III) complex. The concentration-vs-time curves at pH 3 were consistent with consecutive pseudo first-order reactions with the second-order rate constants listed in Table XVII. The results obtained at a pH of 3.8 are difficult to interpret quantitatively because the overall change in absorbance corresponded to only ~82% conversion of Pu(III) to Pu(V). However, the data indicate that the oxidation of Pu(IV) to Pu(V) is about five times faster, and the oxidation of Pu(III) to Pu(IV) is about two times faster, than at the lower pH value.

d. The Pu(V)-Pu(VI) Potential. The reaction

$$PuO_2^{2+} + Os(bipy)_3^{2+} = PuO_2^{+} + Os(bipy)_3^{3+} \quad (2)$$

deserves further comment because it was found not to go to completion at pH 2. Net absorbance change was measured at the Os(II) peak in experiments in which the initial Pu(VI) concentrations were in the range (1.7 to 8.4) x 10^{-6} M, and the initial Os(II) concentrations were (1.9 to 9.4) x 10^{-6} M. In each of seven runs, values for the equilibrium quotient Q and the extinction coefficient difference for the reaction were found that minimize the sum of the squares of the differences between the observed and calculated absorbance values. Values for Q were found to depend very strongly on the initial Pu(VI)/Os(II) ratios, so the analytical determination of the reactants must be very accurate. The average of the seven separate determinations of Q is 14 with a mean deviation

TABLE XVII

REACTION RATES BETWEEN OSMIUM COMPLEXES AND THE VARIOUS OXIDATION STATES OF PLUTONIUM IN AQUEOUS SOLUTIONS AT ROOM TEMPERATURE

Reaction	Concentration			Ionic Strength (M)	Apparent Second-Order Rate Constant ($M^{-1} S^{-1}$)
	Pu ($M \times 10^6$)	Os ($M \times 10^6$)	H^+ (M)		
$Pu(VI) + Os(bipy)_3^{2+} = Pu(V) + Os(bipy)_3^{3+}$	1.7 to 8.4	1.9 to 9.4	0.01	0.01	$(4.45 \pm 0.17) \times 10^4$
$Pu(VI) + Os(dimebipy)_3^{2+} = Pu(V) + Os(dimebipy)_3^{3+}$	2.0	2.0	0.001	0.001	$(3.7 \pm 0.02) \times 10^5$
$Pu(V) + Os(dimebipy)_3^{2+} = Pu(IV) + Os(dimebipy)_3^{3+}$	12	34.5	0.006	0.006	3.2×10^{-3}
$Pu(V) + Os(acac)(bipy)_2^{+} = Pu(IV) + Os(acac)(bipy)_2^{2+}$	21	130	0.002	0.0022	0.013[a]
$Pu(IV) + Os(bipy)_3^{2+} = Pu(III) + Os(bipy)_3^{3+}$	1.5 to 2.0	6.5	0.01 to 0.82	0.82	$(6.2 \pm 0.2) \times 10^3$[b]
	1.5	6.5	0.10	0.10	1.1×10^3
	1.9 to 3.8	1.8 to 9.1	0.01	0.01	$(6.8 \pm 0.2) \times 10^2$
$Pu(IV) + Os(dimebipy)_3^{2+} = Pu(III) + Os(dimebipy)_3^{3+}$	2.1	6.2	$(0.17 \text{ to } 10) \times 10^{-3}$	0.01	$2 \times 10^4 / [1 + 3.56 \times 10^{-4} / (H^+)]$
$Pu(III) + Os(bipy)_3^{3+} = Pu(IV) + Os(bipy)_3^{2+}$	1.9	73	0.001	0.0015	46
$Pu(IV) + Os(bipy)_3^{3+} = Pu(V) + Os(bipy)_3^{2+}$	1.9	73	0.001	0.0015	4

[a] Very approximate because the stoichiometry is not understood.

[b] No significant H^+ dependence.

of 2.4. This average value is readily extrapolated from 0.01 M to zero ionic strength giving 11.7 ± 2.4 for the equilibrium constant. Combining this with 0.8846 V, the accurately determined value for the Os(II)-Os(III) couple,[27] gives 0.948 ± 0.005 V for the Pu(V)-Pu(VI) standard potential. This result is compared to 1.016 ± 0.050 V recommended by Fuger and Oetting[28] and 0.933 V estimated by Allard et al.[18]

e. Ionic Dissociation of the Pu(IV) Polymer. The existence of bright green Pu(IV) polymer suspensions is common knowledge.[29] This polymer is of interest as a possible migrating species from a repository and also because it is probably related to the nonreactive Pu(IV) that is discussed in Sec. II.B.2.f.

Suspensions of the polymer have been prepared by diluting Pu(IV) in HCl-$HClO_4$ mixtures, rather than by using HNO_3 as previously described.[30,31] The formation of polymer was observed to be much slower than reported for HNO_3 solutions,[32] but after ionic species were removed with a cation exchange resin, the spectra of the preparations were essentially the same as those reported earlier.[32] In a second method of preparing the polymer, Pu(IV) in $HClO_4$ was partially neutralized with NaOH solution and then heated to 90°C for 30 minutes. The spectrum of the suspension prepared in this way and treated with a cation exchange resin agreed with published spectra.

The solubility of the polymer $[(PuO_2 \cdot mH_2O)n]$ may be defined in terms of the equilibrium

$$\underset{\text{polymer}}{(1/n)(PuO_2 \cdot mH_2O)_n} + 4H^+ = Pu^{4+} + (2 + m)H_2O \quad . \tag{3}$$

In a previous attempt to measure the solubility,[31] polymer was equilibrated in solutions with $3 \leq pH \leq 7$. Soluble plutonium was defined as all plutonium species that pass through a Centriflo filter with 2-nm pore size. These species were shown to be predominantly Pu(V), although the oxidizing agent was not identified.

A preliminary experiment tested the feasibility of determining the solubility of the Pu(IV) polymer in a way that should avoid the difficulties associated with the above method. In this experiment PuO_2^{2+} was mixed with polymer at pH 3, where the equilibrium reaction is probably

$$(1/n)(PuO_2 \cdot mH_2O)_n + PuO_2^{2+} = 2PuO_2^+ + mH_2O \quad . \tag{4}$$

The concentration of PuO_2^{2+} was determined spectrophotometrically as a function of time. The question is whether concentrations can be identified where the rates of the forward and reverse reactions are equal. If so, the equilibrium quotient for reaction (4) can be determined and that of reaction (3) calculated from it by using the Pu^{4+} - PuO_2^+ and the PuO_2^+ - PuO_2^{2+} potentials.

Three mixtures were prepared in 10^{-3} M $HClO_4$: (A) 10^{-4} N polymer, (B) 5×10^{-5} M PuO_2^{2+}, and (C) 10^{-4} N polymer and 5×10^{-5} M PuO_2^{2+}. The mixtures were placed in 10-cm absorption cells, and the concentrations of PuO_2^{2+} were determined spectrophotometrically at 830 nm for 30 days.

Mixture (A) showed an increase in PuO_2^{2+} concentration corresponding to <0.01% per day based on the total plutonium present. In an experiment in much higher acid, a mixture ~5×10^{-3} N in polymer and 0.04 M in $HClO_4$ was followed spectrophotometrically for 18 days. During this period the Pu(VI) concentration increased at a rate of ~0.11% of the total plutonium per day.

Mixture (B) showed a linear decrease in PuO_2^{2+} concentration because of the net reaction

$$2PuO_2^{2+} + H_2O = 2PuO_2^+ + 2H^+ + \tfrac{1}{2}O_2 \quad , \tag{5}$$

caused by alpha particle self-irradiation from the decay of the ^{239}Pu. The observed rate of this reaction was 1.25% of the total plutonium per day. This is in satisfactory agreement with the value of 1.5% per day reported for solutions in 1 M $HClO_4$.[33]

The mixture of PuO_2^{2+} and polymer, mixture (C), showed a nonlinear decrease in PuO_2^{2+} concentration. The absorbance values were found to agree within 0.002 with the empirical equation

$$A = 0.325 \exp(-0.0299\ t) - 0.050 \quad , \tag{6}$$

where A is the absorbance and t is the time in days. The initial decrease in absorbance, from this equation, is 0.0097 per day or 3.5% of the original Pu(VI) per day, or 1.16% per day based on the total plutonium present.

At the end of the 30-day period, excess Ce(IV) was added to estimate the ionic plutonium species present. Sufficient $Ce(ClO_4)_4$ was added to produce final mixtures that were 3×10^{-4} M in Ce(IV) and 0.079 M in $HClO_4$.

Mixture (A), polymer with no added PuO_2^{2+}, showed a rapid absorbance increase of 0.03 during the first minute after the Ce(IV) was added. This was

followed by a much slower increase with a rate of ~2.5 x 10^{-4} per day for the next 150 minutes. These results indicate that Ce(IV) reacts relatively slowly with the polymer, but ~5% of the plutonium present reacted rapidly, suggesting that small amounts of ionic Pu(III), Pu(IV), or Pu(V) had formed.

Mixture (B), PuO_2^{2+} with no polymer, reacted rapidly with Ce(IV). The final absorbance value was reached within 1 minute and remained constant for the next 163 hours. The PuO_2^+ formed in reaction (5) was apparently reoxidized to PuO_2^{2+}.

Mixture (C), polymer plus PuO_2^{2+}, showed a rapid increase in absorbance when the Ce(IV) was added, followed by a slower increase similar to that observed for mixture (A). The absorbance, extrapolated to the time the Ce(IV) was added, was greater than that of the original mixture. The concentrations of PuO_2^{2+} in mixture (C) before and after adding the Ce(IV) were calculated from the absorbance values and are given in Table XVIII; two derived quantities are also given.

Entry (d) in Table XVIII shows that reaction (4) occurred at a slow but measurable rate. From entry (e) it can be calculated that the average rate of reaction (5) was 0.67% per day, based on the total plutonium present. This is about one-half the rate observed for mixture (B), where no polymer was present. This smaller value indicates that some of the alpha particles from the decay of the ^{239}Pu are absorbed in the colloidal particles and do not lead to chemical reaction.

Because the results in Table XVIII show that most of the reduction of PuO_2^{2+} was by reaction (5), an accurate estimation of the equilibrium quotient for reaction (4) cannot be expected. In addition, an assumption about the rate of reaction (5) must be made. However, the following calculation will demonstrate the process. Equation (6) can be used to show that the observed rate of reduction of PuO_2^{2+} equaled the average rate of reaction (5) at ~18.5 days. If the rate of reaction (5) was essentially constant in the mixture containing the polymer as well as in mixture (B), then the net rate of reaction (4) must have been zero at ~18.5 days. At this time the rates of the forward and reverse reactions would have been equal, and the equilibrium quotient, $Q = [PuO_2^+]^2/[PuO_2^{2+}]$, can be calculated from the concentrations for that time. The value obtained is ~4 x 10^{-5} M, with an experimental uncertainty of 20%.

The potentials for the Pu^{4+} - PuO_2^+ and the PuO_2^+ - PuO_2^{2+} have been estimated as 1.115 and 0.933 V, respectively, at an ionic strength of zero,[18] which

TABLE XVIII

PuO_2^{2+} CONCENTRATIONS IN MIXTURE C

Description	Concentration ($M \times 10^5$)
(a) Original mixture	4.86
(b) After 30 days; room temperature	1.40
(c) After adding Ce(IV); extrapolated to time of mixing	5.34
(d) Consumed by reaction (4), (c)-(a)	0.48
(e) Consumed by reaction (5), (a)-(b)-(d)	2.98

leads to $[Pu^{4+}][PuO_2^{2+}]/PuO_2^{+}]^2[H^+]^4 = 1.2 \times 10^3\ M^{-4}$. Combining this with our provisional estimate of 4×10^{-5} M for $[PuO_2^+]^2/[PuO_2^{2+}]$ gives $5 \times 10^{-2}\ M^{-3}$ for reaction (3). This result is reasonable, so the experiment is being repeated using ^{242}Pu to minimize the complexities caused by alpha particle self-irradiation, reaction (5).

f. Polymer Formed in Dilute Solutions. The rate of Pu(IV) polymer formation has been studied in HNO_3 solutions with plutonium concentrations in the range from 0.009 to 0.05 M and the acid concentration from 0.02 to 0.4 M (Refs. 32, 34). Preliminary experiments at much lower concentrations of both plutonium and acid strongly suggest the formation of polymer under these conditions also.

Studies of the reaction between Pu(IV) and $Os(dimebipy)_3^{2+}$ revealed that the amount of Os(II) oxidized depended on the history of the Pu(IV) solution. Experiments were performed in which a stock solution ~0.04 M in Pu(IV) and 3 M in $HClO_4$ was diluted to a pH of 3. Aliquots were removed periodically and added to excess Os(II), and the absorbance change was determined. The amount of plutonium capable of rapid reaction with Os(II) decreased with time in approximately second-order fashion. Possible reactions to account for this loss include the following.

O_2 oxidation:	$2Pu(IV) + \frac{1}{2}O_2 = 2Pu(V) + H_2O$
disproportionation:	$2Pu(IV) = Pu(III) + Pu(V)$
polymerization:	$nPu(IV) = [Pu(IV)]n$

The effect of oxygen on the disappearance of reactive Pu(IV) was determined by adding concentrated plutonium stock to either oxygen- or argon-saturated

solutions. The concentrations in the diluted solutions were 4.4×10^{-6} M Pu(IV), 1×10^{-3} M $HClO_4$, and 9×10^{-3} M $LiClO_4$. After 30 minutes, during which the appropriate gas was passed over the surface of the solution, a 33% excess of $Os(dimebipy)_3^{2+}$ was added. Fractions of reactive Pu(IV) remaining were determined by measuring absorbance changes caused by oxidation of the Os(II); they were 0.304 ± 0.037 for the oxygen saturated solution and 0.299 ± 0.009 for the argon-saturated solution. These data lead to the conclusion that no more than ~6% of the disappearance of the Pu(IV) is the result of oxygen oxidation.

The fact that Ce(IV) in 0.5 M H_2SO_4 reacts rapidly with Pu(III) and Pu(V) but only slowly with Pu(IV) shows that disproportionation is relatively unimportant. Separate solutions 2×10^{-6} M in Pu(IV), 1×10^{-3} M in $HClO_4$, and 9×10^{-3} M in $LiClO_4$ were prepared from Pu(IV) in 3 M acid and were allowed to stand for 2 and 84 minutes, respectively. A sevenfold excess of Ce(IV) was then added to react with any Pu(III) and Pu(V) that might have formed. Sulfuric acid was added with the Ce(IV), so the final solutions were 0.5 M in H_2SO_4 and 1.4×10^{-5} M in Ce(IV). Unreacted Ce(IV) was determined from the absorbance at 320 nm. The two solutions showed an absorbance difference of 0.009, indicating that slightly more reducing agent was formed in the solution that stood for 84 minutes. These results indicate that ~9 ± 4% of the Pu(IV) may have reacted to produce Pu(III) and Pu(V) in the period between 2 and 84 minutes. Previous experiments under the same conditions showed that in the same time interval the amount of reactive Pu(IV) decreased by at least 54%. This experiment should be repeated using a more sensitive reagent, but the tentative conclusion is that most of the disappearance of reactive Pu(IV) is not caused by disproportionation. This conclusion requires that the reverse of reaction (2) not be rapid in 0.5 M H_2SO_4 compared with the oxidation of Pu(III) and Pu(V) by Ce(IV). This was shown to be the case in a separate experiment.

The discussion given above makes it appear highly likely, but does not prove, that disappearance of reactive Pu(IV) is the result of polymerization.

The effect of reducing the hydrogen ion concentration from 1.0×10^{-3} to 5.0×10^{-4} M was determined in experiments in which $OsCl(py)(bipy)_2^+$ was used as the reducing agent. The second-order rate constants found at the two hydrogen ion concentrations indicate that the empirical rate law is

$$-d[Pu(IV)]/dt = 6.2 \times 10^{-3} [Pu(IV)]^2(H^+)^{-2.2} \text{ M min}^{-1} .$$

This rate law is written in terms of the plutonium species present in the solution in the pH range studied, 3.0 to 3.3. If the hydrolysis constants published by Baes and Mesmer[15] are accepted, the observed hydrogen ion dependence is consistent with a rate determining step in which $Pu(OH)_3^+$ reacts with $Pu(OH)_4^o$.

3. Particulate Transport. One mechanism by which radionuclides may move through geologic media is particulate transport. Dissolved radionuclides can sorb onto particulates consisting of microscopic pieces of rock, dust, fibers, or other debris present in the liquid phase. If these particulates are less than a micrometer in diameter, they are often called radiocolloids. Dissolved radionuclides may also aggregate to form colloids or other stable associations. In addition, leaching of solids containing radioactive material may produce collodial material that is then transported with the aqueous leachant. The extent to which particulate transport may contribute to radionuclide migration in geologic media has not been widely studied. Presumably, such transport would depend on the aqueous flow rate, pore and fracture size of the rock media, ionic composition of the water, and the nature of the particulate, among other factors. Filterable aggregates containing americium and plutonium have been observed in the effluents of crushed-rock columns. Because the feed solutions that were used contained both ionic and aggregated species, it is not clear whether the aggregates in the effluent formed during passage of ions through the column, or whether the aggregates passed intact through the column. Better characterization and control of the feed solutions are necessary in order to do studies of this type.

Particulate size is likely to be a determining factor when particulates pass through connected rock pores or constricted fractures. The Pu(IV) polymers prepared by dilution of Pu(IV) ionic solutions under controlled pH conditions are being studied. The characteristics of these polymers depend somewhat on the conditions of their formation. The size of these colloids varies considerably; ~10% are sufficiently small that the material cannot be centrifuged at 12 000 rpm (28 000 g). Eventually, perhaps, the size of this polymer can be controlled by varying the conditions under which it is formed. To date, particulate transport research in the laboratory has relied upon centrifugation and filtration to separate particulates according to size and on microautoradiography to detect the presence of aggregated radioactive species on filters or other surfaces. Determining the presence of aggregates in the aqueous phase

by microautoradiography has proved to be more difficult. With this technique, an aliquot of the solution is dried, usually on a glass plate, then microautoradiography is used to determine whether the radioactive material was present in dispersed or aggregated forms. Problems may arise because under some conditions dissolved material may form aggregates during the drying process. Experiments with freeze-drying techniques and substrates other than glass have not resolved all the problems associated with this method of identifying aggregates in the liquid phase.

In some preliminary work, fluorescent dyes were incorporated in microscopic plastic particles to trace particulate flow through crushed-rock columns or through solid-tuff disks. This seems to be a promising technique for tracing the transport of particles in the size range of a few micrometers or less.

4. Microautoradiography Studies. Microautoradiography, a technique in which autoradiographs are examined using optical microscopy, has been employed at Los Alamos in speciation studies of actinides (Sec. II.B.1, II.B.3.) and in sorption studies of actinides on specific minerals. Details concerning the application of this technique to sorption investigations are given in two reports and are summarized here.[35,36] Standard 30-μm polished petrographic thin sections are contacted for periods up to several days with groundwater solutions of the actinide of interest. After this solution is rinsed off, a thin photographic emulsion is adhered to the thin section and exposed for a period determined by the level of sorbed activity. The emulsion is then developed in situ, and the alpha-particle tracks are readily visible with an optical microscope at 50 to 400X. Because the emulsion remains adhered to the thin section, the tracks can be related to the mineral site at which the radionuclide was sorbed. Thus, one can distinguish, for example, between sorption on a bulk mineral phase or on the thin layer of alteration phase at the mineral boundary.[36] Also, it is possible to distinguish individual sorbed species from sorbed aggregates (for example, colloids) because the latter give rise to multiple tracks called stars.[35]

The microautogradiography technique can be extended to trace the movement of radionuclides through fracture systems in rock cores and over rock surfaces that are not too rough. There may be difficulties in undercutting such rock samples so that they will transmit light. In some instances, the alpha-particle tracks may be observed using reflected light. Autoradiographs may be prepared using beta particles (for example, from ^{63}Ni, ^{90}Sr, or ^{233}Pa) or Auger electrons (from ^{85}Sr), but the spots left in the emulsion by the electrons are much

more difficult to identify against the mottled background typical of thin sections than are alpha-particle tracks. In general, microautoradiography is a useful adjunct to other analytical techniques commonly used in geochemical investigations.

III. NEAR-FIELD ENVIRONMENT

Possible changes in the solid phases at Yucca Mountain are of concern because they could affect rock properties, especially sorption, strength, permeability, and porosity. This is especially true in the near field where temperature will rise as a result of the repository emplacement. The phases most likely to change are the clays, zeolites, and glass, which may be expected to alter to less hydrous phases having a smaller volume. Anhydrous phase assemblages such as feldspar and silica phases may also be hydrated to zeolites or clays. To predict the mineral assemblages that will be present in Yucca Mountain as a function of time and location, phase changes that may occur in the Yucca Mountain tuffs must be studied in the laboratory. These changes must be studied as a function of pressure, temperature, and bulk composition.

Phase changes in tuffs of varying mineral composition at known values of pressure and temperature are being examined using samples from drill holes in Yucca Mountain. The samples are ground and enclosed in gold capsules with water. The capsules are then placed in standard cold-seal pressure vessels that are pressurized and heated to the desired conditions. In these experiments water pressure is equal to the total pressure. Table XIX shows the mineral composition of the starting materials and the composition of the final products after 2 weeks at 400°C and 400 bars and after 4 weeks at 300°C and 400 bars.

The preliminary hydrothermal experiments illustrate several interesting points. The upper stability limit of mordenite is apparently below 400°C at 400 bars in most of these rocks; however, in sample BH, mordenite is apparently stable at 400°C. Two explanations are possible. The mordenite may be metastable at 400°C, which seems unlikely because clinoptilolite in the other runs at 400°C did not produce mordenite. It is more likely that the stability of mordenite in this sample is caused by a difference in composition. Such a difference might be in the ratio of potassium to sodium. There is also some indication that the mordenite in these samples is stable above 300°C. In the samples that originally contained clinoptilolite and mordenite, mordenite has crystallized at the expense

TABLE XIX

MINERAL COMPOSITION OF STARTING MATERIALS AND HYDROTHERMAL RUN PRODUCTS AT 400 BARS WATER PRESSURE [a]

Sample Number	Starting Composition	Run at 300°C (4 weeks)	Run at 400°C (2 weeks)
BH	clinoptilolite	clinoptilolite	mordenite cristobalite?
G1-1319	glass feldspar cristobalite?	glass feldspar cristobalite?	feldspar glass cristobalite?
G1-1639	clinoptilolite minor mordenite	clinoptilolite mordenite cristobalite feldspar?	feldspar cristobalite
G2-547	feldspar montmorillonite	feldspar montmorillonite?	feldspar cristobalite
G2-762	clinoptilolite minor cristobalite	clinoptilolite cristobalite	feldspar cristobalite minor quartz
G2-2001	mordenite clinoptilolite	mordenite minor quartz cristobalite?	feldspar cristobalite minor quartz
G2-2667	mordenite quartz	mordenite quartz	feldspar quartz

[a] Minerals are listed in approximate order of abundance.

of clinoptilolite. This is, however, not definitive evidence of mordenite stability; mordenite may well be a metastable product of clinoptilolite decomposition. Certainly this is the case for cristobalite, which is known to be metastable with respect to quartz under these conditions. The observation of mordenite growth at the expense of clinoptilolite also indicates that the upper temperature stability limit of clinoptilolite is <300°C at 400 bars water pressure. Results for sample G2-547 indicate that this may also be true for montmorillonite. These conclusions are made somewhat uncertain by lack of knowledge of the exact compositions of the minerals and by questions of metastability.

Experiments have also been performed in which tuff was reacted with J-13 water in Teflon lined Parr Bombs at 152°C. These experiments are discussed in detail in the groundwater chemistry section (II.A.3). The major difference between these experiments and the gold capsule experiments is that the fluid-to-

rock ratio is much greater here. In these experiments, the growth of clays and other fine-grained sheet silicates was observed on glass. This would certainly increase the sorptive capacity of the rock. The dissolution of cristobalite, mordenite, and clinoptilolite was also observed. This, however, should not be taken as proof that clinoptilolite and mordenite are unstable at this temperature. It may be that there was insufficient cristobalite available to the solution to raise the silica activity to an equilibrium value with cristobalite because of the large amount of water present in the experiment. Low silica activity, rather than the temperature may be the reason for mordenite and clinoptilolite instability.

Another study has been conducted on cylinders of intact tuff to examine changes in thermomechanical properties as well as changes in mineralogy. The details of this study are given in Ref. 37. Large changes in tensile strength, compressive strength, and permeability were observed in these experiments, but with a few exceptions, porosity, grain density, and thermal properties were observed to be unaffected. Mineralogic and petrologic examination of the test samples has established the operation of reactions involving the dissolution of silica and feldspar, formation of clays, and possible conversion of clinoptilolite to mordenite. However, it has not been possible to establish a one-to-one correlation of mineralogic and structural changes with physical properties changes. Changes in the volumes of minerals involved in these reactions were observed to be very small, reflecting their sluggish nature. This can explain, in a qualitative way, why some properties were unchanged. For example, thermal properties are dominantly determined by the inherent thermal properties of the constituent mineral phases. Unless there are substantial changes in the amounts of minerals with significantly different thermal properties, the thermal properties of the rock are not expected to change. It should be kept in mind, however, that the duration of this test was short relative to the operational time of a repository. The thermal pulse of a repository will last for hundreds of years. During this time slow processes of the type identified could cause significant changes in the thermomechanical properties of the host rock, and should be taken into consideration. Furthermore, it is believed that the strength changes observed are related to the subtle surface modifications of minerals observed, probably most actively along grain boundaries and fracture surfaces where the catalytic action of water is effective. It is expected that these same processes will be important in controlling the mechanics of discontinuities such as joints. Indeed, there is

evidence that rock friction is time-dependent, reflecting viscoplastic processes at point contacts of the surfaces.

A quantitative inclusion of these time-dependent phenomena will require careful measurements on target-horizon tuff samples held at simulated repository conditions for long time periods. Detailed examination of tested samples should identify the physical-chemical mechanisms involved. In addition, the difficult task of determining the rates of the processes will be required. Once these are determined, they can be incorporated in design and performance models to predict the response of the host rock mass over the lifetime of the repository.

IV. GEOCHEMICAL RETARDATION

A. Sorptive Behavior of Tuff

To predict the retardation possibilities in the Yucca Mountain area, a data base must be established from which models can be produced. Geochemical retardation processes and flow paths between the repository and the accessible environment must be identified. Geochemical retardation will depend on a number of factors, including (1) sorption processes, (2) the horizon and rock type of the repository, (3) temperature variations, (4) groundwater geochemistry, (5) fixation reactions, (6) diffusion processes, and (7) the effect of mineral precipitation. Information collected through studies of these processes will help predict the rates and concentrations in which radionuclides could be released into the environment and assess the hazards associated with such potential releases. The experimental program thus far has addressed various aspects of sorption by tuff, the physical makeup of tuff, the diffusion process, and various transport processes involved in porous and fracture flow. Planned extentions and additions to these retardation studies will be discussed in Chap. 2 of this report.

1. Introduction. The term sorption has generally been used to describe processes by which elements are removed from solution through their interaction with rock, such as ion exchange phenomena, chemisorption, and diffusion into the rock matrix; these processes may ultimately end in a variety of precipitation or coprecipitation reactions. A variety of experimental techniques have been used to gain an understanding of these processes, to study the importance of the parameters involved, and to build up a data base that will be used to model the sorption of nuclides by tuffs in the Yucca Mountain area.

Much effort has been spent studying sorption by a simple batch technique for measuring the distribution of an element between groundwater solutions and crushed tuff. The method is valuable because it is simple and a large number of samples can be processed in a relatively short period (a few days to several months). Other methods may also provide information on speciation, kinetics, diffusion, and surface effects, but they require more elaborate equipment and fewer samples can be studied. They frequently require much more time, and some information cannot be obtained within the time limits of the NNWSI.

One modification of this batch method uses machined wafers, or disks, of tuff instead of crushed-rock samples. The technique, discussed in Sec. IV.C of this report, gives similar results when the two methods can be compared.

Another modification of the batch technique involves a system in which the groundwater is circulated through a column of crushed tuff. This method was studied to investigate whether the agitation of the rock in the batch studies caused effects, such as self-grinding, that might affect results. Also the ratio of rock and solution volume is closer to that in the field geologic setting, relative to the high solution-to-solid ratios that are required in the batch work. The effect of variation in solution-to-rock ratios is discussed in Sec. IV.A.13 of this report.

The behavior of radionuclides eluted through columns of crushed tuff, in which nuclides are eluted as if through ion-exchange resin columns, was studied[38] as a step to a dynamic system. The results are summarized in this section. Another step toward understanding the behavior of transport involves studying elution of tuffs through solid samples (cylinders and blocks) of tuff or samples containing real or artificial fractures. These techniques and results are discussed in Sec. IV.D.

2. Batch Measurements--Experimental Method. In batch measurements of sorptive properties, the distribution of a radionuclide between groundwater and crushed tuff is measured as a function of such parameters as contact time, concentration of sorbing element, particle size, temperature, atmosphere, and lithology.

Considerable time was spent developing a satisfactory procedure; the actinides were particularly difficult, both in preparation of traced solutions and in separation of aqueous and solid phases (Sec. II.B.1). Sorption data collected during procedure development have been included in this section when they are believed valid.

In this batch sorption procedure, the crushed-tuff sample is pretreated by contact for at least 2 weeks with well J-13 groundwater. The groundwater that is used to prepare the solution containing radionuclides (the "traced feed" solution) is pretreated by at least 2 weeks contact with tuff from the same sample as the tuff being studied; it is then filtered through a 0.05-μm Nuclepore membrane. There are slight variations in the procedure, depending on the element to be studied.

Preparation of the tuff sample is accomplished by weighing ~1 g of crushed tuff material into a weighed and washed polyethylene or polycarbonate tube with a cap, adding 20 mℓ of groundwater to the tube, shaking the mixture well, and putting the tube in a shaker to be agitated at a speed of ~200 rpm for not less than 2 weeks. At the end of the 2-week period, the sample is removed from the shaker and centrifuged for 1 hour at ~12 000 rpm. The liquid phase is decanted and the sample is reweighed and then capped; contact with traced feed solutions is started within 2 to 24 hours.

Feed solutions containing barium, strontium, cesium, cerium, europium, lime, nickel, cobalt, sodium, tin, iron, manganese, or selenium are prepared using commercially produced nuclides. The final concentrations of the elements studied in these feed solutions generally range from 10^{-6} to 10^{-9} M. The tracer is evaporated at room temperature in a polyethylene or polycarbonate container. After a few drops of HCl are added, a second evaporation is carried out. The appropriate amount and type of pretreated groundwater is added, the container is capped, and the traced solution is agitated in a shaker for 1 or 2 days. The traced feed solution is then filtered through a 0.05-μm Nuclepore membrane just before use.

Exceptions to the above general procedure include technetium, uranium, and the actinides. Because technetium volatilizes when heated in acid solution and is more stable in base, the tracer is delivered in 0.1 M amonium hydroxide solution. It is added in a small volume to the appropriate tuff-treated water in amounts to produce 10^{-3} to 10^{-9} M feed solutions. Once the dilution has been made, the solution is equilibrated for a few days and then passed through a 0.05-μm filter just before use.

Uranium-traced feed solutions are prepared from a dilution of a stock solution prepared by dissolving a weighed amount of uranyl nitrate in water that has been purified with a Millipore de-ionizing system and filtering this solution through a 0.05-μm membrane. The final preparation of a uranium-traced

feed solution consists of adding an appropriate amount of the uranium stock solution to tuff-treated water, shaking the mixture for a period of up to a week, and then filtering the solution through a 0.05-μm membrane just before use. The resulting solutions are approximately 10^{-7} M in uranium.

The preparation of americium-, plutonium-, and neptunium-traced feed solutions is done in the following manner. Americium tracer obtained from Oak Ridge National Laboratory, ^{237}Pu obtained from Argonne National Laboratory, or ^{239}Pu tracer (weapons grade) from Los Alamos is dried at room temperature in air in a polycarbonate or polypropylene container. The plutonium is treated with sodium nitrite before drying to ensure the (IV) oxidation state. The dried activity is removed from the container in two steps: (1) a 1- or 2-minute contact with tuff-treated groundwater using a vibrator or ultrasonic bath and (2) a second 1- or 2-minute contact with a fresh portion of tuff-treated water, again using an ultrasonic bath. After each contact the aqueous phase is added to a large polyethylene bottle. The solution is shaken from 1 to 2 days and then passed through 0.4- and 0.05-μm filters serially just before use. Final solutions are approximately 1×10^{-6} M for americium solutions, 1×10^{-6} M for ^{239}Pu solutions, and 4×10^{-13} M for ^{237}Pu solutions.

Contact starts when 20 mℓ of traced feed solution are added to 1 g of groundwater-treated tuff in a polyethylene or polycarbonate tube (Tube 1), the two phases are mixed thoroughly, and the sample is placed in a shaker to be agitated for a predetermined time. The time at which contact starts is noted. At the end of the sorption period, the time is noted again, and the sample is removed from the shaker and centrifuged for 1 hour at ~12 000 rpm (28 000 g). A portion of the liquid phase (the top 15 to 18 mℓ) is pipetted to a clean polyethylene or polycarbonate tube (Tube 2) and capped. The remaining liquid is carefully removed to another separate tube (Tube 3). The solid phase in Tube 1 is weighed and then prepared for counting. The liquid phase in Tube 2 is centrifuged at ~12 000 rpm for 1 hour. A portion of the liquid (the top 12 to 16 mℓ) is pipetted to a clean polyethylene or polycarbonate tube (Tube 4), capped, and centrifuged for 2 hours at ~12 000 rpm. The 2 to 3 mℓ remaining in Tube 2 is added to Tube 3. When the 2-hour centrifugation is finished, a portion of the liquid (the top 9 to 10 mℓ) is pipetted to a clean polyethylene or polycarbonate tube (Tube 5) and prepared for counting (see below). Any liquid remaining (0 to 3 mℓ) in Tube 4 is combined with the previously saved liquid (Tube 3), and the combination is used to measure pH.

After the solid phase has been sampled for counting, or after counting is complete if the solid phase is counted, the desorption step of the procedure can be started. Twenty milliliters of tuff-treated water is added to the remaining solid phase in its tube. The tube is capped and weighed and the two phases are thoroughly mixed. The sample is placed in a shaker to agitate at ~200 rpm for a predetermined time. The time at the start of desorption is noted. At the end of the desorption period, the sample is treated and separated in exactly the same manner as were the solid and liquid phases of the sorption sample.

The tracer activity in the separated phases is determined in several ways. The gamma-emitting actinides, except for uranium, are counted in the following manner. The solid phase in its polyethylene or polycarbonate container is counted in a NaI(Tl) well detector. Standards are prepared by using a known amount of the appropriate activity in geometry and conditions identical to those of the samples; these standards are counted whenever the samples are counted. Three milliliters of the liquid phase is transferred by automatic pipettor to a polyethylene counting vial and acidified by adding 1 mℓ of concentrated hydrochloric acid. The mixture is mixed well and the tube capped. These liquid samples are counted in both the NaI(Tl) well counter and in an automatic gamma scintillation counter. Alternative methods for counting plutonium samples when the tracer used is plutonium other than ^{237}Pu include radiochemical analysis of both the liquid and the dissolved solid sample or liquid scintillation counting of both fractions. The uranium sorption ratio is such that it is necessary to count only the liquid phase. When the tracer used is ^{237}U, a portion of the liquid phase is placed in a vial and gamma counted with a Ge(Li) detector. At present, natural uranium is being used as tracer, and the liquid samples are being counted by a delayed neutron counting method. The remaining elements are prepared for gamma counting in the following manner. A fraction of the solid phase is dried and weighed, then transferred to a vial, sealed, and counted with a Ge(Li) detector. The liquid samples are prepared by acidifying 10 mℓ of the aqueous phase in a vial with 1 mℓ of concentrated HCl and sealing the vial. The liquid sample is also counted with a Ge(Li) detector.

A value of the sorption ratio R_d is obtained from the batch measurements. It is defined by

$$R_d = \frac{\text{activity on solid phase per unit mass of solid}}{\text{activity in solution per unit volume of solution}} .$$

Many investigators refer to this quantity as the distribution coefficient K_d. Los Alamos prefers not to use this term except under equilibrium conditions. Los Alamos data indicate that equilibrium is not achieved in many instances, but the sorption ratio is a measurement of an element's distribution between phases under specified conditions, although not necessarily at equilibrium. Sorption from near-neutral groundwater onto a rock is complicated on tuff; it may involve many competing cations and complexed or hydrated species. Many equilibria would have to be described in equations leading to the thermodynamic quantities for sorption of an element. Later in this section some simplifying assumptions will be applied in relationships between an equilibrium constant and the distribution coefficient.

Los Alamos' previously published[1-3] and recent unpublished data are consolidated in App. A, which gives data from individual batch sorption and desorption experiments on tuffs, including the (1) parameters of contact time, (2) concentration of sorbing element in the groundwater, (3) particle size of crushed tuff, (4) temperature, and (5) atmosphere in which the experiment was conducted. Tuff samples from drill holes J-13 (Ref. 4), UE25a-1 (Ref. 39), and USW-G1 (Refs. 40 and 41) have been assigned the prefixes JA-, YM-, and G1-, respectively. At this time, in an attempt to put the results of these measurements on a common basis, any lateral variation of properties within tuff units in the Yucca Mountain region is ignored, and depth equivalents in drill hole USW-G1 are assigned to samples from the other two drill holes (Table XX). These depths are designated according to the sample's relative position within a given stratigraphic unit and compensate for vertical variations between holes. The thicknesses of the Bullfrog Member in drill hole UE25a-1 and the Tram Member in drill hole J-13 are not known at this time and are assumed to be the same as in drill hole USW-G1. Although this treatment is fairly successful for the three drill holes considered, it cannot be applied to all of Yucca Mountain because of lateral variation in other drill holes.

Previous discussions[1-3] and examination of the data in App. A indicate that sorption ratios change only slowly with contact time >1 week or that there is no definite correlation with the length of contact. For devitrified tuffs, which contain some clays but not zeolites, sorption ratios are greater (usually by factors of 2 to 3) for the finest (<38-μm) fractions of ground tuff than for the coarser fractions (Sec IV.A.9). Accordingly, in averaging the values in App. A, values for fractions containing <75-μm particles were not used except with cores for which only data for a <500-μm fraction was available.

TABLE XX

DEPTH INTERVALS OF MAJOR TUFF

STRATIGRAPHIC UNITS[a]

Tuff Stratum	Symbol[b]	Drill Hole J13	Drill Hole UE25a-1	Drill Hole USW-G1
Yucca Mountain	Tpy			60-235
Tiva Canyon	Tpc	426-1037	30-270	
Topopah Spring	Tpt	1037-1476	270-1362	235-1426
Calico Hills	Tht	1476-1821	1362-1834	1426-1802
Prow Pass	Tcp	1821-1991	1834-2333	1802-2173
Bullfrog	Tcb	1991-2851	2333-	2173-2640
Tram	Tct	2851-		2640-3558
Dacite Flow-Breccia	Tb			3558-3946

[a]Depths are given in feet.

[b]These symbols are used in the figures in this section.

The average values are given in Table XXI for sorption and in Table XXII for desorption experiments. Samples are ordered according to depth equivalent in drill hole USW-G1. Some of the values in these tables are not the exact averages of those in App. A because the numbers in the appendix have been rounded off. Data[1,2] for the cation exchange capacity and surface area are given in Table XXIII.

The uncertainties associated with averages of sorption data (such as in Table XXI) are the standard deviations of the means σ_m, defined by

$$\sigma_m = \left(\frac{\Sigma\, d_i}{n(n-1)} \right)^{1/2} ,$$

where

d_i is the deviation from the mean of the ith experimental value, and

n is the number of values.

The standard deviation of the mean is used rather than the standard deviation of the sample or the population so as to avoid including zero in the range of uncertainty when, for example, averaging a large range of

TABLE XXI

AVERAGE SORPTION RATIOS FOR PULVERIZED TUFF FROM SORPTION EXPERIMENTS[a]

Sample	Depth (ft)	USW-G1 Depth[b] (ft)	R_d (mℓ/g) Sr	Cs	Ba	Ce	Eu	Am	Pu	U	Tc	Np
JA-8	606	172	270(5)	2700(400)	435(15)		2100(300)					
YM-5	251	221	280(80)[c]	5800(800)[c]	1100(200)[c]	450000(240000)[c]	230000(40000)[c]					
YM-22	848	868	53(4)	290(30)	900(30)	1270(40)	1390(110)	1200(130)[c,d]	64(20)[c]	1.8(0.2)[c]	0.30(0.14)[c]	7.0(1.0)[c]
G1-1292	1292	1292	200(6)[e]	430(28)[e]	2100(300)[e]	66(8)[e]	140(14)[e]					
YM-30	1264	1318	260(80)	855(5)	3400(1500)	230000(100000)	160000(50000)					
JA-18	1420	1339	17000(3000)	16000(1000)	38000(18000)	2800(1400)[d]	1400(200)[d]	180(30)	120(20)	2.5(0.4)		
G1-1436	1436	1436	36000(3000)	7800(500)	150000(24000)	59000(7000)	30000(2000)					
YM-38	1504	1538	17000(2000)	13000(2000)	100000(10000)	760(140)	1600(200)	4600(1100)	140(30)	5.3(0.2)		11.0(0.7)
YM-42	1824	1802	3900(600)	17000(1000)	94000(14000)	49000(7000)	52000(4000)					
G1-1854	1854	1854	60000(14000)	13000(2000)	45000(7000)		>15000					
YM-45	1930	1873	194(14)	520(90)	1200(100)	730(100)	1600(200)					
G1-1883	1883	1883	22.0(0.2)	187(3)	182(12)	140(20)		4700(300)	77(11)			6.4(0.6)
YM-46	2002	1926	190(60)	840(6)	14000(6000)	310000(110000)	307000(110000)					
G1-1982	1982	1982	55(4)	1120(110)	700(50)	560(40)[e]	970(150)					
YM-48	2114	2019	2100(400)	9000(4000)	18000(6000)	1400(500)	2200(500)				0.15(0.02)	
YM-49	2221	2090	3200(300)	36000(3000)	42000(8000)	550(100)	1200(100)	4300(1400)	230(50)[d]		0.21(0.02)	9(3)
JA-26	1995	2173	95(35)	1500(600)	800(300)							
JA-28	2001	2178	94(20)	1640(210)	820(50)		2100(1000)					
G1-2233	2233	2233	48000(3000)[e]	13500(800)	250000(30000)	1400(300)	900(200)					
G1-2289	2289	2289	7300(500)	37000(13000)	66000(9000)		797(10)					
YM-54	2491	2330	62(12)	180(40)	400(150)	150(40)	470(40)	153(6)	80(20)	1.3(0.3)	4.2(0.5)	
G1-2333	2333	2333	180(20)	1400(130)	1500(200)		2300 (400)					
G1-2363	2363	2363	64(3)	470(40)	235(9)		730(50)					
G1-2410	2410	2410	169(1)	1250(50)	1780		440(80)					
JA-32	2533	2467	57(3)	123(4)	380(30)	82(14)	90(20)	130(30)	110	2.2(0.9)		
G1-2476	2476	2476	41(1)	700(40)	385(11)		3200(100)					
G1-2698	2698	2698	42000(3000)[e]	7700(400)[e]	63000(5000)[e]	240(30)[e]	200(30)[e]					
G1-2840	2840	2840	160(1)	2200(200)	2070(70)		4900(400)					
G1-2854	2854	2854	94(1)	1080(120)	1000(50)		1300(200)					
G1-2901	2901	2901	68(1)[e]	1290(110)[e]	1600(200)[e]	42000(3000)[e]	160000(50000)[e]					
G1-3116	3116	3116	2400(17)[e]	6600(500)[e]	12000(4000)[e]	100(10)[e]	760(60)[e]					
JA-37	3497	3286	287(14)	610(40)	760(150)		6000(800)	28000(10000)[d]	400(70)[d]	4.6(0.3)		28(7)
G1-3658	3658	3658	13000(0)	4950(50)	13500(500)	1000(200)[e]	530(40)					

[a] Ambient conditions, air, 20 ± 4°C; fractions do not contain <75-μm-diam particles except those designated by footnote e.

[b] Depth equivalent in drill hole USW-G1 according to position in geologic unit.

[c] Nonweighted average; values in parentheses are the absolute-value standard deviations of the means.

[d] Some data were rejected in averaging.

[e] Average of data for <500-μm-diam particle-size fraction (contains some <75-μm particles); no other data available.

TABLE XXII

AVERAGE SORPTION RATIOS FOR PULVERIZED TUFF FROM DESORPTION EXPERIMENTS[a]

Sample	Depth (ft)	USW-G1 Depth[b] (ft)	R_d (mℓ/g) Sr	Cs	Ba	Ce	Eu	Am	Pu	U	Tc	Np
JA-8	606	172	311(3)	4600(400)	480(50)		10000(3000)					
YM-5	251	221	320(30)[c]	8900(600)[c]	1200(120)[c]	310000(30000)[c]	36000(14000)[c]					
YM-22	848	868	59(2)	365(7)	830(100)	6500(800)	3500(200)	2500(400)[c]	1330(140)[c]	5(2)[c]	1.2(0.3)[c]	33(5)[c]
G1-1292	1292	1292	120(5)[e]	510(20)[e]	1500(100)[d,e]	600(200)[e]	600(70)[e]					
YM-30	1264	1318	210(30)	1500(100)	3100(600)	170000(15000)	11000(700)					
JA-18	1420	1339	15000(2000)	17500(700)	280000(50000)	1600(500)[d]	2400(300)[d]	1100(300)	350(140)	9.4(1.4)		
G1-1436	1436	1436	87000(12000)	24000(2000)	340000(90000)	6700(600)	5300(600)					
YM-38	1540	1538	22000	13000	260000	2600	7300	7100(1200)	1600(300)	14.8(1.0)		24(2)
YM-42	1824	1802	4100(1000)	21000(2000)	90000(30000)	44000(5000)	64000(3000)					
G1-1854	1854	1854	72000(13000)[d]	14000(2000)	150000(40000)		4800(700)					
YM-45	1930	1873	210(20)	620(110)	1310(60)	5800(600)	7300(900)					
G1-1883	1883	1883	59(1)[e]	430(4)[e]	440(10)[e]	2200(100)[e]	1350(50)[e]	7200(900)	890(60)			36(10)
YM-46	2002	1926	260(20)	1800(300)	21000(3000)	300000(50000)	31000(2000)					
G1-1982	1982	1982	322(8)[e]	2300(200)[e]	2780(120)[e]	7000(900)[e]	6370(130)[e]					
YM-48	2114	2019	2700(200)	27000(4000)	34000(7000)	128000(300)	8100(1200)				1.6(0.2)	
YM-49	2221	2090	4400(100)	39000(1000)	65000(7000)	1040(40)	2100(500)	3400(400)[d]	720(90)		2.0(0.3)	12(4)
JA-26	1995	2173	39(3)	1580(90)	450(13)		2900(200)					
JA-28	2001	2178	114(3)	2400(100)	1160(20)		12300(500)					
G1-2233	2233	2233	90000(40000)[e]	23000(6000)[e]	240000(80000)[e]	20000(13000)[d]	5000(2000)[e]					
G1-2289	2289	2289										
YM-54	2491	2330	97(9)	310(20)	660(20)	1000(200)	1840(110)	550(80)	720(40)	12(8)	2.0(0.3)	
G1-2333	2333	2333	140(13)	1230(100)	1460(130)		9900(1200)					
G1-2363	2363	2363	150(6)[e]	1200(30)[e]	820(20)[e]	130000(6000)[e]	6100(300)[e]					
G1-2410	2410	2410	140(14)	1120(100)	1760(150)		6000(3000)					
JA-32	2533	2467	53(3)	175(11)	490(40)	530(120)	850(130)	2200(600)		8(2)		
G1-2476	2476	2476	200(4)	1520(0)								
G1-2698	2698	2698	210000(50000)[e]	17000(1100)[e]	190000(80000)[e]	2000(400)[e]						
G1-2840	2840	2840	150(4)	2300(130)	2500(200)		9000(1100)					
G1-2854	2854	2854	96(1)	1160(20)	1330(0)		5000(200)					
G1-2901	2901	2901	67(1)[d,e]	1380(30)[e]	1980(30)[e]	39000(1000)[e]	210000(50000)					
G1-3116	3116	3116	24000(13000)[e]	11000(3000)[e]	160000(80000)[e]	3000(1000)[e]	8000(3000)[e]					
JA-37	3497	3286	312(9)	850(50)	920(40)		11000(2000)	32000(10000)	1400(300)	9.9(0.4)		170(50)
G1-3658	3658	3658	12000(3000)[e]	12000(2000)[e]	10000(4000)[e]	9000(4000)[e]	9000(3000)[e]					

[a] Ambient conditions, air, 20 ± 4°C; fractions do not contain <75-μm diam-particles except those designated by footnote e.

[b] Depth equivalent in hole drill USW-G1 according to position in geologic unit.

[c] Nonweighted average; values in parentheses are the standard deviations of the means.

[d] Some data were rejected in averaging.

[e] Average of data for <500-μm-diam particle-size fraction (contains some <75-μm particles); no other data available.

TABLE XXIII

CATION EXCHANGE CAPACITY AND SURFACE AREA

Sample	Mesh Size (μm)	Cation Exchange Capacity (meq/100 g) Cs	Sr	Surface Area (m^2/g)
JA-18	106-150	75	48	31
JA-18	355-500	80	44	46
JA-32	106-150	2	2	8,8[b]
JA-32	355-500	2	3	9
JA-37	106-150	17	63	94,115[b]
JA-37	355-500	18	30	131
YM-22	106-500	2	3	22
YM-38	106-500	109	54	103
YM-45	106-500	6	6	43
YM-48	106-500	51	21	19
YM-49	106-500	107	47	
YM-54	106-500	4	4	

[a]By the glycol method.[1]

[b]The two values are from separate determinations.

R_d values from individual determinations, all of which indicate a high sorption ratio. The total spread of values averaged in the measurements is often a factor of 5 larger than σ_m. This is the result of the choice of σ_m just discussed, the nonweighted averaging, and the simplifying assumption that the samples belong to the same population when averaging results for different times, particle sizes, etc. These uncertainties should not necessarily be used in assessment calculations as bounds for K_d values within a given unit.

3. Lithology. The lithologies of the samples were determined by a number of analytical techniques,[4,39,40] including x-ray diffraction, optical microscopy, and electron microprobe. Table XXIV lists the petrologic characterization of samples selected for this work in the various particle size ranges. The actual depths of the samples from the drill holes, the equivalent depth in drill hole USW-G1, and the stratigraphic unit are also listed. The

TABLE XXIV

PETROLOGIC CHARACTERIZATION OF TUFF SAMPLES[a]

Sample	Depth (ft)	Equiv. USW-G1 Depth[b] (ft)	Particle Size (μm)	Abundance (%) Smectite	Illite Muscovite	Clinoptil-olite	Quartz	Cristob-alite	Alkali Feldspar	Glass	Other[c]	Dry Bulk Density (g/cm^3)	Degree of Welding[d]	Oxidation State[e]	Crystals (%)	Lithics (%)	Unit[f]
JA-8	606	172	all	25-50	--	--	--	10-20	tr	25-50	--		N		8.9	6.7	Tpc
"	"	"	75-500	30-60	--	--	<5	10-20	--	20-50	--						"
"	"	"	<75	30-60	--	--	--	10-20	--	30-60	--						"
YM-5	251	221	all[g]	10	--[h]	--	<5	<5	10-20	~70	--		N		10.9	4.3	Tpc
YM-22	848	868	all	5-10	--	--	40-60	--	40-60	--	--	2.3	D	C6(2-7)	1.0	0.4	Tpt
"	"	"	106-500	<5	<2	--	30-50	--	30-50	--	--						"
"	"	"	38-106	<2	tr	--	30-50	--	30-50	--	--						"
"	"	"	<38	<5	<2	--	30-50	--	30-50	--	--						"
G1-1292	1292	1292	all	tr	--	--	--	5-10	10-20	80-90	--		V	C1			
"	"	"	75-500	--	--	--	--	15-30	10-20	40-60	--						
YM-30	1264	1318	all	5-10	5	5-10	40-60	5-15	30-50	--	--	2.1	D	C5(2-7)	2.1	21.6	"
"	"	"	75-500	--	--	15	30	20	35	--	--						
"	"	"	<75	--	--	15	30	20	35	--	--						
JA-18	1420	1339	all	5	5	5-10	--	15-25	15-25	~50	--		N	C3(2-5)	1.8	11.9	"
"	"	"	355-500	~5	--	10-20	--	30-50	30-50	~40	--						"
"	"	"	106-150	~5	~5	10-20	--	30-50	30-50	~40	--						"
G1-1436	1436	1436	75-500	<5	<5	75-90	5-10	--	~5	--	--	1.6		C6(5-7)	5.2	3.2	Tht
YM-38	1504	1538	106-500	5-10	<2	30-50	15-30	10-20	5-15	--	A,tr	1.8	N	C5(4-6)	4.0	7.7	"
"	"	"	38-106	5-10	<5	40-60	2-10	10-20	5-15	--	--						"
"	"	"	<38	5-15	<5	40-60	2-10	10-20	10-20	--	A,tr						"
YM-42	1824	1802	75-500	tr	<5	20	35-40	--	40	--	--	2.3			15.6	46.6	"
"	"	"	<75	tr	tr	20	40	--	40	--	--						"
G1-1854	1854	1854	75-500	5-10	--	30-50	5-15	15-30	20-40	--	--						Tcp
"	"	"	<75	5-10	--	40-60	20-40	15-30	10-30	--	--						"
YM-45	1930	1873	all	1-5	--	--	40-60	tr	30-50	--			N	C4(3-5)	13.5	0.6	"
G1-1883	1883	1883	75-500	<2	<5	--	30-50	--	50-70	--	--	1.7	P	C4(3-5)	16.6	1.0	"
"	"	"	106-500	<2	<2	--	20-40	0-10	40-60	--	--						"
"	"	"	38-106	<2	<5	--	30-50	0-10	30-50	--	--						"
"	"	"	<38	2-5	<2	--	20-40	0-10	40-60	--	--						"
YM-46	2002	1926	all	<5	<5	--	40-60	--	35-55	--	--	2.1	D		12.7	0.3	"
"	"	"	75-500	<5	--	--	50	--	45	--	--						"

TABLE XXIV (cont)

Sample	Depth (ft)	Equiv. USW-G1 Depth[b] (ft)	Particle Size (μm)	Abundance (%) Smectite	Illite Muscovite	Clinoptilolite	Quartz	Cristobalite	Alkali Feldspar	Glass	Other[c]	Dry Bulk Density (g/cm^3)	Degree of Welding[d]	Oxidation State[e]	Crystals (%)	Lithics (%)	Unit[f]
G1-1982	1982	1982	all	tr	<5	--	5-15	40-60	30-50	--	--	1.8	N	C2	13.2	0.4	"
"	"	"	75-500	5-10	<2	--	--	--	70-90	--	--						"
"	"	"	38-106	<2	--	--	--	40-60	40-60	--	--						"
"	"	"	<38	10-20	--	--	--	30-50	20-40	--	C,<2						"
YM-48	2114	2019	all	tr	--	10-20	--	--	20-30	40-60	--						"
"	"	"	108-500	<2	--	20-40	5-10	5-15	20-40	10-30	--						"
YM-49	2221	2090	all	tr	tr	10-20	--	--	20-30	40-60	--	2.0	P	C6(5-7)	8.0	1.4	Tcp
JA-26	1995	2173	all	--	--	tr	30-50	tr	10-20	--	A,30-50		N		18.3	1.0	"
JA-28	2001	2178	all	tr	2.5	--	30-50	--	10-20	--	A,30-50				20	5	Tcb
G1-2233	2233	2233	<500	<5	<5	20-40	15-20	10-20	10-20	--	M,20-40	1.5	N	C6(6-7)	15.4	0.4	"
"	"	"	75-500	<5	5-15	15-30	5-10	--	40-60	--	M,<5						"
"	"	"	38-106	<5	~5	20-40	15-30	10-20	10-20	--	M,20-40						"
G1-2289	2289	2289	75-500	--	5-10	30-50	<5	--	30-50	--	M,10-20	1.6	N	C6(5-7)	15.8	1.0	"
YM-54	2491	2330	all	tr	tr	--	50-70	--	20-40	--	--	2.1	W	C5(4-7)	17.8	0	"
"	"	"	106-500	5-10	2-5	--	30-50	--	25-45	--	--						
"	"	"	38-106	5-10	5-10	--	30-50	--	30-50	--	--						
"	"	"	<38	5-10	2-10	--	15-30	--	40-60	--	--						
G1-2333	2333	2333	75-500	2-5	2-5	--	15-30	10-30	50-70	--	--						
"	"	"	<75	5-10	<5	--	15-30	20-40	20-40	--	--						
G1-2363	2363	2363	all	10-20	5-10	--	30-50	--	30-50	--	--	1.9	M	C6(5-7)	20.4	0.2	"
"	"	"	106-500	5	<2	--	30-50	0-10	30-50	--	--						"
"	"	"	38-106	5	<2	--	30-50	0-10	30-50	--	--						"
"	"	"	<38	5-10	<2	--	20-40	0-10	40-60	--	--						"
G1-2410	2410	2410	75-500	5-10	<2	--	20-40	0-10	30-50	--	--						"
"	"	"	<75	5-10	<5	--	20-40	5-15	30-50	--	--						"
JA-32	2533	2467	106-500	<5	5-15	--	30-50	--	30-50	--	--						"
"	"	"	355-500	--	5-10	--	40-50	--	30-40	--	--						"
"	"	"	150-180	--	10-15	--	35-50	--	40-65	--	--						"
"	"	"	106-150	<5	5-15	--	30-50	--	30-50	--	--						"
"	"	"	38-106	<2	tr	--	30-50	--	30-50	--	--						"
"	"	"	<38	5-10	--	--	20-40	--	40-60	--	A,tr						"
G1-2476	2476	2476	75-500	<2	~2	--	30-50	5-15	40-60	--	--						"
"	"	"	<75	2-5	~2	--	30-50	5-15	40-60	--	--						"

TABLE XXIV (cont.)

Sample	Depth (ft)	Equiv. USW-G1 Depth[b] (ft)	Particle Size (μm)	Abundance (%) Smectite	Illite Muscovite	Clinoptilolite	Quartz	Cristobalite	Alkali Feldspar	Glass	Other[c]	Dry Bulk Density (g/cm^3)	Degree of Welding[d]	Oxidation State[e]	Crystals (%)	Lithics (%)	Unit[f]
G1-2698	2698	2698	all	<5	10-15	30-50	<5	--	30-50	--	M,<5	1.8	N	C6(5-7)	13.2	1	Tct
G1-2840	2840	2840	75-500	2-5	2-5	--	40-60	0-10	30-50	--	--						"
"	"	"	<75	2-5	2-5	--	40-60	0-10	30-50	--	--						"
G1-2854	2854	2854	75-500	<2	5-10	--	30-50	0-10	30-50	--	--						"
"	"	"	<75	<2	5-10	--	30-50	0-10	30-50	--	--						"
G1-2901	2901	2901	all	5-10	5-10	--	20-40	--	40-60	--	--		W	C6(6-7)	16.5	2	"
G1-3116	3116	3116	all	5-10	5-10	5-15	20-40	--	20-40	--	A,10-30	1.9		C6(6-7)	4.0	21.4	"
JA-37	3497	3286	all	20-40	5	~5	30-60	--	15-30	--	--						Tct
"	"	"	355-500	10-15	--	tr	40-50	--	30-40	--	C,tr						"
"	"	"	106-150	5-10	--	--	40-50	--	30-40	--	C,tr						"
G1-3658	3658	3658	75-500	40-60	--	--	--	--	40-60			2.3		C3	23.4	0	Tl
"	"	"	106-500	40-60	--	--	--	--	40-60								"
"	"	"	38-106	30-50	--	--	--	--	50-70								"
"	"	"	<38	50-70	--	--	--	--	30-50								"

[a] Analyses were performed by Los Alamos ESS Division; methods are discussed in Ref. 43.

[b] Equivalent depth in hole USW-G1 according to relative position in stratigraphic unit. The thickness of the Bullfrog and Tram units in drill holes UE25a-1 and J-13, respectively, are assumed to be of the same thickness as the corresponding units in drill hole USW-G1.

[c] A = analcime; C = calcite; and M = mordenite.

[d] N = nonwelded; P = partly welded; M = moderately welded; D = densely welded; V = very densely welded (vitrophyre); and W = intermediate degree of welding.

[e] The empirical stage of oxidation of iron-titanium exsolution oxide phases; C1 denotes unoxidized and C7 denotes completely oxidized. See Ref. 44 for a discussion of oxide mineral alteration trends.

[f] Tpc = Tiva Canyon Member of the Paintbrush Tuff; Tpt = Topopah Spring Member of the Paintbrush Tuff; Tht = tuffaceous beds of Calico Hills; Tcp = Prow Pass Member of the Crater Flat Tuff; Tcb = Bullfrog Member of the Crater Flat Tuff; Tct = Tram unit of the Crater Flat Tuff; and Tl = lava flow and flow breccia.

[g] Beginning with whole rock.

[h] A blank indicates that no analysis was performed, and a dash indicates that the mineral was not detected; tr = trace ($\lesssim$1%).

average composition of >75-μm-diam. particles is plotted as a function of depth in Fig. 8 for unaltered glass and for the secondary minerals smectite, illite or muscovite, and clinoptilolite. In Fig. 9 the values are plotted in Fig. 9 for the devitrification minerals quartz, cristobalite, and feldspar and for the sum of the three. In Fig. 10, the abundances are plotted for the sum of the silica minerals quartz and cristobalite and for the zeolites analcime and mordenite. Because the Tiva Canyon Member does not occur in the USW-G1 hole, the plot includes the values measured for samples from this member in drill holes J-13 and UE25a-1 instead of the Yucca Mountain Member in drill hole USW-G1. The compositions determined[40] for a more complete suite of samples from the USW-G1 drill hole are also plotted. The compositions of the samples used for sorptive studies are in reasonable agreement with those characterized in Ref. 40, and the compositions of the samples from the three drill holes show fairly consistent trends. In a search for a glass sample, the two samples from the UE25a-1 hole in the Prow Pass Member (Tcp), which contain high percentages of unaltered glass, were selected. The lithologies of samples from the three drill holes are detailed in Refs. 4, 6, 39, 41, and 42.

The plots indicate that additional samples from some regions of high clinoptilolite and smectite should be studied to complete the analysis and that more samples in the Topopah Member (Tpt) and bedded tuffs of Calico Hills (Tht) should be studied. Because the unsaturated zone has only recently been seriously considered for a repository site, these units had not been studied in detail earlier. The plots also indicate that more samples containing high percentages of smectite, mordenite, analcime, and glass should be studied.

4. Sorption as a Function of Stratigraphic Position. The data for sorption in Table XXII are plotted in Figs. 11 through 20 as a function of the drill hole USW-G1 depth for the elements studied. Figures 12-14 indicate that the data for strontium, cesium, and barium from the three drill holes follow approximately the same trends. Sorption ratios increase from a fairly low level (relative to the maximum values) near the base of the Topopah Spring Member (Tpt), stay high through the bedded tuffs of Calico Hills (Tht), and then decrease below the top of the Prow Pass Member (Tcp) in the upper third of the unit. The ratios increase again through the rest of the unit, but the two samples from the J-13 drill hole have lower sorption ratios for the three elements. Sorption ratios in the Bullfrog Member (Tcb) are high, whereas

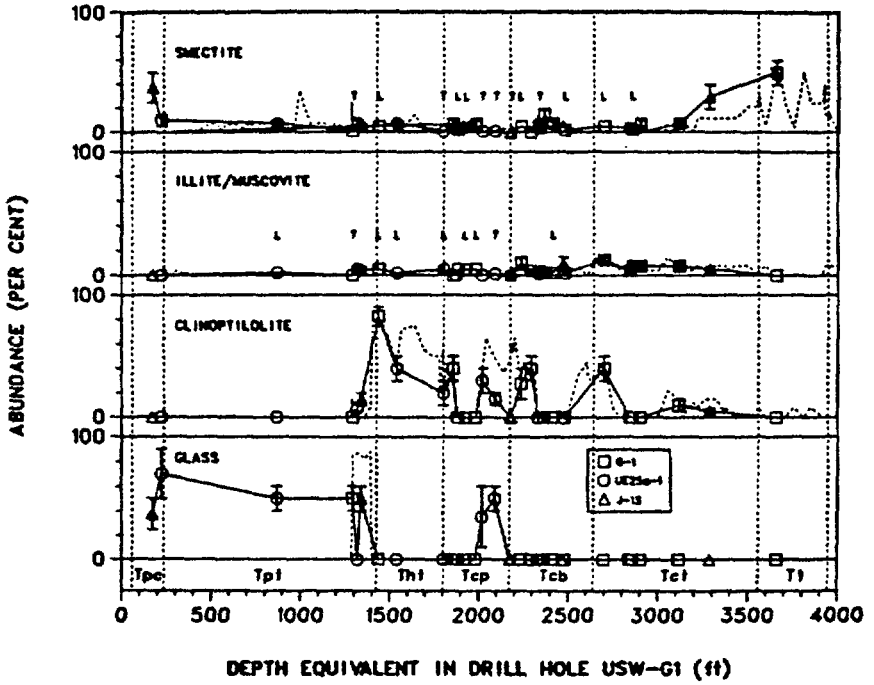

Fig. 8. Variation in mineralogy with depth for alteration minerals smectite, illite or muscovite, and clinoptilolite. Dashed lines are data for a more complete set of samples.[40] The letters T and L indicate trace (≲1%) amounts and upper limits, respectively.

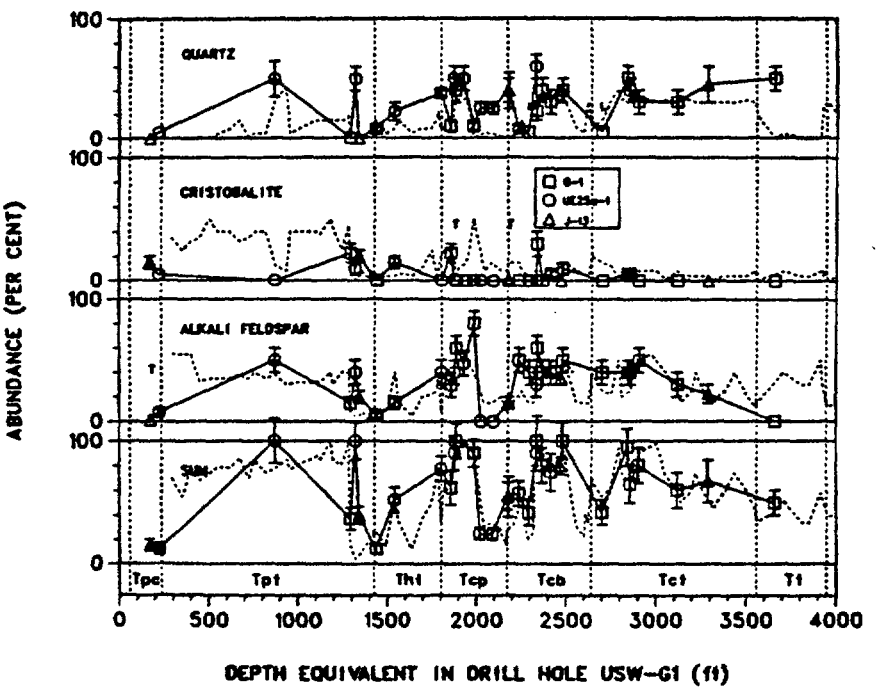

Fig. 9. Variation in mineralogy with depth for devitrification minerals quartz, cristobalite, and feldspar. Dashed lines are data for a more complete set of samples.[40] The letter T indicates trace (≲1%) amounts.

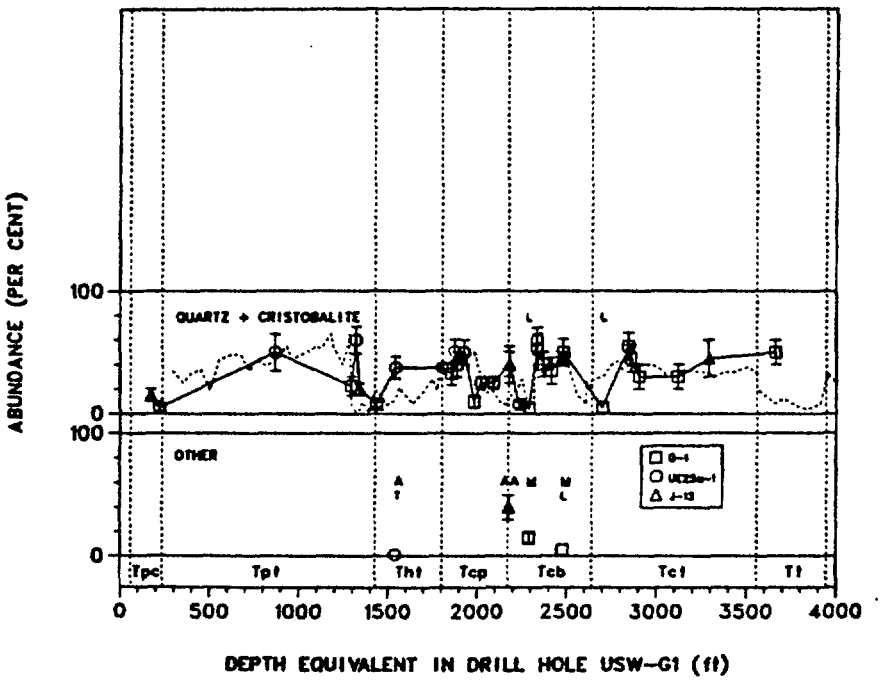

Fig. 10. Variation in mineralogy with depth (a) for the sum of silica minerals quartz and cristobalite and (b) for the zeolites analcime (A) and mordenite (M). The letters T and L indicate trace ($\lesssim$1%) amounts and upper limits, respectively.

those in the center of this unit are lower. In the Tram Member (Tct), sorption ratios are again high at the top of the unit and start to decrease with depth; however, one sample in the center of the Tram Member exhibits higher sorption ratios.

The physical and mineralogic variations within tuff units are related to the mode of emplacement and to alteration processes both during cooling and by interaction with groundwater (see, for example, Refs. 6 and 40). The lowest sorption ratios for strontium, cesium, and barium, which are thought to sorb mainly by ion-exchange reactions, are associated with devitrified tuffs. These tuffs are generally welded to some degree and contain principally quartz, cristobalite, and alkali feldspars (with some clays). The maximum sorption ratios correspond to nonwelded tuffs that contain the zeolite clinoptilolite.

The variations of sorption of cerium, europium, plutonium, and americium with stratigraphy (Figs. 15, 16, 19, and 20) are not as regular as those for strontium, cesium, and barium. The chemistry of these elements is more complex in the near-neutral groundwater (Sec. II.B). The sorption ratios for plutonium cover a fairly narrow range and are independent of sample position or mineralogy.

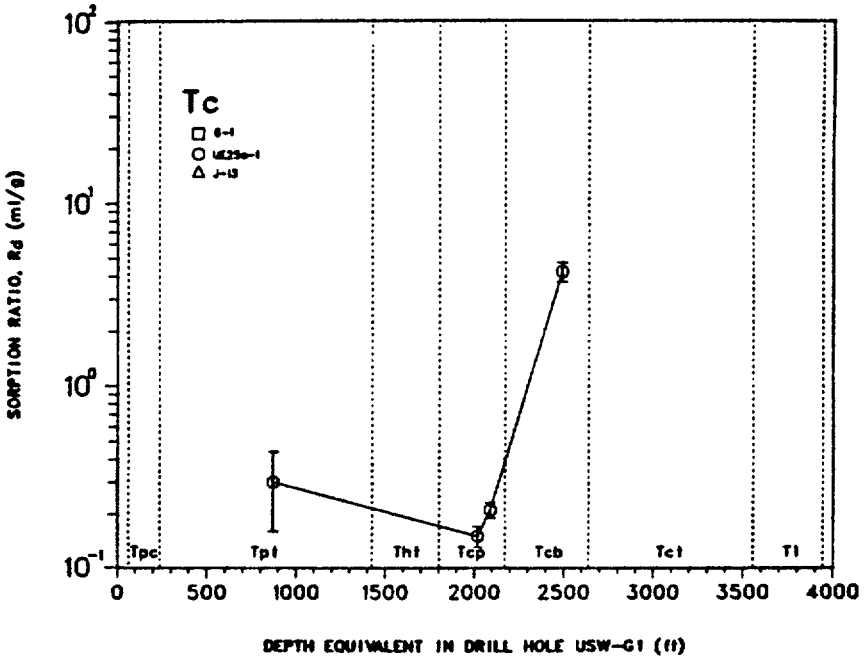

Fig. 11. Sorption ratio variation for technetium as a function of stratigraphic position. Samples are from drill hole UE25a-1.

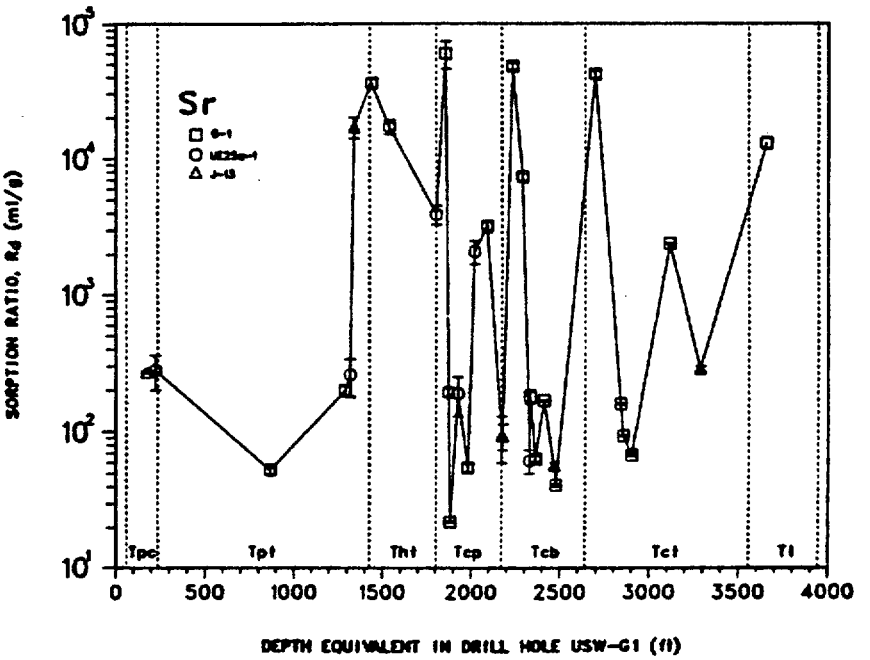

Fig. 12. Sorption ratio variation for strontium as a function of stratigraphic position. The drill holes from which each sample originated are indicated by symbols in this and subsequent figures.

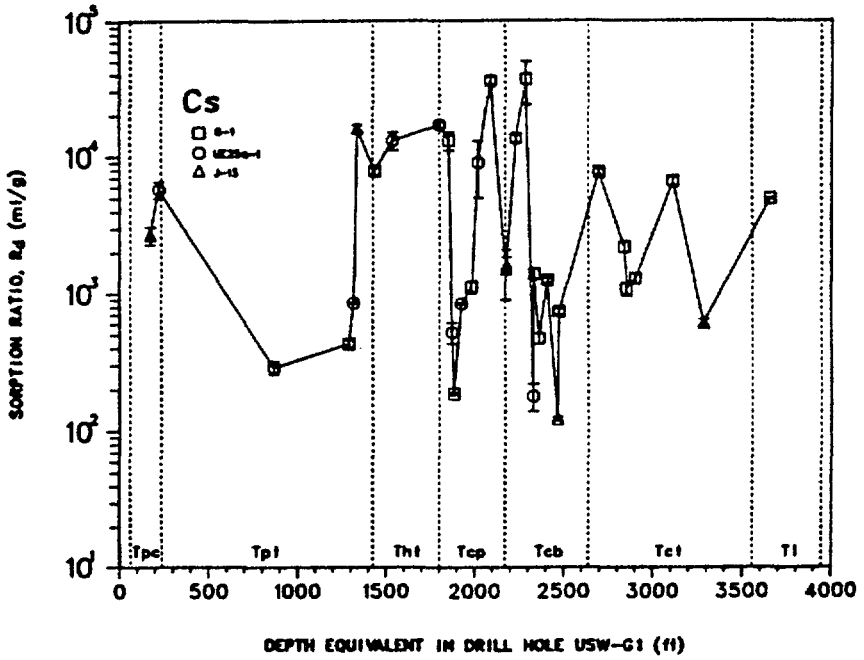

Fig. 13. Sorption ratio variation for cesium as a function of stratigraphic position.

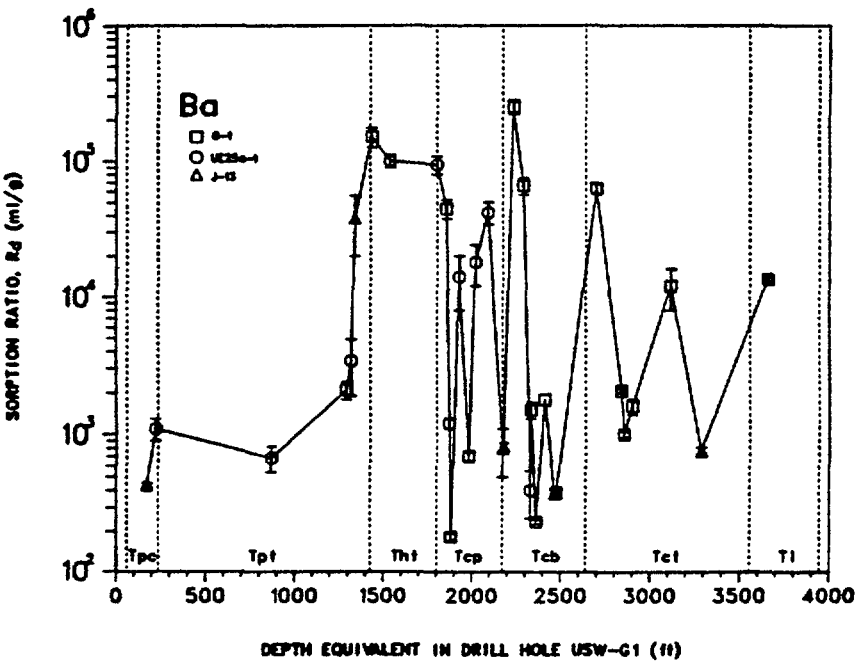

Fig. 14. Sorption ratio variation for barium as a function of stratigraphic position.

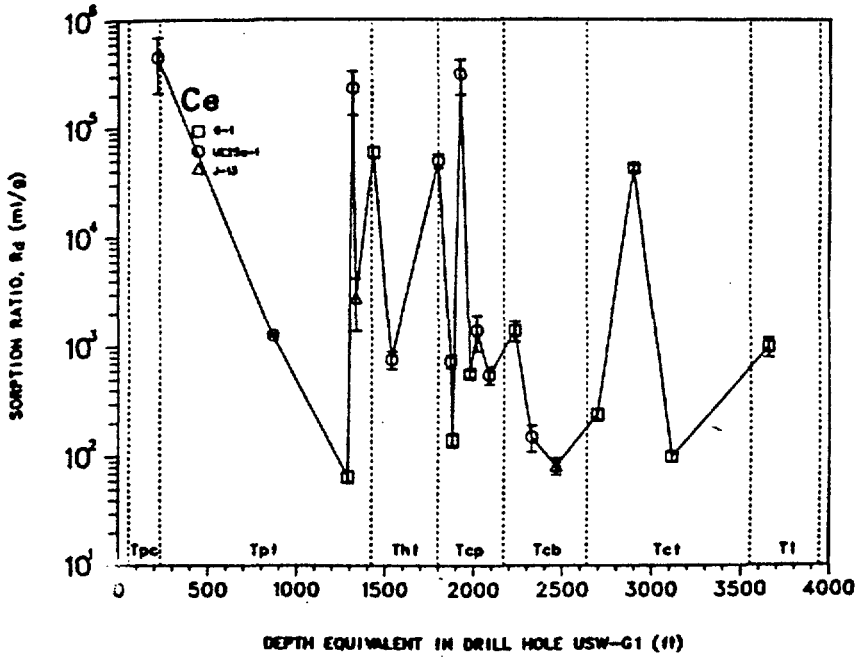

Fig. 15. Sorption ratio variation for cerium as a function of stratigraphic position.

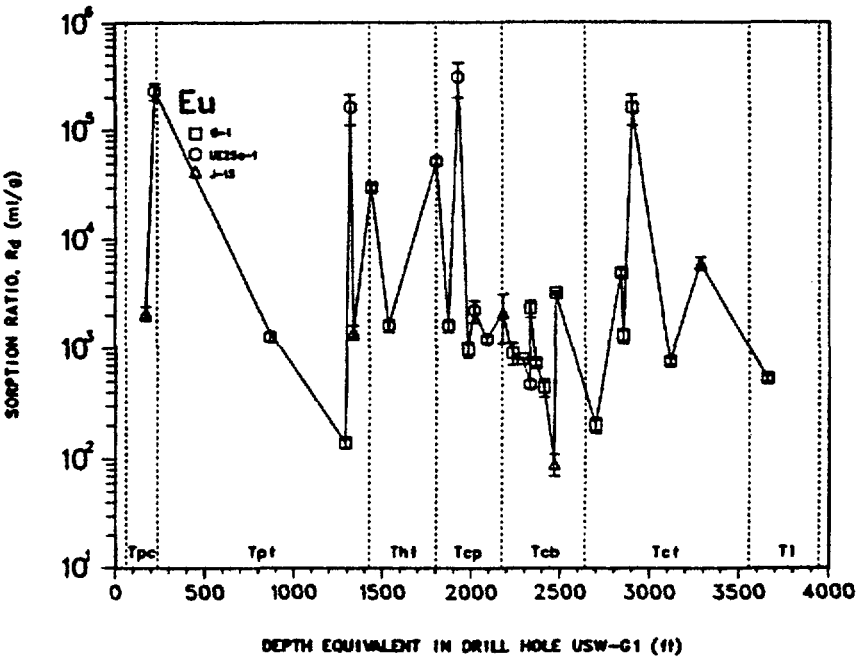

Fig. 16. Sorption ratio variation for europium as a function of stratigraphic position.

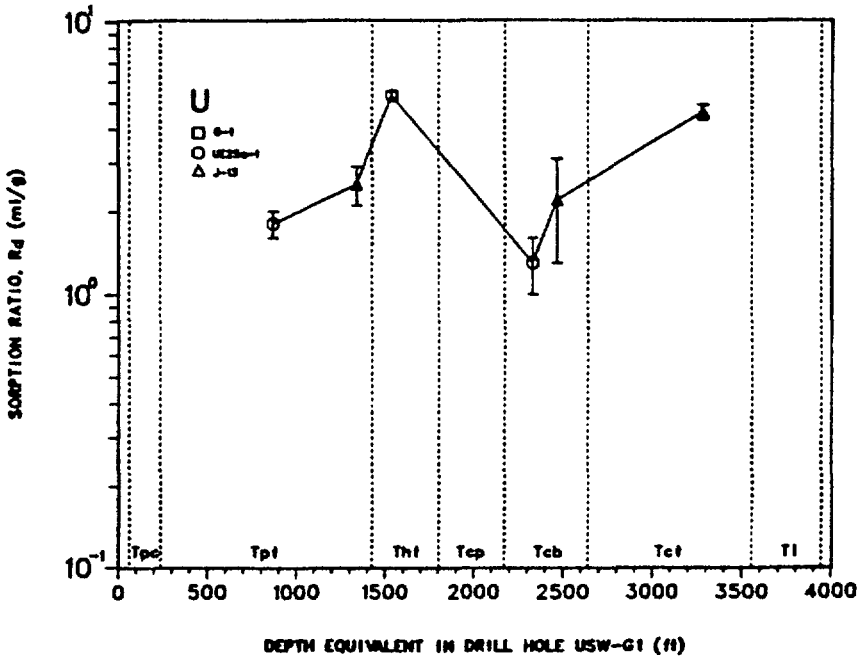

Fig. 17. Sorption ratio variation for uranium as a function of stratigraphic position.

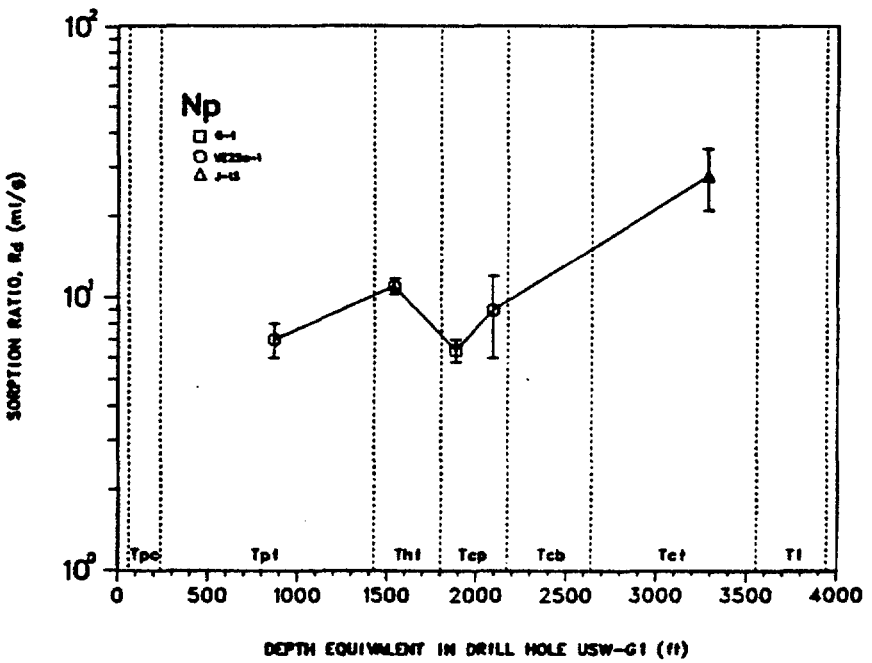

Fig. 18. Sorption ratio variation for neptunium as a function of stratigraphic position.

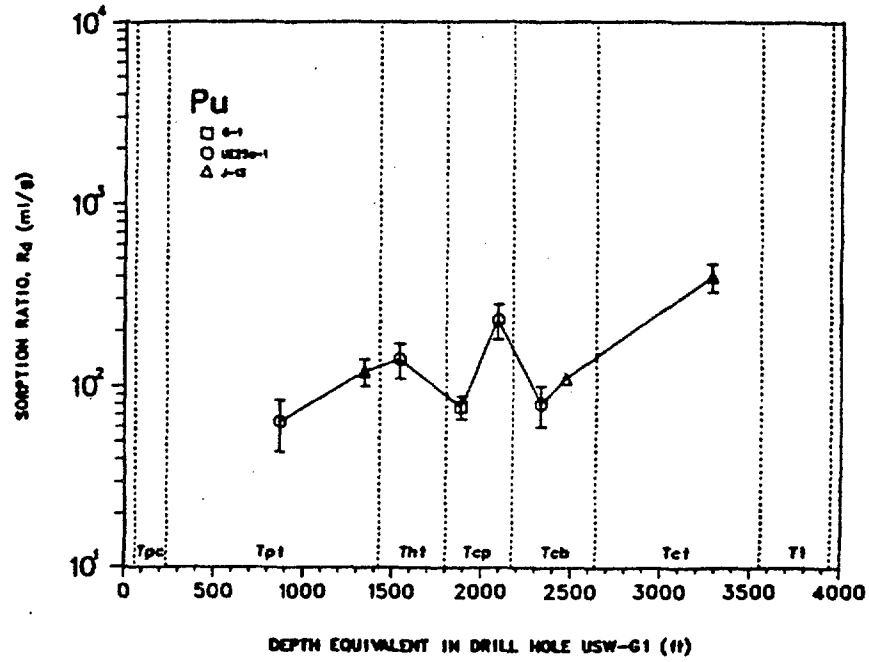

Fig. 19. Sorption ratio variation for plutonium as a function of stratigraphic position.

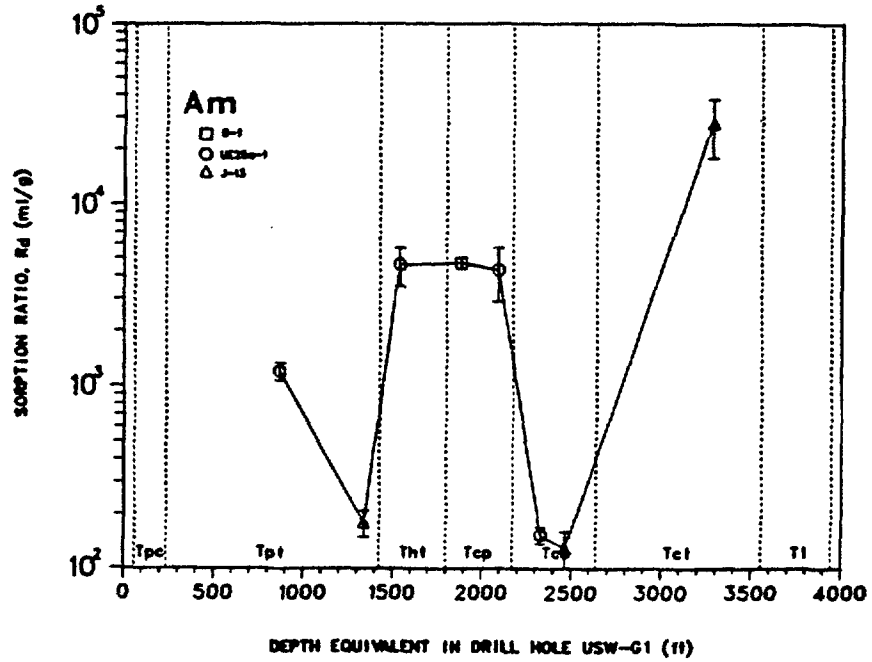

Fig. 20. Sorption ratio variation for americium as a function of stratigraphic position.

In comparing the sorption ratios for americium with sample mineralogy, there is a rough correlation of high sorption with samples containing clinoptilolite and smectite and low sorption with samples containing devitrification minerals.

Although sorption of technetium, uranium, and neptunium (Fig. 11, 17, and 18) has not been measured for many samples, the sorption ratios are relatively low; correlations with stratigraphic position cannot be made.

5. Sorption as a Function of Tuff Mineralogy. The variations of sorption of strontium and cesium (Figs. 12 and 13) and the abundance of the zeolite clinoptilolite (Fig. 8) are compared as a function of stratigraphic position in Figs. 21 and 22. The stratigraphic correspondences are quite striking, showing the correlation of increasing strontium and cesium sorption with increasing clinoptilolite abundance. A similar correlation can be made for sorption of barium by comparing the plot in Fig. 14 with the plot of clinoptilolite abundance in Fig. 8.

Sorption ratios are plotted as a function of clinoptilolite abundance in Figs. 23-25, for strontium, cesium, and barium for all of the samples studied. Again, the samples containing no clinoptilolite have significantly lower sorption ratios than those containing more than a few per cent of the zeolite. If the abundance of this zeolite is the only factor influencing sorption ratios, with no differences in sorptive properties caused by changes in the composition of the clinoptilolite (or heulandite), then there should be a linear relationship of the form

$$K_d = kc \quad ,$$

where

k is a constant, and

c is the clinoptilolite abundance (in per cent).

A nonweighted least squares fit[45] to the data points, for which the abundance of clinoptilolite is $\geq$10%, gave values of 690 ± 170, 430 ± 150, and 2300 ± 700 for strontium, cesium, and barium, respectively. The fits for strontium and cesium give K_d values of 6.9×10^4 and 4.3×10^4 mℓ/g for 100% of the pure minerals. These values are compared with those calculated (see below) using simplifying assumptions from Ames' thermodynamic data,[46,47] which used different

mineral samples, of 1.8×10^5 and 3.8×10^4 mℓ/g for strontium and cesium, respectively.

The lines in Figs. 23-25 represent these fits with the dashed lines defining $\pm 2\sigma$ envelopes. Although the least square fits are not particularly good, the points fall within the uncertainty envelopes fairly well. The dotted lines in Fig. 23 through 25 define an uncertainty of a factor of ±3 for later comparison. Most values for cesium with clinoptilolite abundances of $\geq$10% fall within this larger envelope.

One could equally well argue that all tuffs containing >10% clinoptilolite fall into one grouping for cesium and two groupings (10 to 25% and >25%) for both strontium and barium with the sorption ratio in each group known within one order of magnitude.

In Figs. 26-29, sorption ratios for technetium, cerium, europium, and americium are shown as a function of clinoptilolite abundance. There are no obvious correlations or trends with zeolite abundance; sorption ratios of samples with no clinoptilolite scatter among those for samples with the zeolite.

Sorption ratios for uranium, neptunium, and plutonium are plotted similarly in Figs. 30-32. Although there are no trends with increasing zeolitization, for each element, sorption ratios are higher for the zeolitized tuffs than for the nonzeolitized one.

Can simple correlations be made for other minerals in tuffs where clinoptilolite is absent? Consider the smectite clays: Fig. 33 shows the absence of any obvious trend for cesium when considering smectite alone in nonzeolitized samples. Similar plots for other nuclides, not shown, do not indicate any apparent correlations. Possible explanations are that (1) trace quantities of clinoptilolite, undetected by x-ray diffraction, may mask any influence of smectites, (2) combinations of all sorbing minerals contribute to the sorption ratio, and (3) sorption by clays involves other factors, such as their texture or their availability to the groundwater. One of these possibilities is discussed later in this section.

Tuff samples JA-26 and JA-28 contain the zeolite analcime. The sorption ratios for these samples, shown as triangles at the bottom of the Prow Pass Member in Figs. 8-16, do not exhibit the large values expected for clinoptilolite. Evidently, the more random structure of analcime, compared to the

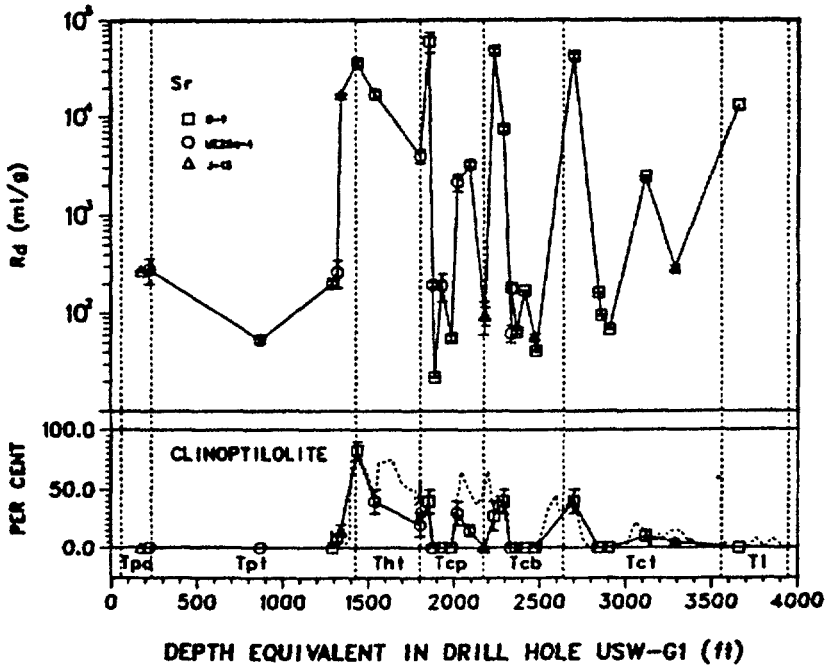

Fig. 21. Sorption ratio variation for strontium with abundance of clinoptilolite and stratigraphic position.

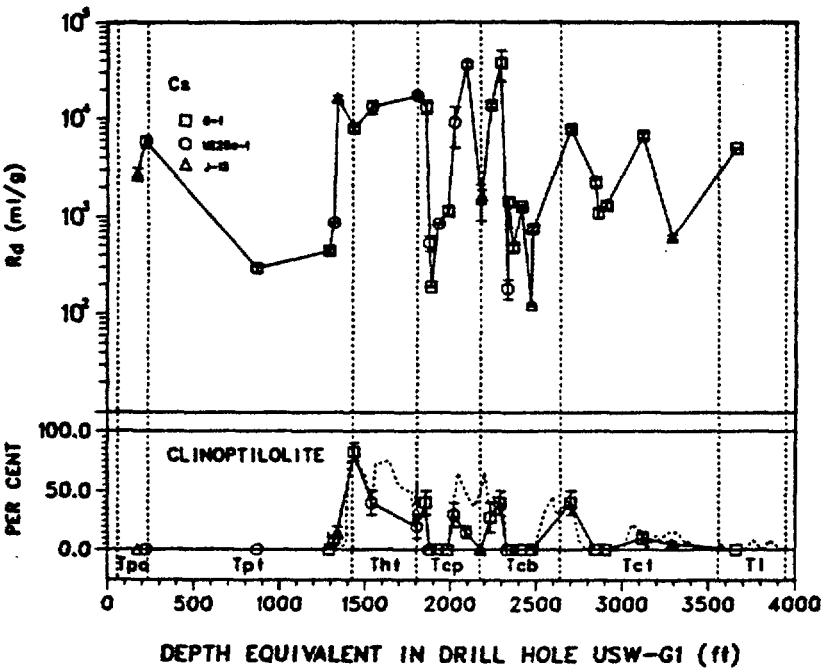

Fig. 22. Sorption ratio variation for cesium with abundance of clinoptilolite and stratigraphic position.

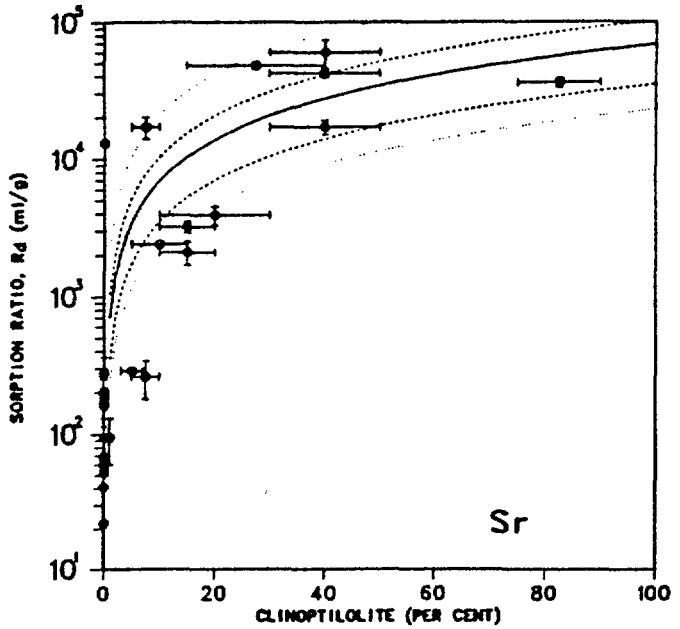

Fig. 23. Sorption ratio variation for strontium with clinoptilolite abundance. Solid line represents K_d = 6.9 x 10^4 mℓ/g for pure clinoptilolite. Dashed and dotted lines for Figs. 23, 24, and 25 indicate error bands for 2σ and factor of ±3, respectively.

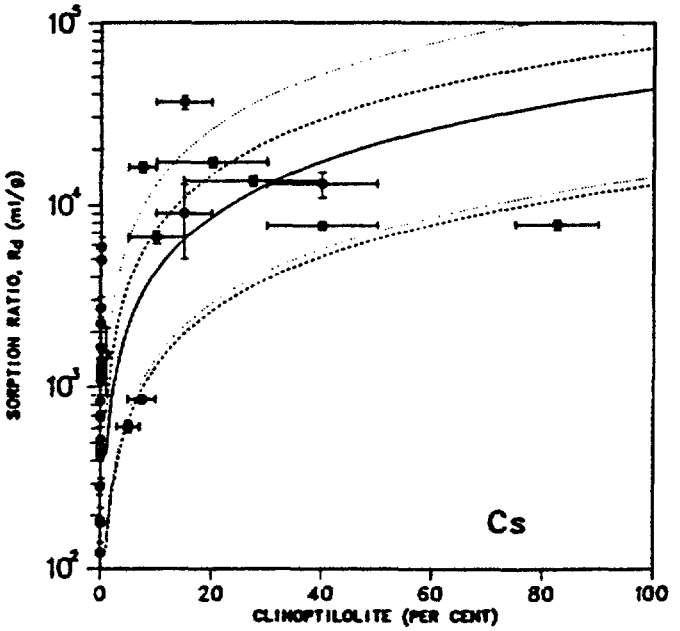

Fig. 24. Sorption ratio variation for cesium as a function of clinoptilolite abundance. Solid line represents K_d = 4.3 x 10^4 mℓ/g for pure clinoptilolite.

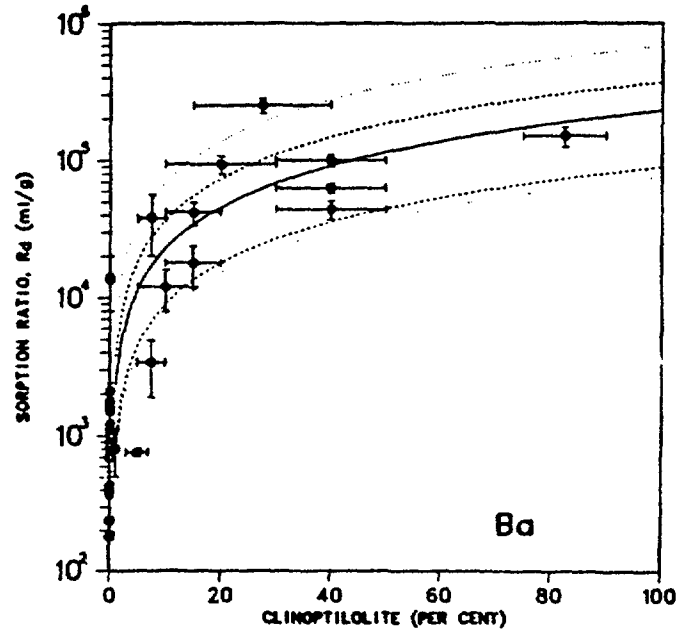

Fig. 25. Sorption ratio variation for barium. Solid line represents K_d = 2.3×10^5 mℓ/g for the pure mineral.

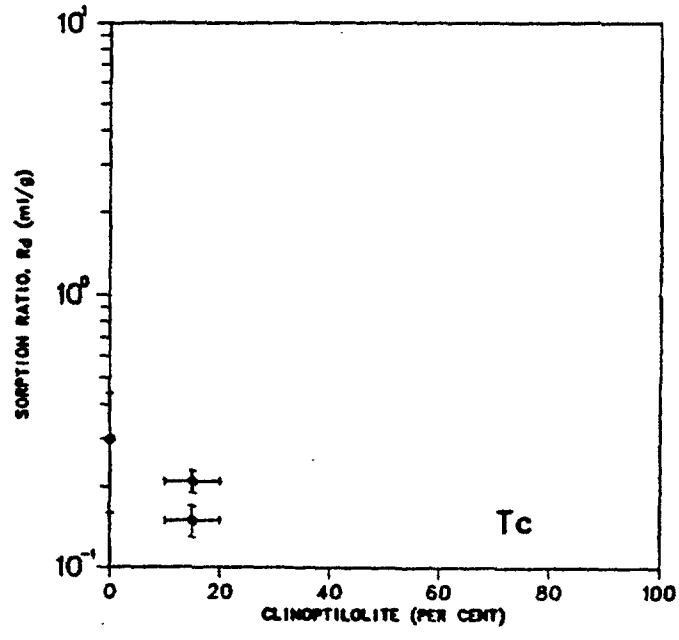

Fig. 26. Sorption ratio variation for technetium as function of clinoptilolite abundance.

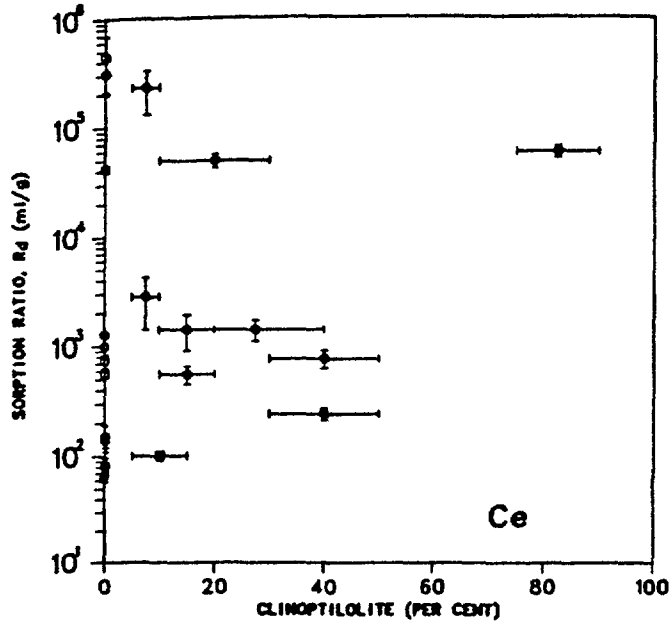

Fig. 27. Sorption ratio variation for cerium as a function of clinoptilolite abundance.

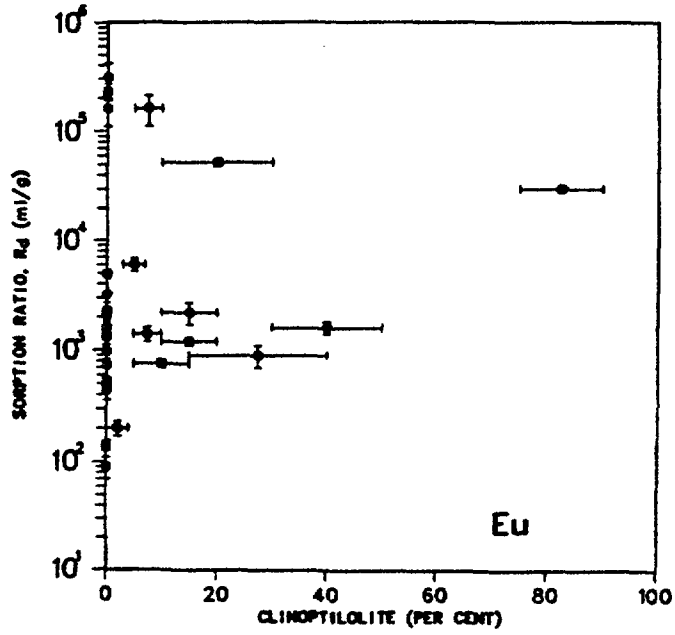

Fig. 28. Sorption ratio variation for europium as a function of clinoptilolite abundance.

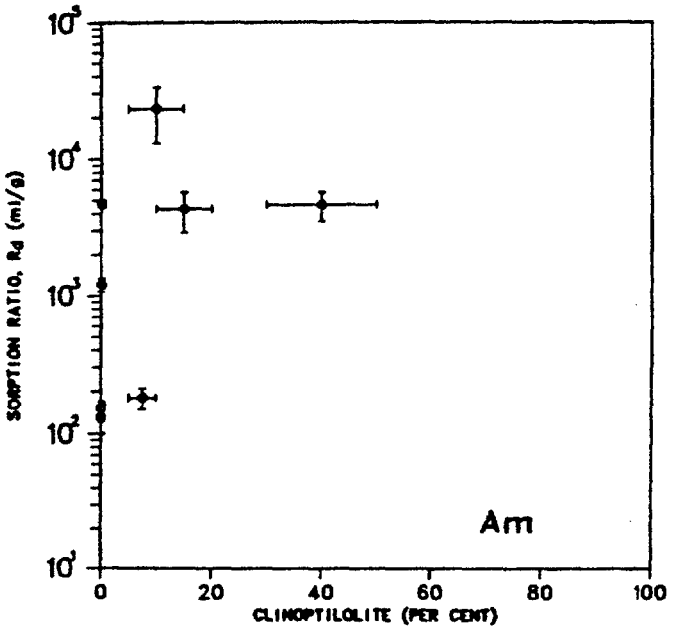

Fig. 29. Sorption ratio variation for americium as a function of clinoptilolite abundance.

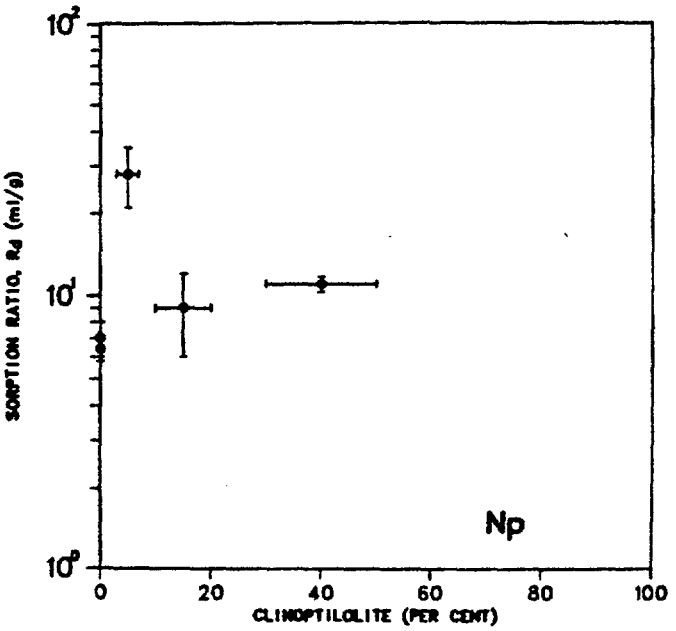

Fig. 30. Sorption ratio variation for neptunium as a function of clinoptilolite abundance.

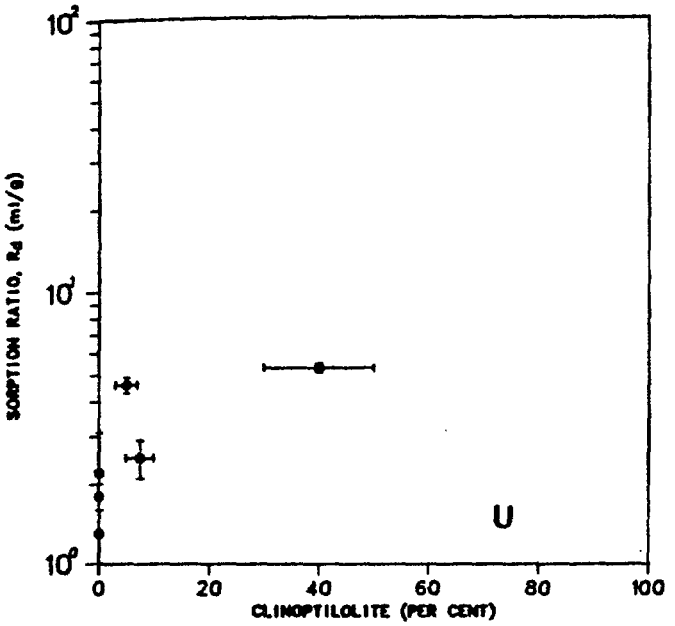

Fig. 31. Sorption ratio variation for uranium as a function of clinoptilolite abundance.

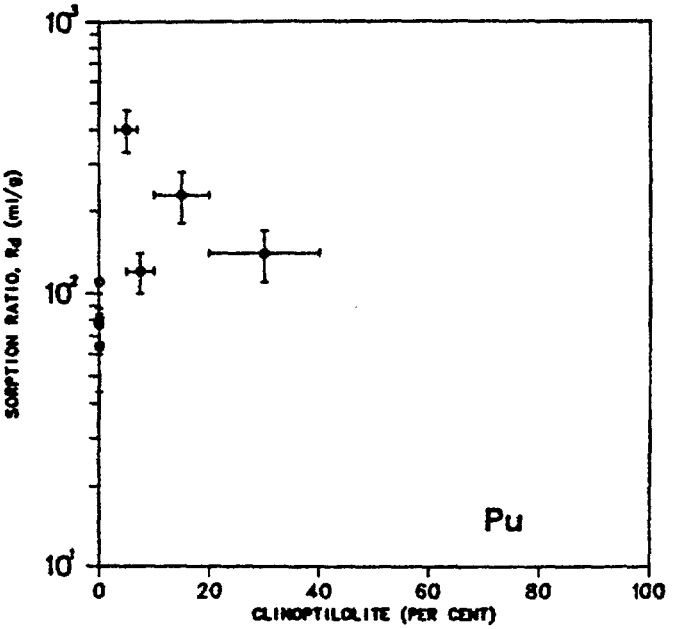

Fig. 32. Sorption ratio variation for plutonium as a function of clinoptilolite abundance.

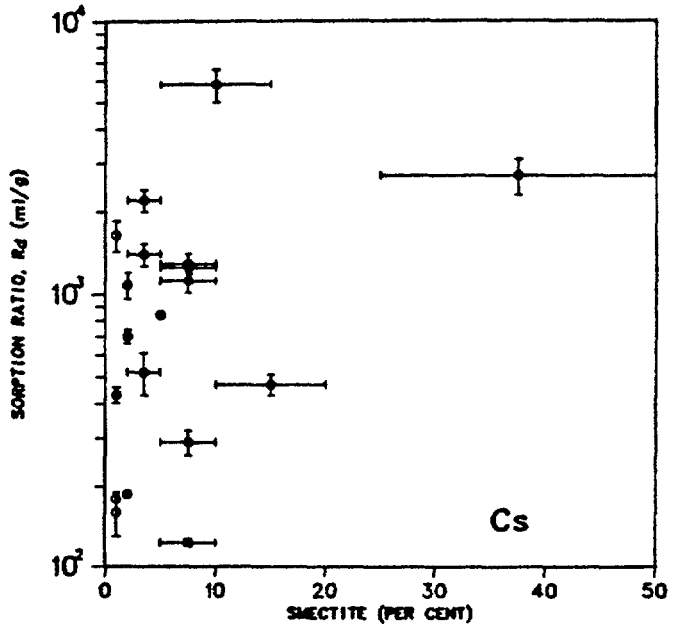

Fig. 33. Sorption ratio variation for cesium with smectite content for nonzeolitized samples.

open-cage structure of clinoptilolite,[48] inhibits exchange of ions such as strontium, cesium, and barium. The ring sizes[49-51] in analcime, ~2.2 Å, are smaller than those in clinoptilolite, 3.5 x 7.9 and 3.0 x 4.4 Å, which further inhibits in analcime an exchange of ions larger than K^+. The two mordenite-containing samples studied also contain clinoptilolite, which may have masked any effect of the mordenite.

The three tuffs containing fresh glass and no zeolites are samples YM-5, JA-8, and G1-1292. For cesium, which exchanges strongly on glass, the first two samples show sorption ratios approximately an order of magnitude higher than the third. Sample G1-1292, although very high in glass, is from the vitrophyre and probably has much less surface area, even in pulverized form, than the other two fine-grained samples. Trends for divalent strontium and barium are not as evident as for cesium.

Because tuff samples may be composed of more than one sorbing mineral, Los Alamos is currently researching ways to predict sorption ratios by combining the effects of several minerals. Tentatively, the combined effect is defined as a weighted sum, the "sorptive mineral content (SMC)," determined by

$$SMC = \Sigma W_i X_i \quad ,$$

where

W_i is the weighting factor for each mineral phase and

X_i is the abundance (%) of each phase.

The weighting factors are determined relative to clinoptilolite, to which a value of 1.0 is assigned because it is the most strongly sorbing mineral in the group. A set of values for sorption of cesium on other minerals must be obtained from data for the pure minerals or inferred from mixtures. The K_d values for clinoptilolite, mordenite, and montmorillonite are calculated from published thermodynamic data.[46,47,49-51] Some simplifying assumptions (mentioned earlier in this section) were made in applying the data to calculate K_d values for the specific tuff/groundwater cases. The assumptions are that (1) all mineral phases observed in the x-ray diffraction analyses, which are performed[40] on samples ground to <10 μm, are available for sorption, and the only competition for sorption sites is, in this case, between trace amounts of cesium and sodium; (2) the sodium concentration in the assumed groundwater is 3×10^{-3} M (the approximate ionic strength of the trace groundwater); and (3) one set of thermodynamic data applies to all samples of each mineral. The last assumption is not strictly true because samples of the same mineral from different localities, when prepared differently, gave different thermodynamic constants.[47]

Consider the following equilibrium

$$Cs^+ + Na\text{-}R = Cs\text{-}R + Na^+ \quad , \qquad (7)$$

where

Cs-R and Na-R represent the ion sorbed on a mineral.

Define

K = the equilibrium constant for equilibrium (7),

CEC = cation exchange capacity in meq/g, and

$[Na^+]$ = sodium concentration;

then,

$$K_d = (CEC)\ K/[Na^+] \quad .$$

Table XXV gives the values used for K and CEC. If clinoptilolite is the only mineral available for exchange in the samples listed in Table XXIII, then CECs of 1.7 to 5.3 and 0.7 to 3.5 meq/g for cesium and strontium, respectively, are inferred for the pure zeolite. The values obtained by Ames[46] for two clinoptilolites are 1.7 and 2.0 meq/g, and Barrer[49] gives a value of 3.3 for heulandite. Thus, there are some differences in the properties of clinoptilolite, depending on the sample.

The weighting factor for illite was somewhat arbitrarily set at 0.05 because the CEC for this mineral[52,53] is ~10 times less than that for montmorillonite. The factor for analcime was set at 0.10 to correspond to the sorption ratio for sample JA-26, which contains 40% analcime as the only sorbing mineral. The factor for glass was likewise adjusted to give the observed results for samples G1-1292 and YM-48, which contain glass as the principal sorbing phase. Quartz, cristobalite, and feldspars are assumed to have negligible contributions to sorption. The K_d values, calculated or assumed, and the corresponding weighting factors W_i are given in Table XXVI.

The sorption ratios in Table XXI are plotted as a function of SMC in Fig. 34. Figure 35 is the same plot for low values of R_d. The solid line is the theoretical line for clinoptilolite with a K_d value of 3.8×10^4 mℓ/g. The dashed lines represent an error envelope for uncertainties of a factor of 3;

TABLE XXV

VALUES USED FOR CALCULATING K_d FOR CESIUM

Mineral	K	CEC
Clinoptilolite	50[a]	2.3
Mordenite	1.8[a]	2.3[b]
Analcime		4.5[b]
Montmorillonite	48[c]	1.17[c]

[a]Ref. 47.

[b]Ref. 49.

[c]Ref. 51.

TABLE XXVI

K_d AND W_i VALUES USED IN SMC EVALUATION OF CESIUM

Mineral	K_d (mℓ/g)	W_i
Clinoptilolite	3.8×10^4	1.00
Montmorillonite	1.9×10^4	0.50
Mordenite	1.4×10^3	0.04
Analcime		0.05
Glass		0.016

most of the experimental R_d values fall within the envelope. This treatment will help predict sorptive properties for nonzeolitized as well as zeolitized tuffs; sorption of cesium is probably the simplest test of this type of concept.

6. Desorption Experiments: Reversibility. If equilibrium were established and if observed R_d values for tuffs were true K_d values, the same R_d values should be obtained from desorption and sorption experiments. The values from sorption and desorption experiments are compared as a function of stratigraphic position in Figs. 36-45. Some differences between the two types of measurement arise from large ranges in individual determinations (App. A); the averaging process, which assumed that the samples represent the same population, may not have been proper for such cases. The results for strontium and cesium from the two methods agree within ~20% for most measurements. In general, values from desorption experiments are slightly higher than those from sorption experiments. For barium there is reasonable agreement when R_d values are low (devitrified tuffs). For some of the zeolitized tuffs, however, values for barium from desorption experiments are greater than those from sorption experiments by factors of ~2 for most samples to ~10 for a few. It appears that barium sorbs on clinoptilolite somewhat more irreversibly than do strontium and cesium. For cerium, europium, and americium, the differences in R_d values (which are reasonably high) by the sorption and desorption methods are greater. A large fraction of these elements is sorbed irreversibly, although in most cases the trends from the sorption measurements with stratigraphic position are qualitatively retained in the desorption results. The differences for plutonium, which do not show discernible trends, are also approximately a

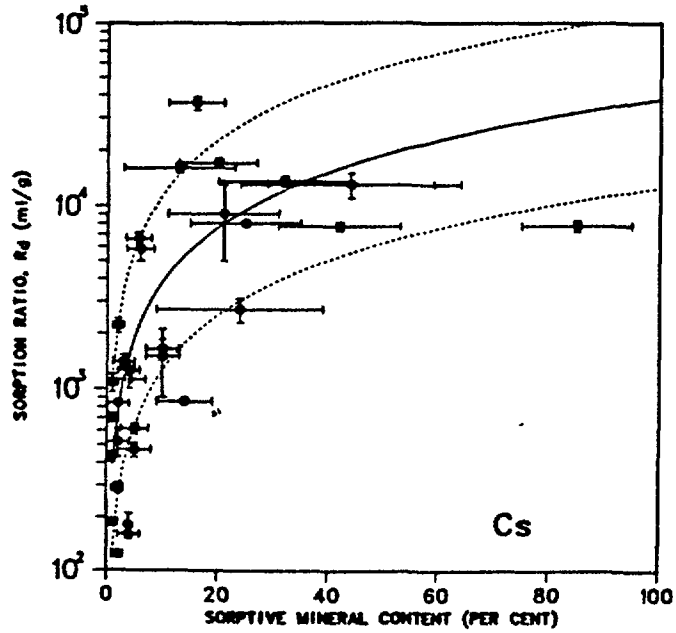

Fig. 34. Sorption ratios for cesium as a function of sorptive mineral content. Solid line is theoretical line for clinoptilolite with $K_d = 3.8 \times 10^4$ mℓ/g. Dashed lines give an uncertainty envelope of a factor of ±3.

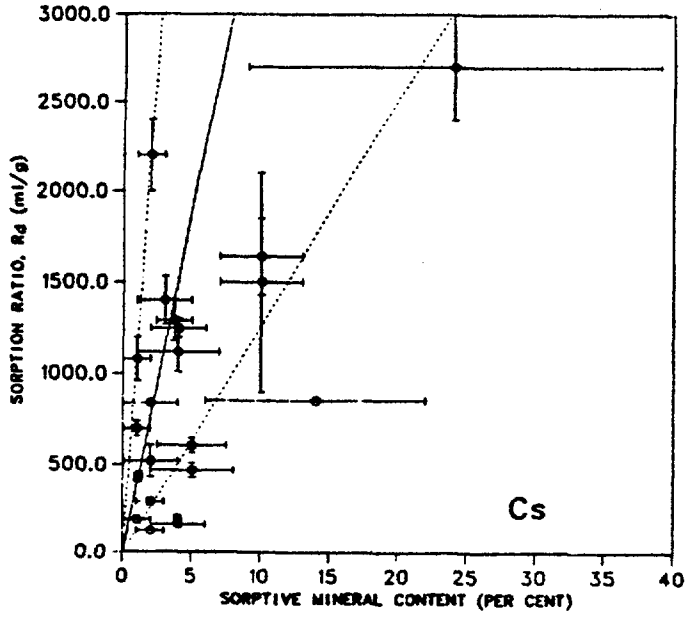

Fig. 35. Early part of Fig. 34 on linear scale.

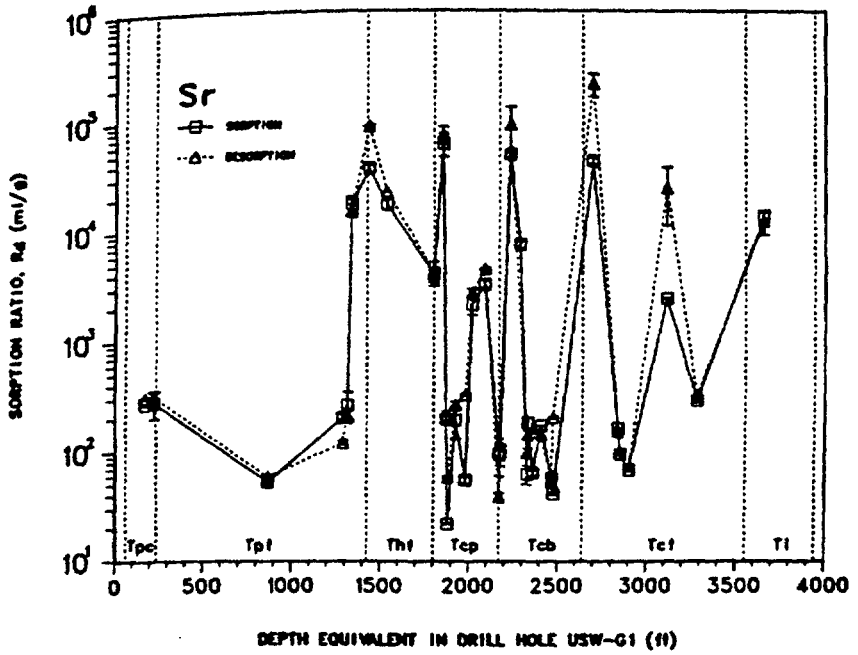

Fig. 36. Comparison of strontium ratios for sorption and desorption as a function of stratigraphic position.

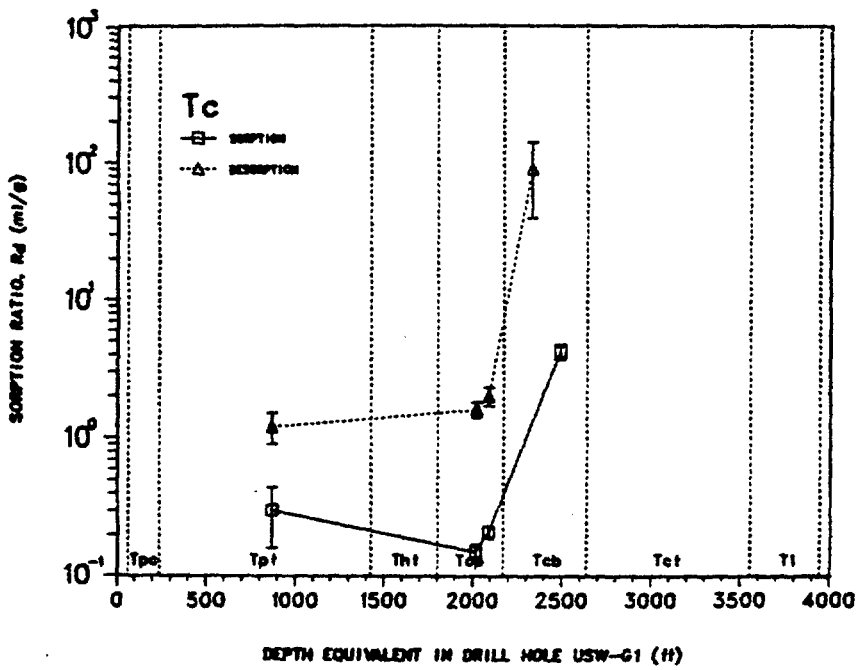

Fig. 37. Comparison of technetium sorption ratios for sorption and desorption as a function of stratigraphic position.

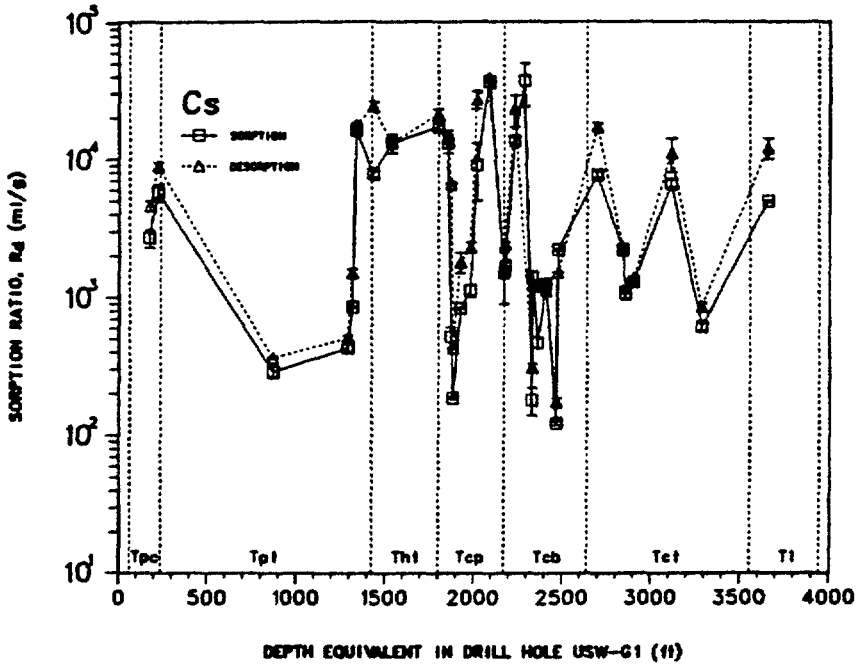

Fig. 38. Comparison of cesium sorption ratios for sorption and desorption as a function of stratigraphic position.

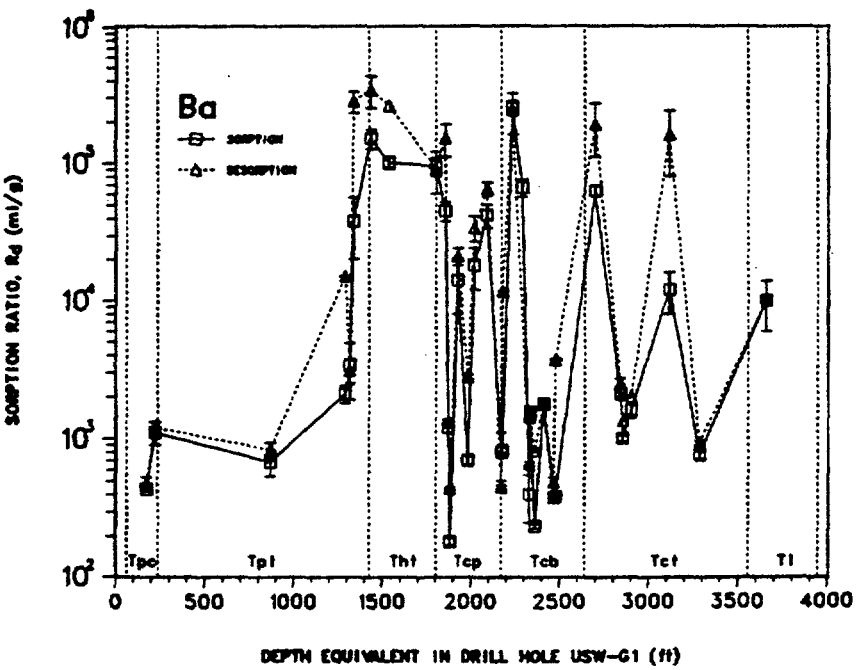

Fig. 39. Comparison of barium sorption ratios for sorption and desorption as a function of stratigraphic position.

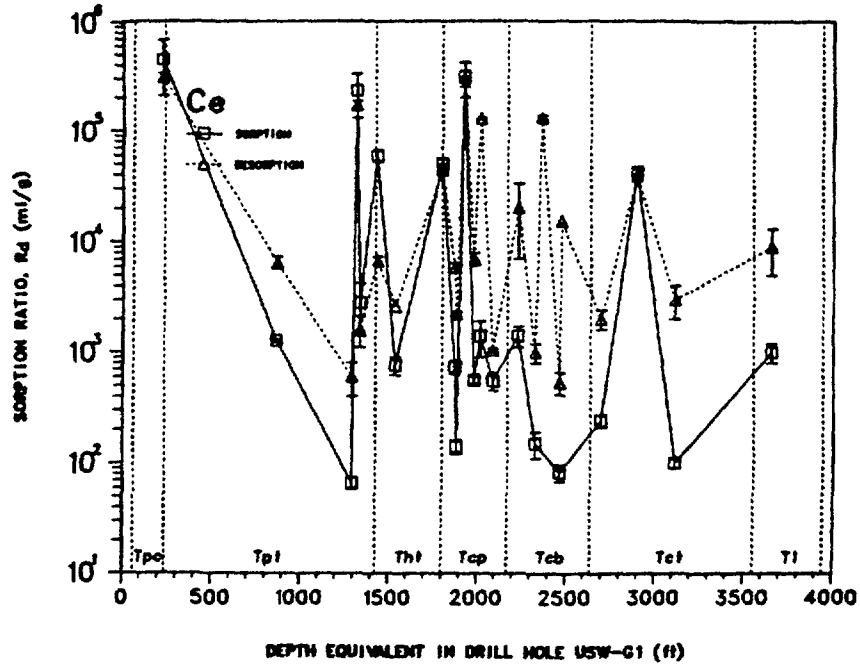

Fig. 40. Comparison of cerium sorption ratios for sorption and desorption as a function of stratigraphic position.

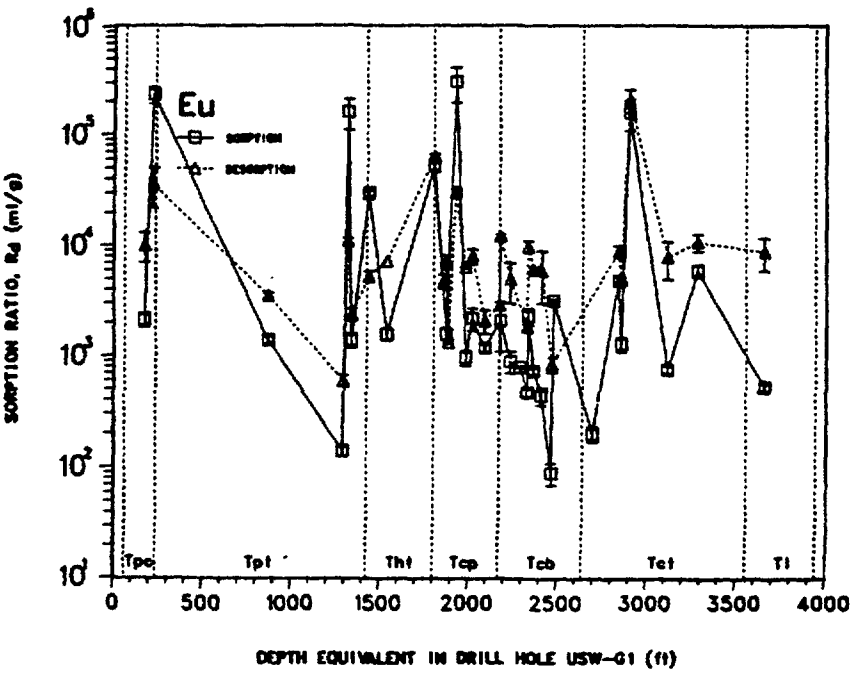

Fig. 41. Comparison of europium sorption ratios for sorption and desorption as a function of stratigraphic position.

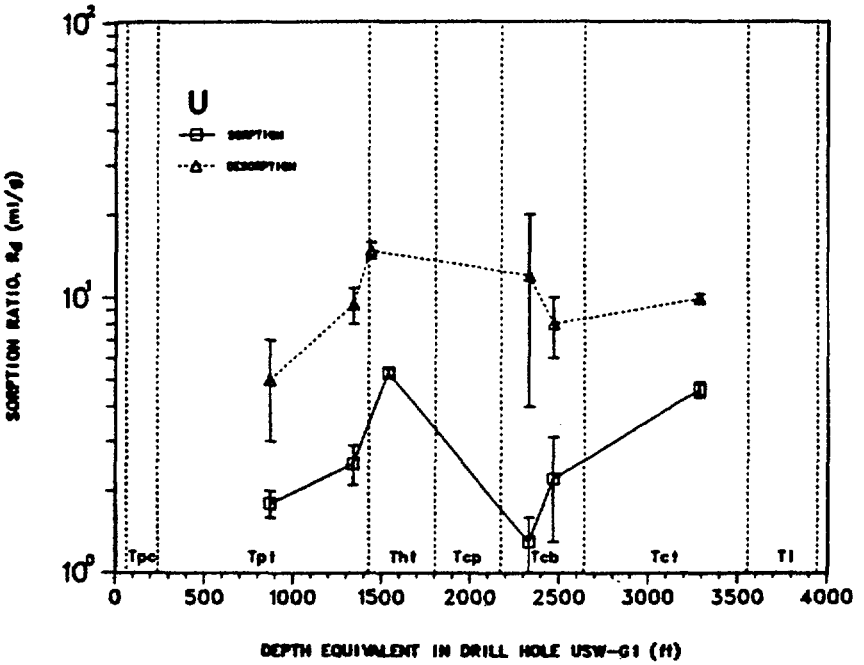

Fig. 42. Comparison of uranium sorption ratios for sorption and desorption as a function of stratigraphic position.

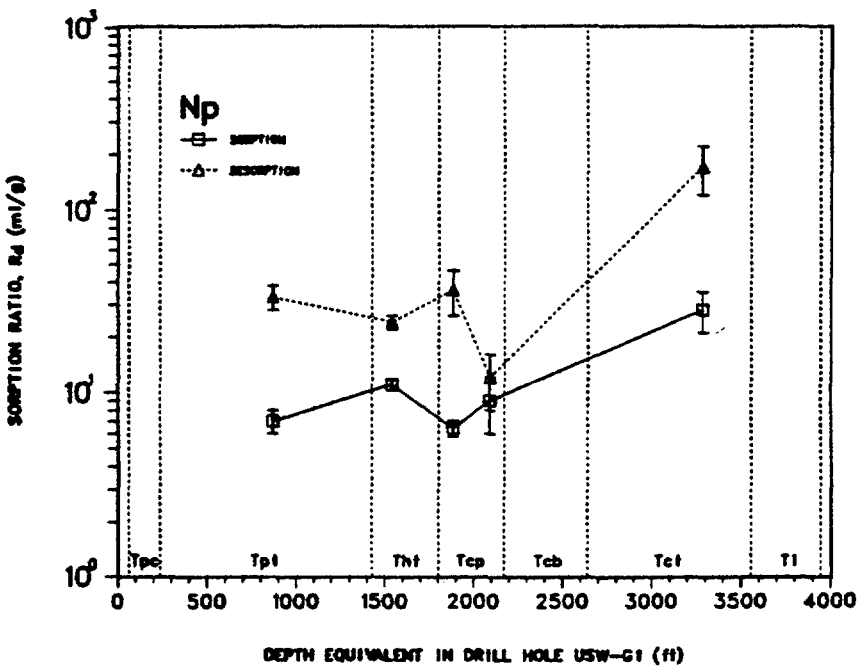

Fig. 43. Comparison of neptunium sorption ratios for sorption and desorption as a function of stratigraphic position.

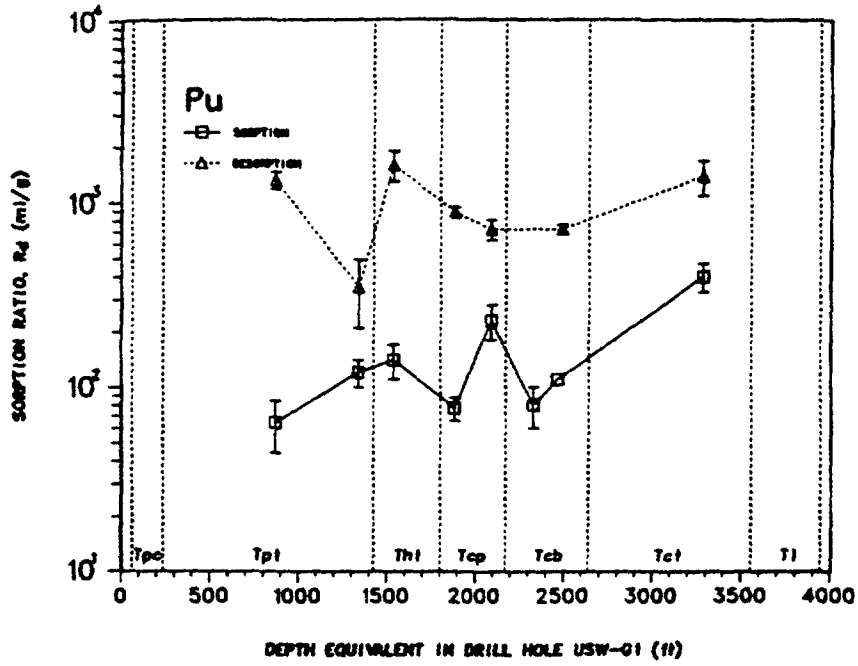

Fig. 44. Comparison of plutonium sorption ratios for sorption and desorption as a function of stratigraphic position.

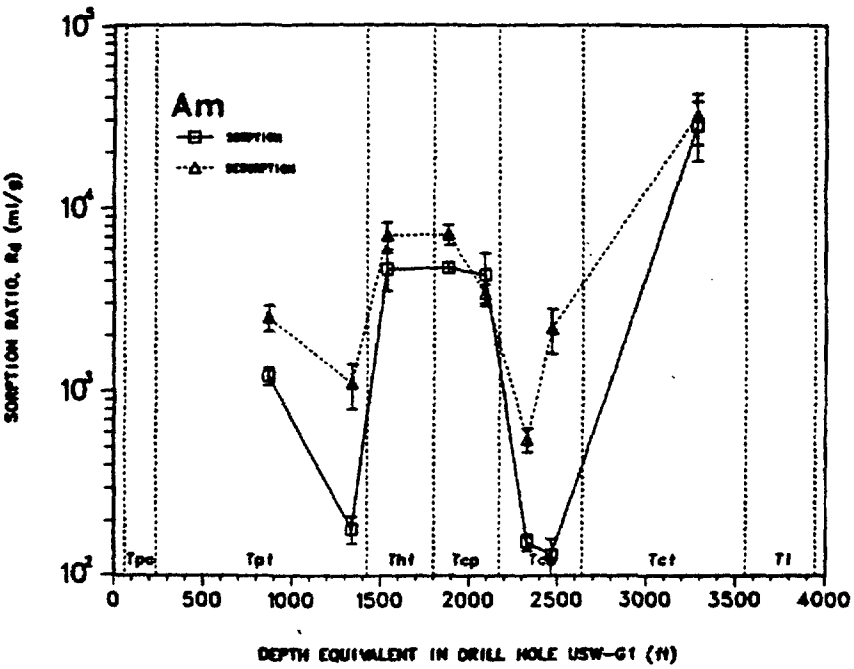

Fig. 45. Comparison of americium sorption ratios for sorption and desorption as a function of stratigraphic position.

factor of 10. Sorption ratios for technetium, uranium, and neptunium, which are low, are nevertheless significantly greater for desorption than for sorption.

7. Sorption of Actinides and Technetium. The chemistry of these elements is complex in near-neutral groundwater (Secs. II and IV.A.11). Sorption ratios for plutonium cover a fairly narrow range (less than a factor of 10) that is independent of sample position or mineralogy. Based on the limited data available, neptunium exhibits similar behavior with a range of less than a factor of 5, although the R_d values are about an order of magnitude less than those for plutonium. Americium sorption ratios show a much wider variation, from just over 100 mℓ/g to nearly 30 000 mℓ/g, but again with essentially no correlation to mineralogy. Sample JA-37 gave the highest R_d values for all three actinides, which could be related to its relatively high clay content (Table XXIV). It is worth noting that this sample gave the most unusual results among those whose sorptive behaviors were compared using both batch and circulating system techniques (Sec. IV.A.11). Obviously, additional sorption ratio measurements must be made for these elements, particularly for neptunium. Although sorption of technetium and uranium (Fig. 11-18) has not been measured for many samples, the sorption ratios are relatively low; correlations with stratigraphic position or mineralogy cannot be made.

It is interesting to compare the Los Alamos results for actinide sorption with those of Allard et al.,[54,55] who examined the sorption of americium and neptunium on common rock-forming minerals: quartz, biotite, bytownite, albite, microcline, olivine, kaolinite, hornblende, and augite. They used a synthetic groundwater and a somewhat different batch technique and observed a difference of about a factor of 10 between the low-sorbing quartz and high-sorbing biotite. The sorption ratios they report (for pure minerals) tend to be somewhat higher (factors of 10) than those reported here (for tuff) for neptunium, but they are quite similar for americium.

8. Effects of Elevated Temperature. The averages of results from three batch experiments performed at 70°C are given in Table XXVII. These values are compared with those for room temperature given in Tables XXI and XXII. The values are generally similar but higher than those for room temperature by factors up to 5. A limited number of experiments should be performed for other elements.

9. Effects of Particle Size on Sorptive Behavior. Sorption measurements were performed by the batch technique to determine whether the presence of

TABLE XXVII

AVERAGE SORPTION AND DESORPTION RATIOS FOR PULVERIZED TUFF AT 70°C[a]

Sample	Depth (ft)	Equiv. USW-G1 Depth[b] (ft)	R_d (mℓ/g) Sr	Cs	Ba	Ce	Eu	Am	Pu	U
					Sorption					
JA-18	1420	1339	18000(2000)[c,d]	18000(1000)	49000(7000)					4.0(0.2)
JA-32	2533	2467	113(9)	97(6)	110(120)	80(20)	140(30)	110(20)		11.7(1.7)
JA-37	3497	3286	1050(130)	1360(85)	3670(700)		4200(400)	1000(200)	240	16(2)
					Desorption					
JA-18	1420	1339	21000(2000)	19300(1300)	108000(13000)					14(3)
JA-32	2533	2467	100(8)	108(4)	1160(100)	640(8)	1800(300)			21.1(1)
JA-37	3497	3286	1340(110)	2700(500)	5900(900)		14000(1000)			47(6)

[a] Air; fractions do not contain <75 μm-diam particles.

[b] Depth equivalent in drill hole USW-G1 relative to position in geologic unit.

[c] Nonweighted average; values in parentheses are the absolute-value standard deviations of the means.

[d] Some data were rejected in averaging.

very small (<38-μm) particles in the samples would result in large differences in the ratios measured for tuff samples. This investigation was motivated by the observation that sorption ratios from crushed-rock column measurements are frequently 2 to 3 times lower than batch measurements for a <500-μm fraction (Sec. IV.A.11). All material in the crushed-rock columns was >35 μm, the size of the end frits.

The experimental samples were the zeolitized tuffs YM-38, G1-2289, and G1-3658 and the devitrified tuffs YM-54, G1-1883, G1-1982, and G1-2363. For all samples except G1-1982, the fractions were <38, 38 to 106, and 106 to 500 μm. For sample G1-1982 the fractions were <38, 38 to 75, 75 to 250, and 250 to 500 μm. The larger fractions were wet-sieved to remove very fine particles. Rock samples were contacted with traced groundwater solutions at ambient temperature under atmospheric conditions for 3 weeks. (Contact periods for sample G1-1982 were both 2 and 3 weeks.)

Tables XXVIII and XXIX show the dependence of the sorption ratio on particle size. Samples YM-54, G1-1883, G1-1982, and G1-2363 (all of which are devitrified and do not contain zeolites) show higher sorption ratios (by factors of 2 to 5 for the <38-μm fraction) for strontium, cesium, and barium. The <38-μm fraction of the devitrified tuff samples contains a higher percentage of smectite clays than do the larger size fractions (Table XXIV). These clays may be responsible for the increased sorption by ion exchange of strontium, cesium, and barium.

For a different set of samples (Table XXIX), all of which are devitrified except G-1854 [zeolitized with some clinoptilolite (Table XXIV)], the <75-μm fraction gave R_d values averaging a factor of only ~1.4 greater than those for the 75- to 500-μm fraction. Apparently, the large number of particles between 38 and 75 μm in the <75-μm fraction significantly reduces the difference in sorption between the two fractions studied, and particles in the 38- to 75-μm range have sorption ratios similar to those in the 75- to 500-μm fraction for each tuff. Unfortunately, no data are available for direct comparison of <38-μm and <75-μm fractions of the same samples.

For the zeolitized tuff samples YM-38, G1-1854, G1-2289, and G1-3658, sorption ratios for strontium, cesium, and barium are very high. In general, the smaller fractions have R_d values less than a factor of ~2 higher than the coarser fractions. The increase in sorption ratios for the fine fractions of sample G1-2289, which exhibited the largest fractionation of minerals after sieving (Table XXIV), is no greater than would be expected from the increase in

TABLE XXVIII

DEPENDENCE OF SORPTION RATIO ON PARTICLE SIZE

Sample	Element	R_d (mℓ/g) <38 μm	38-106 μm	106-500 μm
YM-38	Sr	13900[a]	20300[a]	17600[a]
"	"	20500[a]	19600[a]	17600[a]
"	"	17000(3000)	20000(400)	17600(0)
"	Cs	11100	16600	14300
"	"	19600	14900	14000
"	"	15000(4000)	16000(900)	14200(200)
"	Ba	69000	119000	56500
"	"	187000	102000	103000
"	"	130000(60000)	110000(9000)	80000(23000)
"	Eu	2250	1350	1330
"	"	2990	1340	1510
"	"	2600(400)	1340(10)	1400(100)
YM-54	Sr	277	56.8	37.1
"	"	274	56.1	56.1
"	"	276(2)	56.5(0.4)	47(10)
"	Cs	937	188	114
"	"	889	186	132
"	"	910(30)	187(1)	120(10)
"	Ba	1720	476	134
"	"	1610	471	148
"	"	1670(60)	474(3)	140(7)
"	Eu	1610	255	489
"	"	1590	420	444
"	"	1600(10)	340(80)	470(20)
G1-1883	Sr	26.2	22.2	22.4
"	"	80.2	21.7	21.8
"	"	50(30)	22(1)	22(1)
"	Cs	306	198	186
"	"	717	183	181
"	"	500(200)	190(10)	184(3)

TABLE XXVIII (cont)

Sample	Element	R_d (mℓ/g) <38 μm	38-106 μm	106-500 μm
G1-1883	Ba	234	208	161
"	"	753	199	162
"	"	500(300)	204(5)	162(1)
"	Eu	375	108	173
"	"	653	119	153
"	"	510(200)	110(10)	160(10)
G1-2289	Sr	16600	6340	7830
"	"	11700	6410	8450
"	"	14000(3000)	6380(40)	8100(300)
"	Cs	43400	33800	12100
"	"	27100	29100	72100
"	"	35000(8000)	31000(3000)	42000(30000)
"	Ba	173000	54000	90300
"	"	114000	48500	69600
"	"	140000(30000)	51000(3000)	80000(10000)
"	Eu	1650	780	817
"	"	1400	778	812
"	"	1500(100)	779(1)	815(3)
G1-2363	Sr	179	73.9	58.2
"	"	168	62.2	61.4
"	"	170(10)	70(10)	60(2)
"	Cs	1390	553	414
"	"	1270	520	382
"	"	1300(100)	540(20)	400(20)
"	Ba	918	243	230
"	"	865	255	212
"	"	890(30)	250(10)	220(10)
"	Eu	5650	778	780
"	"	5440	794	578
"	"	5500(100)	786(8)	680(100)

TABLE XXVIII (cont)

Sample	Element	R_d (mℓ/g) <38 μm	38-106 μm	106-500 μm
G1-3658	Sr	9830	11600	13100
"	"	15700	13500	13400
"	"	13000(3000)	13000(1000)	13200(200)
"	Cs	13900	6140	4910
"	"	18500	7080	5040
"	"	16000(2000)	6600(500)	4980(70)
"	Ba	11700	9020	12700
"	"	18600	10200	14200
"	"	15000(4000)	9600(600)	13000(1000)
"	Eu	14600	414	488
"	"	15700	477	566
"	"	15000(600)	440(30)	530(40)

		R_d (mℓ/g) <38 μm	38-75 μm	75-250 μm	250-500 μm
G1-1982[b]	Sr	1200	59	49	51
"	"	1200	66	53	66
"	"	1200(0)	63(4)	51(2)	59(7)
"	Cs	3800	1200	960	1200
"	"	3500	1300	1100	1200
"	"	3650(200)	1250(50)	1000(70)	1200(0)
"	Ba	10000	670	568	693
"	"	10000	844	780	780
"	"	10000(0)	760(90)	670(100)	740(40)
"	Eu	1200	535	614	864
"	"	2500	885	1300	1100
"	"	1900(700)	710(180)	960(300)	980(120)

[a] For all samples except G1-1982, the first two lines for each element give duplicate measurements for 3-week contact periods. The third line gives the average of the duplicate measurements. Values in parentheses are standard deviations of the means.

[b] For sample G1-1982, the first two lines give measurements for 2- and 3-week contact periods, respectively; the third line gives the average of the two. Values in parentheses are the standard deviations of the means.

TABLE XXIX
DEPENDENCE OF SORPTION RATIO ON PARTICLE SIZE[a]

Sample	Element	R_d (mℓ/g) <75 μm	R_d (mℓ/g) 75-500 μm
G1-1854	Sr	71000	32000
"	"	92000	43500
"	"	81000(11000)	38000(6000)
"	"	15100	11400
"	"	14900	10000
"	"	15000(100)	10700(700)
"	Ba	63000	34000
"	"	48000	34000
"	"	56000(8000)	34000(0)
"	Eu	>131000	>122000
"	"	>100000	>14000
G1-2333	Sr	220	152
"	"	216	144
"	"	218(2)	148(4)
"	Cs	1700	1200
"	"	1510	1120
"	"	1600(100)	1160(40)
"	Ba	1900	1200
"	"	1820	1140
"	"	1860(40)	1170(30)
"	Eu	2000	1400
"	"	3120	2870
"	"	2600(600)	2200(800)
G1-2410	Sr	283	170
"	"	276	168
"	"	280(4)	169(1)
"	Cs	2000	1200
"	"	2040	1300
"	"	2020(20)	1250(50)
"	Ba	3040[b]	1780[b]
"	"	3040	1780
"	Eu	390	360
"	"	440	510
"	"	420(30)	440(80)

TABLE XXIX (cont)

Sample	Element	R_d (mℓ/g) <75 μm	R_d (mℓ/g) 75-500 μm
G1-2476	Sr	49	41
"	"	51	40
"	"	50(1)	41(1)
"	Cs	815	660
"	"	919	741
"	"	870(50)	700(40)
"	Ba	480	374
"	"	518	396
"	"	500(20)	385(10)
"	Eu	4600	3300
"	"	5080	3110
"	"	4800(300)	3200(100)
G1-2840	Sr	170	160
"	"	171	159
"	"	170(1)	160(1)
"	Cs	2800	2400
"	"	2480	2020
"	"	2600(200)	2200(200)
"	Ba	2300	2000
"	"	2620	2140
"	"	2500(200)	2070(70)
"	Eu	5000	4500
"	"	6200	5330
"	"	5600(600)	4900(400)
G1-2854	Sr	120	94
"	"	59	93
"	"	90(30)	94(1)
"	Cs	1700	1200
"	"	510	952
"	"	1100(600)	1080(120)
"	Ba	1600	950
"	"	6510	1040
"	"	4000(2000)	1000(50)
"	Eu	1100	1100
"	"	2560	1530
"	"	1800(800)	1300(200)

[a]The first two lines are measurements for 2- and 3-week contact periods, respectively; the third line gives the average of the two. Values in parentheses are the standard deviations of the means.

[b]Only one measurement available.

zeolite content (Sec. IV.A). Sample G1-3658 exhibited similar variations without a corresponding variation in mineral abundances.

Sorption ratios are higher for europium for the <38-μm fractions of both zeolitized and devitrified tuffs, which may be a result of sorption on the increased surface areas by processes other than ion exchange.

Preliminary results from whole-core column studies indicate that there is better agreement with the results of batch experiments when batch work is performed with samples from which the very fine particles have been removed. However, greater variation should be expected in whole-core samples because of the heterogeneity of tuff; as more whole-core experiments are completed, samples having R_d values greater than those from the batch experiments may be found. Perhaps the fine clays are not generally available to fluids for sorption in real situations or they have been enriched in the samples studied. Of course, there is better agreement between batch results from sorption on larger particles and crushed-rock column measurements because the fine particles were deliberately removed for the crushed-rock column work.

The presence of very fine particles in larger fractions apparently can change the observed sorption ratio of an element by a factor of 2 to 5, especially in the case of devitrified tuffs. Therefore, it is advisable to wet-sieve larger fractions to avoid the presence of fine particles that might increase the observed sorption in an irreproducible manner. The removal of small particles may result in measurements on material that is not completely representative of the tuff; however, the results are useful for comparative purposes and are probably not far from the "true" values. Any errors should be in the conservative direction, that is, too low R_d values for samples that do not contain very fine particles.

10. Comparison of Batch Studies Made Under Atmospheric and Controlled-Atmosphere Conditions. Because reducing conditions are expected for some groundwater/rock systems, the sorptive behavior of some elements in such systems may be different from that under normal atmospheric conditions. Differences in the sorptive capacity of a rock type could be expected if the rock's surface were altered by exposure to air. These effects were investigated by comparing the results of batch studies performed on the same geologic materials in a nitrogen atmosphere ($\leq$0.2 ppm oxygen and $\leq$20 ppm carbon dioxide) with similar measurements made under normal atmospheric conditions. However, the controlled-

atmosphere studies were not truly representative of the conditions to be found in deep geologic systems because very little carbon dioxide was present.

The pH values of the groundwaters after the experiments in the controlled atmosphere were ~0.5 unit higher than for similar experiments in air. This might be a consequence of some loss of carbon dioxide (and total carbonate) from solution and might affect sorption of U(VI), which is strongly complexed by carbonate. The changes in pH may decrease significantly the solubility of some multivalent ions and also might result in changes in ionic charge, degree of hydration, etc.

For most experiments, the radionuclides were ^{85}Sr, ^{137}Cs, ^{133}Ba, ^{141}Ce, ^{152}Eu, $^{95}Tc^{m}$, ^{237}U, ^{237}Pu, ^{241}Am, and ^{235}Np; the rock samples were from tuff cores YM-22, YM-38, and YM-54. Experiments were also performed with ^{22}Na, ^{54}Mn, ^{75}Se, and ^{113}Sn and tuff core G1-2233. The groundwaters used for the determinations in air and nitrogen atmospheres had the same initial composition. Fractions of <75 and 75 to 500 μm were used for most studies under both conditions; fractions of <106 and 106 to 500 μm were used in some experiments under atmospheric conditions.

The R_d values from both sorption and desorption studies, given in Table XXX, are the averages of measurements for 3-, 6-, and 12-week contact periods. The effects of atmosphere on the sorptive behavior of the 14 elements studied are summarized in Table XXXI and are discussed below.

Strontium, cesium, and barium R_d values are essentially the same for atmospheric and controlled-atmosphere conditions. The sorptive behavior of tuff for these elements appears to be independent of the atmosphere involved.

Cerium and europium R_d values are similar for the two different atmospheres. The sorption of cerium and europium may be strongly dependent on the formation of insoluble forms of these elements, such as precipitates or colloids.

Americium has lower R_d values for both sorption and desorption in the YM-22 (devitrified) tuff under the controlled atmosphere. For samples YM-54 (devitrified) and YM-38 (zeolitized), americium R_d values for both sorption and desorption are either the same or slightly greater under the controlled atmosphere. Americium has exhibited a tendency toward large variations in behavior when experimental conditions are changed, which may be the result of speciation effects.

TABLE XXX

SORPTION RATIOS (mℓ/g) FOR ATMOSPHERIC AND CONTROLLED-ATMOSPHERE CONDITIONS

		Sorption		Desorption	
Sample	Element	Atmospheric	CA[a]	Atmospheric	CA[a]
YM-22	Sr	56(4)[b]	63(6)[b]	63(4)[b]	104(12)[b]
YM-38	"	11900(3200)	10600(2600)	21700	17000(2300)
YM-54	"	90(4)	110(13)	94(9)	126(7)
YM-22	Cs	340(60)	330(50)	400(30)	420(60)
YM-38	"	8600(1700)	9300(1200)	13000	12000(1600)
YM-54	"	250(20)	300(30)	310(20)	360(50)
YM-22	Ba	980(80)	550(130)	1000(210)	830(210)
YM-38	"	66000(13000)	>62000	260000	64000(9000)
YM-54	"	620(80)	560(70)	660(20)	600(40)
YM-22	Ce	1300(100)	920(170)	6100(700)	2300(100)
YM-38	"	820(100)	570(90)	2640	7000(5000)
YM-54	"	140(40)	520(140)	1000(200)	1500(400)
YM-22	Eu	1400(100)	970(110)	3600	2400(300)
YM-38	"	3000(1000)	850(110)	7300	7000(5000)
YM-54	"	510(80)	900(200)	1800(100)	2000(200)
G1-2233	Na	141(4)	150(2)	160(10)	150(3)
"	Mn	6000(400)	1500(900)	>9300	2300(800)
"	Se	11(2)	14(0)	46(5)	99(31)
"	Sn	460(130)	210(2)	580(70)	740(240)
YM-22	Am	4000(1200)	1400(200)	4700(1000)	3700(800)
YM-38	"	5500(1000)	5600(1000)	9500(1300)	14000(2000)
YM-54	"	590(210)	1000(400)	600(50)	2600(400)

TABLE XXX (cont)

Sample	Element	Sorption		Desorption	
		Atmospheric	CA	Atmospheric	CA
YM-22	Pu	140(40)	220(50)	1400(100)	1600(300)
YM-38	"	250(90)	800(90)	2000(500)	>2300
YM-54	"	90(20)	130(20)	720(5)	1300(200)
YM-22	U	1.8(0.2)	0.6(0.3)	5.3(1.9)	
YM-38	"	5.3(0.2)	15(1)	15(1)	
YM-54	"	1.7(0.2)	1.5(0.2)	13(3)	
YM-22	Np	5.9(0.6)	8.6(0.7)	33(5)	23(3)
YM-38	"	11(1)	100(30)	23(3)	270(80)
YM-22	Tc	0.3(0.1)	2.6(1.0)	1.2(0.3)	18(5)
YM-38	"		14(4)		120(20)

[a]CA = controlled atmosphere; nitrogen, ≤0.2 ppm oxygen, and ≤20 ppm carbon dioxide.

[b]Average of all measurements taken at 3-, 6-, and 12-week contact times; fraction sizes: <75 and 75 to 500 μm for most atmospheric and controlled-atmosphere conditions and <106 and 106 to 500 μm for some atmospheric conditions. Values in parentheses are absolute-value standard deviations of the means. No error is given for single measurements.

Plutonium R_d values for both sorption and desorption for the zeolitized tuff YM-38 are significantly higher under controlled-atmosphere conditions than in air. This is perhaps consistent with the tendency of plutonium to exhibit variations in behavior when experimental conditions are changed, presumably the result of speciation effects (Sec. II). Technetium sorbs relatively more strongly in a controlled atmosphere where conditions are presumably more reducing. The sorption ratios on zeolitic tuffs are about 15 times larger under controlled-atmosphere conditions than in air. The values for devitrified tuffs are 10 to 25 times larger under the controlled-atmosphere conditions. Uranium sorption ratios under controlled-atmosphere conditions are similar to those in air for YM-22 and YM-54 samples (devitrified) but somewhat

TABLE XXXI

COMPARISON OF SORPTION RATIOS (R_d) MEASURED UNDER ATMOSPHERIC AND CONTROLLED-ATMOSPHERE CONDITIONS[a]

Element	Effect on R_d Value
Cs	none
Sr	none
Ba	none
Ce	none
Eu	none
Na	none
Se	none
Mn	lower in CA (factors of 3 to 4)
Sn	lower in CA (factor of 2)
Am	none
Pu	higher in CA (factor of 2)
Tc	higher in CA (factor of $\geq$10)
U	higher in CA[b] (factors of 2 to 3)
Np	higher in CA (factor of 2)

[a]CA = controlled atmosphere; nitrogen, $\leq$0.2 ppm oxygen, and $\leq$20 ppm carbon dioxide.

[b]YM-38 (zeolitized) tuff only; otherwise no effect.

higher for YM-38 samples (zeolitized). The U(VI) apparently remains strongly complexed by carbonate in the groundwater even though the total carbonate concentration is reduced in the controlled atmosphere.

Neptunium sorption and desorption ratios are higher in the controlled-atmosphere than in air, especially for the zeolitized tuff. There is perhaps a change in the oxidation state of neptunium in the controlled atmosphere, which could favor increased sorption.

Sodium and selenium show no observable difference in R_d values for sorption and desorption when measured in air or in the controlled atmosphere.

Manganese has lower R_d values for both sorption and desorption when measured in the controlled atmosphere; tin values for sorption are also lower in the controlled atmosphere, but values for desorption are about the same. It seems that there is less formation of insoluble

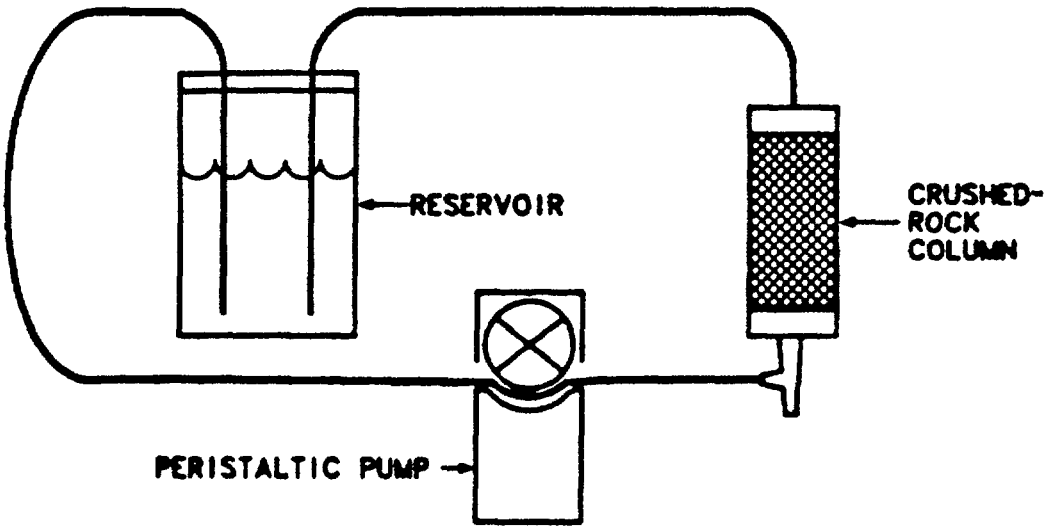

Fig. 46. Circulating system for crushed-rock system studies.

oxidized compounds of tin and manganese in the controlled atmosphere, resulting in lower sorption ratios.

If reducing conditions exist in any tuff/groundwater system, the effect would probably be enhanced sorption or precipitation for a number of elements. Furthermore, if Fe(II) is present in solution under reducing conditions, the precipitation of ferric hydroxide from such groundwaters under oxidizing conditions should result in scavenging other waste elements from solution.

11. Comparison of Sorption Ratios Measured by Batch and Circulating-System Methods. The circulating system (Ref. 3 and Fig. 46) is a hybrid that incorporates features of both batch and column methods. The batch and circulating-system procedures are similar in some ways, but the solid phase remains stationary in the circulating system and is not subject to the possible self-grinding of the batch measurements. The presence of smaller particles could result in greater sorption as a result of greater surface area or differences in mineralogy.

Sorption ratios for strontium, cesium, and barium were determined using one feed solution for the circulating system and another for the batch measurements. The actinide series of comparisons was made using the same feed solution for both circulating-system and batch measurements for each actinide. Although the feed solutions for both the batch and circulating systems were prepared

just before the start of batch sorptions, there was a delay of from 6 to 16 days before the feed solution could be introduced in the circulating system.

The traced feed solutions were made in the standard manner by drying the tracer (Sec. IV.A.2). The concentrations of tracer and element added were approximately 5×10^{-9} M for cesium, 5×10^{-8} M for barium, and 5×10^{-7} M for strontium. Solutions traced with americium or plutonium varied with each preparation. The concentrations of plutonium were 3.1×10^{-12} M for experiments with YM-49 and 4.1×10^{-12} M for JA-37 and G1-1883. Americium concentrations in feed solutions were 1.2×10^{-7} M for YM-49, 1.3×10^{-7} M for JA-37, and 1.2×10^{-7} M for G1-1883. Desorption experiments were performed with the circulating-system columns from the actinide measurements with fresh, untraced groundwater that had been pretreated with the appropriate tuff.

Table XXXII shows the results of individual sorption measurements for strontium, cesium, and barium that were taken using circulating systems. Results of batch sorption measurements for these same elements are summarized in Table XXI. Pertinent data from the batch and circulating-system sorption and desorption measurements are presented in Tables XXXIII and XXXIV.

The actinide R_d values for desorption measurements with the circulating system are higher than for sorption, just as they are for the batch technique. This apparent irreversibility was discussed earlier (Sec. IV.A.6).

The average R_d values for sorption by the two methods are given in Table XXXV, and the ratios of these results are given in Table XXXVI. Considering the spread of experimental values, the agreement between the two methods is good. In most cases, the results fall within the spread of individual experiment values (see the tables in this section and in App. A). The errors given in Table XXXVI arise from propagating the standard deviation of the mean, which is discussed in Sec. IV.A.2 above. The barium sorption ratio obtained for sample YM-22 by the column method[38] (137 mℓ/g) is in much better agreement with the results from the circulating-system method than is the batch data.

The devitrified tuffs tended to give slightly higher sorption ratios by the batch method than by the circulating-system method. The observed difference could well be the result of the presence of smaller particles arising from self-grinding in the batch measurements. Similar particle-size effects have been observed in other experiments (Sec. IV.A.9). The results are quite similar for the simple cations, which presumably sorb by ion exchange, and the

TABLE XXXII

STRONTIUM, CESIUM, AND BARIUM SORPTION RATIOS FROM CIRCULATING-SYSTEM SORPTION MEASUREMENTS

Core	Contact Time (days)	R_d (mℓ/g) Sr	Cs	Ba
YM-22	26	9[a]	99[a]	33[a]
	49	29	405	129
	63	28	441	129
	84	30	616	133
	112	21	494	102
Average		27(2)[b]	490(50)[b]	120(10)[b]
YM-54	26	39	105	111
	49	53	158	153
	63	49	131	146
	84	44	112	132
	112	41	99	116
Average		45(3)	120(10)	130(10)
JA-37	26	401	1770	948
	49	390	1890	819
	63	398	1800	891
	84	420	1920	729
	112	365	1480	899
Average		390(10)	1800(80)	860(40)

[a]Value not included in average.

[b]Values in parentheses are the absolute-value standard deviations of the means.

actinides, which probably sorb by a more complex process. The R_d value ratios for zeolitized tuffs, which in general have higher R_d values than the devitrified tuffs, scatter considerably and show no consistent pattern; the differences may be the result of experimental uncertainties. Results from other experiments (Sec. IV.A.9) indicate a much smaller effect for zeolitized tuffs than for devitrified tuffs as a result of small particles present in the samples.

TABLE XXXIII

AMERICIUM SORPTION RATIOS FROM

BATCH AND CIRCULATING-SYSTEM MEASUREMENTS

Core (μm particle size)	Contact Time (Weeks)	R_d (mℓ/g) Batch Sorption	Batch Desorption	Circulating System Sorption	Circulating System Desorption
G1-1883	3	4200		2900	25000
(106-250)	3			3000	36000
	12		5900		
	6	4500		3500	24000
	6			3300	56000
	9		6900		
	9			3300	10000
	9			3600	48000
	12	5300		3100	14000
	12			3500	57000
YM-49	3		8900		
(106-260)	3	2900		3300	34000
	3			2500	41000
	12		19000[b]		
	6	2800		1800	30000[b]
	6			1600	5400[b]
	9		3800		
	8			2400	10500
	8			1500	13000
	12	7100		2800	28000
	12			1600	10000
	3		3000		
JA-37	3	18000		2700	51000
(106-250)	3			300	36000
	12		54000		
	6	37000		3900	190000
	6			4100	170000
	9		59000		
	9			4700	2200000[b]
	9			3900	240000
	12	46000[a]		3600	290000
	12			3600	500000
	3		43000		

[a]Value not included in calculation. Value is from filtered sample; unfiltered sample analogous to those for all other data from these batch measurements was unavailable.

[b]Value not included in calculations.

TABLE XXXIV

PLUTONIUM SORPTION RATIOS FROM
BATCH AND CIRCULATING-SYSTEM MEASUREMENTS

Core (μm particle size)	Contact Time (Weeks)	R_d (mℓ/g) Batch Sorption	Batch Desorption	Circulating System Sorption	Circulating System Desorption
G1-1883 (106-250)	3	51			
	4			46	
	6				465
	12		830		
	6	52[a]		67	
	6	91			
	8		740[a]		
	8		1100		
	9				700
	13	82[a]			
	13	107			
	3		960[a]		
	3		850		
YM-49 (106-250)	3	140			
	4			410	
	12		390[a]		
	6	160			
	6	200[a]		740	
	9		410		
	9		445[a]		
	12	210			
	12	820[a]			
	3		660		
	3		930[a]		
JA-37 (106-250)	3	300		260	
	12		870		
	6	420[a]		305	
	6	560			
	9		890[a]		
	9		1700		
	12	760[a]		320	
	12	1900			
	3		1300[a]		
	3		2400		

[a]Pretreatment of crushed rock was for 4.5 months rather than the normal 2 weeks.

TABLE XXXV

AVERAGE SORPTION RATIOS FROM BATCH AND CIRCULATING-SYSTEM SORPTION MEASUREMENTS

Element	Tuff Core	R_d (mℓ/g) Batch[a]	R_d (mℓ/g) Circulating System
Sr[a]	YM-22	53(3)[b]	27(2)[b]
	YM-54	62(12)	45(3)
	JA-37	287(14)	390(10)
Cs[a]	YM-22	290(30)	490(50)
	YM-54	180(40)	120(10)
	JA-37	610(40)	1800(80)
Ba[a]	YM-22	900(30)	120(10)
	YM-54	400(150)	130(10)
	JA-37	760(150)	860(40)
Am	YM-49	4300(1400)	2200(300)
	JA-37	28000(10000)	3400(600)
	G1-1883	4700(300)	3300(100)
Pu	YM-49	230(50)	570(170)
	JA-37	400(70)	290(20)
	G1-1883	77(11)	56(11)

[a]From Table XXI.

[b]Values in parentheses are the absolute-value standard deviations of the means.

TABLE XXXVI

COMPARISON OF AVERAGE SORPTION RATIOS FROM BATCH AND CIRCULATING-SYSTEM SORPTION MEASUREMENTS

	Batch R_d-to-Circulating System R_d Ratio				
	Sr	Cs	Ba	Am	Pu
Zeolitized Tuffs					
JA-37[a]	0.74(0.04)[b]	0.34(0.03)	0.88(0.18)	8.2(3.3)	1.4(0.3)
YM-49				2.0(0.7)	0.40(0.15)
Devitrified Tuffs					
YM-22	2.0(0.2)	0.59(0.09)	7.5(0.7)		
YM-54	1.3(0.2)	1.3(0.3)	1.6(0.6)		
G1-1883				1.4(0.1)	1.4(0.4)

[a]JA-37 also contains a small amount of clinoptilolite.

[b]Values in parentheses are the errors propagated from errors given in Table XXXV.

The very large differences between R_d values measured by the two methods for sorption of barium on tuff YM-22 and americium on tuff JA-37 are currently unexplained. They do, however, indicate the complexity of sorption processes and sorption measurements and, further, the need for additional study. The americium result for sample JA-37 may be related to the relatively high concentration of montmorillonite in this tuff (Table XXIV). The presence of a large number of highly sorptive fine clay particles in the batch samples could possibly lead to the high R_d value. Early attempts to measure the sorption ratio for americium on tuff JA-37 by using the original inadequate phase-separation technique (Sec. II) resulted in much lower values. This might also be attributable to the presence of highly sorptive, fine clay particles that might be particularly difficult to remove from the aqueous phase (thereby resulting in a low R_d value). The situation is not clear because the plutonium results do not show the same behavior; there is much better agreement between circulating-system and batch measurements and between old and new separation techniques. However, the behavior of americium has consistently been more of a problem than that of plutonium. The extremely high R_d values for americium desorption that were obtained in the circulating-system measurement (Table XXXIII) may in some way be related.

The possibility of transport on small particles may have a bearing on the results of the circulating system measurements and is discussed in Sec. II.B.

12. Crushed-Rock Column Studies. A complete report on these studies is available[38] and is only summarized here. Elutions of radionuclides from columns of crushed tuff, granite, and argillite have been used as a simple first step in trying to relate laboratory batch-type measurements to a flowing system.[2,3,38] Although primarily tuffs were studied, granite and argillite were also included to obtain a more general data base. Because radionuclides are often sorbed quite strongly by these rock types, small columns ($\lesssim$0.5 cm in diameter by 2 to 5 cm long) were used to minimize the duration of an experiment. However, the elutions of nuclides from some of the columns still required 2 to 3 years. The columns were loaded with ~5- to 10-μℓ spikes of groundwater containing one or more radioisotopes. Groundwater was pushed upward through the column by syringe pumps at flow rates of 11 to 77 m/year, although faster flow rates were used in a few cases. The velocity of the radionuclide was measured directly and then compared to the groundwater velocity (measured using HTO or ^{131}I, which does not sorb) to calculate the retardation factor

R_f. In simple ion-exchange theory, the R_f is related to the sorption ratio R_d (or more precisely, the distribution coefficient K_d) by the expression

$$R_f = 1 + (\rho/\varepsilon)R_d \quad ,$$

where ρ is the density of the rock column and ε is the porosity.

Several general observations can be made from the data of approximately 40 columns.[38] (1) The sorption ratios of strontium, cesium, and barium, measured with the columns, generally fall within the range of measured batch R_d values when the batch measurements are made on fractions washed free of fine ($\lesssim$35-μm) particles. Previous reports[2,3] indicated that R_d values inferred from the column studies were 1 to 5 times smaller than from batch study R_d values; however, these earlier comparisons were made with batch measurements using material containing fine particles, and they should not be considered valid. (2) Elution of strontium from a tuff from a vitrophyre was unusual, giving a broad, asymmetric peak; strontium peaks were generally narrow and symmetric. (3) Broad, asymmetric peaks were typical of cesium elutions. In addition, cesium frequently seemed to be eluted either in two broad, partially overlapping peaks or in one major peak with a distinct shoulder. On granite columns, cesium seemed to be fixed at the load end, possibly as a result of irreversible sorption on biotite; such irreversible sorption was not observed on any of the tuffs.

In addition to ^{85}Sr, ^{137}Cs, and ^{133}Ba behavior, that of the radionuclides $^{95}Tc^m$, ^{152}Eu, and ^{141}Ce has been studied. Cerium was loaded on two columns but decayed before eluting. The $^{95}Tc^mO_4^-$ was strongly affected by kinetics. This is not surprising because the retardation mechanism of technetium is probably by reduction of TcO_4^- to Tc(IV), perhaps as TcO_2, rather than by ion exchange. At flow rates of ~2000 m/year, either in air or in a controlled atmosphere of nitrogen with $\leq$0.2 ppm O_2 and $\leq$20 ppm CO_2, argillite-column sorption ratios were 0.29 to 0.43 mℓ/g. The corresponding batch sorption ratio in air was 18 to 222 mℓ/g. When the flow rate was slowed to 20 m/year, allowing more time for reaction, the R_d value for technetium increased to 72 mℓ/g.

Five columns were loaded with ^{152}Eu; for three of the columns, the measured batch sorption ratios fell between the R_d values corresponding to a small amount of ^{152}Eu, which was eluted initially, and the majority of the ^{152}Eu, which remained on the columns. (The columns were sectioned, and the distribution of activity along each column was measured to estimate an R_d value.) It

is not clear whether the europium that eluted initially from the columns was the result of colloidal species. Of the last two columns loaded with ^{152}Eu, one was contaminated with iron and the other gave a sorption ratio that overlapped with the large range of batch sorption ratios. Conclusions can not be drawn for ^{152}Eu until additional measurements are made--ideally using a continuous feed "loading" technique, rather than a spike. The use of spikes can lead to problems because of the isotherm effects discussed in the next section.

A crushed-tuff column (YM-54-4) was loaded with spikes of tritium, ^{131}I, and ^{237}U. Groundwater elution curves result in an R_d value of 0.72 mℓ/g for uranium, whereas the value obtained by batch measurements is 1.5 mℓ/g. The uranium peak was quite asymmetric, and the activity per milliliter slowly decreased; by drop 23, when most of the iodine had been eluted, only 50% of the uranium had been removed from the column. The marked asymmetry may be an effect of the complicated sorption illustrated by the large difference between sorption (1.5 mℓ/g) and desorption (11 mℓ/g) R_d values when measured by the usual batch method.

The general agreement between column and batch measurements for ^{85}Sr, ^{137}Cs, and ^{133}Ba on washed samples is encouraging, because the results of batch measurements are often used to show relative sorption under a variety of conditions, and their relevance to the migration of radionuclides under flowing conditions has been questioned. Whether sample-crushing influences the rock chemistry in both the batch and crushed-rock columns will be determined by studying radionuclide migration through columns of intact rock, larger blocks of intact rock, and in the field.

13. Sorption Isotherms. The study of sorption isotherms is used to

(a) determine the influence of groundwater/tuff interactions on the sorptive properties of tuff,

(b) accurately model the retardation of waste elements under various source-term and groundwater conditions,

(c) detect irreversible sorption processes that could be very positive properties if discovered in tuff,

(d) interpret and model diffusion into the tuff matrix as it would occur in fracture flow, and

(e) explain the observed dependence of the distribution coefficient on the solution-to-solid ratio and predict real conditions from laboratory measurements.